ISSN Print: 2518-4245
ISSN Online: 2518-4253
Vol. 59(3), September 2022

PROCEEDINGS
OF THE PAKISTAN ACADEMY OF SCIENCES:
A. Physical and Computational Sciences

PAKISTAN ACADEMY OF SCIENCES
ISLAMABAD, PAKISTAN

Proceedings of the Pakistan Academy of Sciences: Part A
Physical and Computational Sciences

Proceedings of the Pakistan Academy of Sciences A. Physical and Computational Sciences is the official flagship, the peer-reviewed quarterly journal of the Pakistan Academy of Sciences. This open-access journal publishes original research articles and reviews on current advances in the field of Computer Science (all), Materials Science (all), Physics and Astronomy (all), Engineering Sciences (all), Chemistry, Statistics, Mathematics, Geography, Geology in English. Authors are not required to be Fellows or Members of the Pakistan Academy of Sciences or citizens of Pakistan. The journal is covered by Print and Online ISSN, indexed in Scopus, and distributed to scientific organizations, institutes and universities throughout the country, by subscription and on an exchange basis.

Annual Subscription: **Pakistan:** Institutions, Rupees 4000/-; Individuals, Rupees 2000/- (Delivery Charges: Rupees 150/-)
Other Countries: US$ 200.00 (includes air-lifted overseas delivery)

HEC Recognized, Category Y; Scopus Indexed

Published by **Pakistan Academy of Sciences**, 3 Constitution Avenue, G-5/2, Islamabad, Pakistan
Email: editor@paspk.org; **Tel:** 92-51-920 7140 & 921 5478; **Websites:** www.paspk.org/proceedings/; www.ppaspk.org

Printed at **Graphics Point.,** Office 3-A, Wasal Plaza, Fazal-e-Haq Road Blue Area Islamabad.
Ph: 051-2806257, **E-mail:** graphicspoint16@gmail.com

PROCEEDINGS OF THE
PAKISTAN ACADEMY OF SCIENCES: PART A
Physical and Computational Sciences

CONTENTS

Volume 59, No. 3, September 2022 **Page**

Submission of Manuscripts: Manuscripts may be submitted as an e-mail attachment at editor@paspk.org or submit online at http://ppaspk.org/index.php/PPASA/about/submissions. Authors must consult the ***Instructions for Authors*** at the end of this issue or at the Website: www.paspk.org/proceedings/ or www.ppaspk.org.

Proceedings of the Pakistan Academy of Sciences: A Physical and Computational Sciences 59(3): 1-16 (2022)

ISSN (Print): 2518-4245; ISSN (Online): 2518-4253
https://doi.org/10.53560/PPASA(59-3)782

Pakistan Academy of Sciences

Review Article

Machine Learning Methods of IoT Security and Future Application

Aqib Ali[1*], Samreen Naeem[1], Sania Anam[2], and Muhammad Munawar Ahmed[3]

[1]College of Automation, Southeast University, Nanjing, China
[2]Department of Computer Science, Govt Degree College for Women Ahmadpur East, Bahawalpur, Pakistan
[3]Department of Information Technology, The Islamia University of Bahawalpur, Pakistan

Abstract: One of the technologies that are now expanding rapidly is called the Internet of Things (IoT). It is a technology that enables billions of smart devices or things, collectively referred to as "Things," to collect a variety of data about themselves and the environment in which they are located using a variety of sensors. They can then share data with parties who have been permitted to do so for a variety of objectives, such as the management and monitoring of industrial services or the expansion of company services or operations. However, there are presently more security risks associated with the Internet of Things than ever. The field of machine learning (ML) has recently experienced significant advancement in technology, which has resulted in the opening of various new lines of inquiry that may be used to address existing and upcoming issues related to the Internet of Things. Nevertheless, machine learning is a robust technology that can recognize suspicious dangers and activities in smart devices and grids. This paper presents an extensive literature review on Machine Learning methods and the significance of IoT security in the context of various types of potential attacks as well as the comparison of several different ML algorithms regarding the detection of attacks and anomalies. Additionally, many machines learning-based Internet of Things protection systems have been presented.

Keywords: Internet of Things, Cyberattacks, Machine Learning, Security

1. INTRODUCTION

The Internet of things (IoT) is a network of intelligent devices that share data online. In a new context, smart objects gather information and initiate events [1]. Smart cities, houses, transit, agriculture, hospital, supply chain, seismic detection, and smart grid are IoT applications as shown in Figure 1. The Networking, Cloud, and Cybersecurity Solutions (CISCO) predicts 31.3 billion IoT devices by 2025. IoT device growth is rapid and global. IoT devices create massive data. Physical, network, and application architectures make up classical IoT [2]. The gadgets are environmentally conscious and may be wired or wirelessly linked. As in a smart home, the refrigerator may automatically make an order at the registered merchant when the fruit bowl empties and notify home users. Sensors and computers can monitor smart hospital patients in an emergency. Little-end sensors have various features and low computing power. IoT implementation is complex. IoT problems are standardization, interoperability, data storage, processing, trust management, identification, confidentiality, integrity, availability, security, and privacy [3].

IoT devices employ web-enabled sensors and hardware to send, gather, and act on data. Connecting IoT or edge devices to a gateway collects data for cloud analysis. Smart gadgets sometimes communicate with other devices and work on the information delivered between them [4]. Intelligent devices communicate by transferring data packets over a network, saving time and money. IoT gadgets make the network insecure. Unsecured devices abuse the network. Since IoT devices are tightly linked, an attacker can exploit a single weakness to modify all data and damage humans [5]. Several

Received: July 2022; Accepted: September 2022
*Corresponding author: Aqib Ali <aqibcsit@gmail.com>

preventative strategies are explored to avert cyber risks, and a fog security gateway is created. The fog layer's primary purpose is to increase safety and efficiency and minimize cloud data processing, analysis, and archiving [6].

Fog computing explores data's outer edges—the fog layer stores construction data in a customer's cloud or data center. The fog layer improves efficiency and reduces redundancy in cloud data transit, maximizing cloud computing security. Data won't be transferred straight to the cloud layer since it establishes a high-latency network connection between devices and the analytics endpoint and has more bandwidth than the fog layer. In other cases, there's no bandwidth to transport data since it's processed locally [7]. An IDS analyzes data flow to detect and safeguard system information. IDS activities include monitoring, analysis, and detection. The monitoring phase depends on the host-based or network-based sensor, the analysis phase on model identification or feature extraction, and the detection phase on detecting abnormalities or abusive intrusions [8]. IoT is a new technology that has many uses. Many applications struggle with security and privacy. IoT security and privacy have been studied. New technologies can handle IoT security, though [9]. This article identified three prominent security technologies: ML, Blockchain, and AI.

2. LITERATURE REVIEW

This section contains relevant works on anomaly detection using machine learning methods in the IoT network. Using distributed deep learning fog for ML algorithm-based computing in IoT, an NSL-KDD dataset is utilized to compare the model to the surface algorithm. The outcome may be better. As a signature-based IDS [10]. ADFA-LD dataset used with Raspberry pi for a perceptron-based fog IDS. When improving calculating accuracy and efficiency. Traditional intrusion detection systems consist of a host and network-based or hybrid IDS, which may detect cyber-attacks differently. Standard IDS are designed to identify intrusion activity on single or complete network traffic. First, host-based IDS installs antivirus software and identifies suspicious network traffic by scanning and analyzing system calls, application logs, file systems, etc. Some IoT devices have restricted capability and resources [11]. Therefore, this solution fails.

The second kind, network-based IDS, analyzes all network traffic and identifies known and unknown threats (HIDS) using an anomaly-based and signature-based hybrid approach. Signature-based technique uses more resources and doesn't identify attacks, only database records [12]. Anomaly-based NIDS is better at monitoring

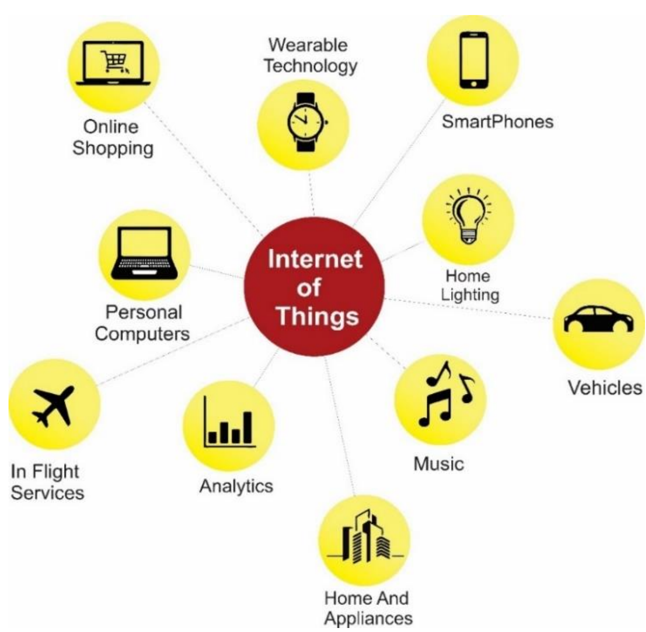

Fig. 1. IoT Applications

network traffic and identifying threats. Anomaly detection promises to identify NIDS attacks.

Random Forest (RF) is utilized to detect malicious activity using the UNSW-NB15 dataset and the AD-IoT detection approach, which uses binary classification to characterize packet behavior as usual or dangerous. Only package behavior limits it—unknown packet attack. AD-IoT hasn't been utilized to designate an attack. Hence this will be the inquiry [13]. Most of the advanced research work done in current days should provide excellent direction for future researchers [14-22].

3. CURRENT RESEARCH GAPS IN IOT SECURITY

Understanding the underlying privacy and security problems is critical to properly implementing the IoT. In the past, the IoT was built on top of existing technology [23]. As a result, it's critical to determine if the IoT's security concerns are novel or a revolution in the security challenges experienced by previous technologies. Several characteristics, such as incorporating apps, networks, hardware, and software, are comparable to the last security issues [24]. The fundamental problem with the IoT is resource limits, which make it challenging to employ present advanced IoT security solutions. In addition, IoT privacy and security issues necessitate optimal algorithms and layered architecture. IoT systems, for example, require more robust cryptographic optimization and new algorithms to handle privacy and security owing to IT limits. On the other hand, various IT gadgets bring new problems to existing security methods [25]. ML approaches may be used to increase the security of text data by automated organizing in this situation. These methods will be addressed in more detail later in the paper.

4. IOT LAYERS

The Internet of Things architecture functions as a portal to a variety of different hardware applications [26]. This allows for the establishment of a connection as well as the extension of IoT services to each gateway. When transmitting and receiving information or data from different levels of Internet of Things architecture [27], several network protocols are used. Some examples of these protocols are Bluetooth, Wi-Fi, RFID, narrow and wide band, ZigBee, and LPWAN. A typical Internet of Things architecture consists mostly of three layers: the physical layer, the network layer, and the application layer as shown in Figure 2 [28].

- **The Physical Layer:** This layer is characterized by sensing and knowledge gathering and collection about the world in which intelligent

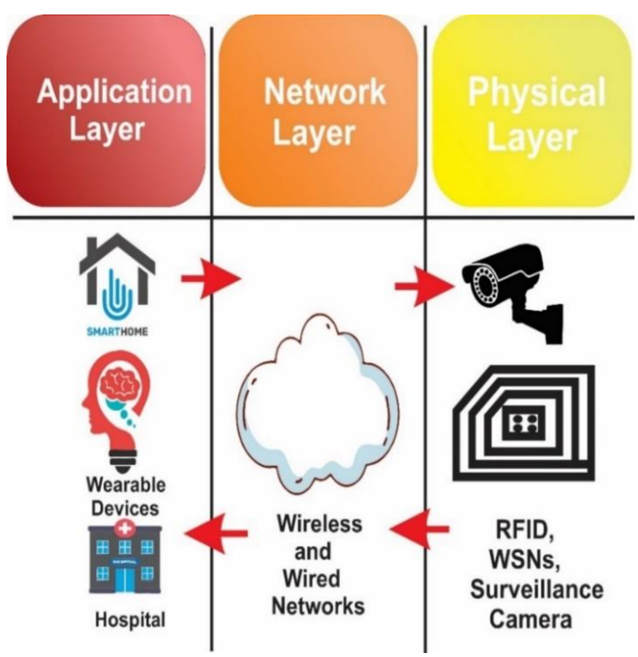

Fig. 2. IoT Layers: The Architecture

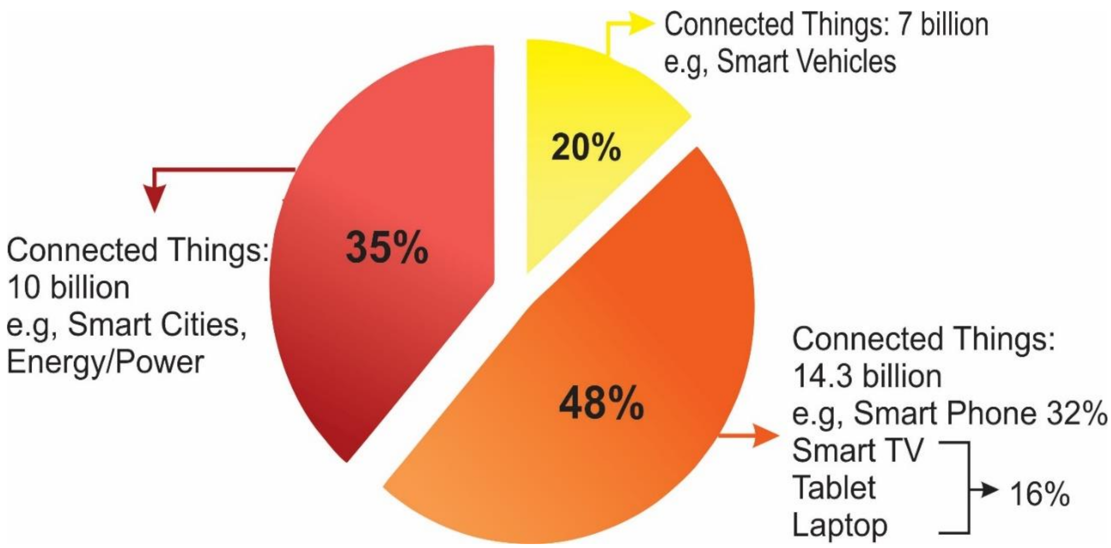

Fig. 3. Users of IoT devices Estimated by the year 2025.

things are available [29].

- **The Network Layer:** The layer feature allows data to be delivered and processed utilizing various devices' internet connections [30].
- **The Application Layer:** Its primary purpose is to give a specific application-based service to the user [30].

4.1 Security in the IoT

21st-century IoT device security is a prominent subject. IoT connects the universe. It opens several doors for attacks [31]. IoT apps running on an open network make gadgets easier to use. The Internet of Things endangers human life by exposing it to various hazards and threats. Still, it also makes compliance more straightforward. [32] Internet of Things devices may be accessed from any location without user authentication. Several security measures will need to be developed to ensure the safety of IoT devices. Because of their physical construction, Internet of Things devices has limited computing capabilities, which makes it impossible to devise an all-encompassing security protocol. A reliable IoT must have security qualities. Standard IoT security criteria include confidentiality, integrity, and authentication [33]. An estimated percentage of IoT device users by 2025 is presented in Figure 3.

- Confidentiality involves prudence through concealing information. Sensitive sensors need concealment, such as with military data. WSN is a highly-requested feature. If WSN reports could be altered, the enemy may be misled. Social and industrial uses need secrecy [34].
- To preserve IoT data integrity, the recipient must confirm no messages were modified during transmission or delivery. The data integrity check ensures that the information provided has not been modified. This is very important because even if intruders cannot get the data, the network may still fail to function correctly if any of the nodes have been infiltrated and altered the data. Data may be modified automatically without human involvement if the connection is unstable. Integrity check detects unintentional and purposeful message modifications [35].
- The authentication procedure verifies a message's origin. Sensor nodes assess the peer node's identification and validity. Authenticity ensures a simple message. The Message Authentication Code (MAC) offers message integrity and authenticity [36].

5. IOT ATTACKS

In recent years, the IoT has been attacked, raising awareness among businesses and consumers. Describes IoT attacks, impacts, and surfaces. Cyber and physical attacks against IoT [37]. Figure 4 shows IoT security threats, including different types of attacks, effects of the attack, anomaly detection,

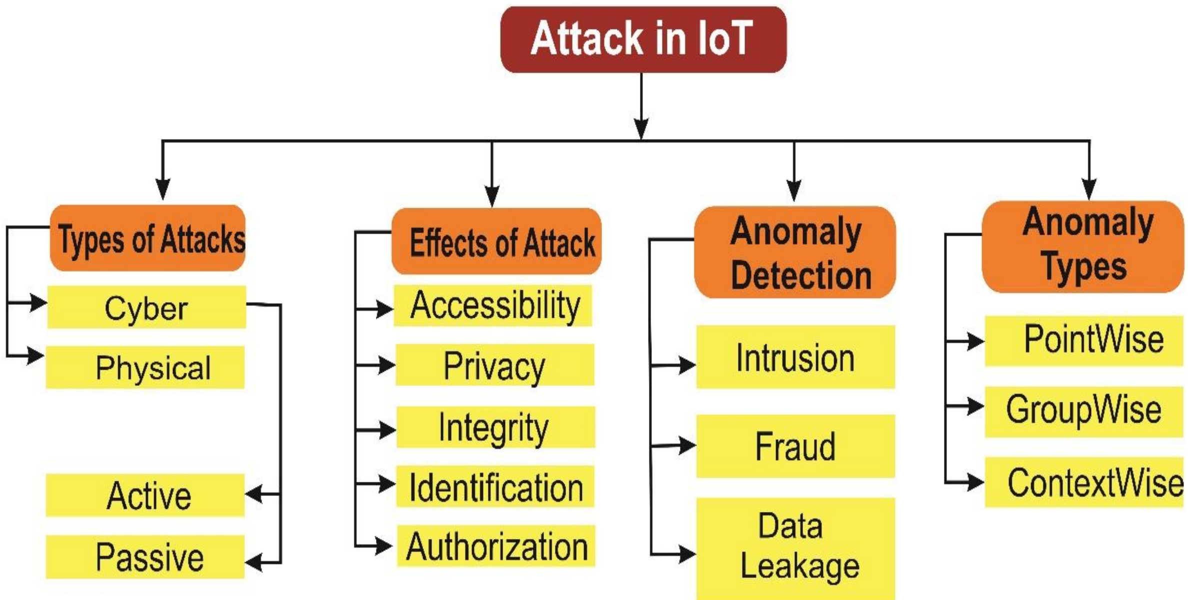

Fig. 4. Graphical representation of IoT security threats, including different types of attacks, effects of the attack, anomaly detection, and anomaly types.

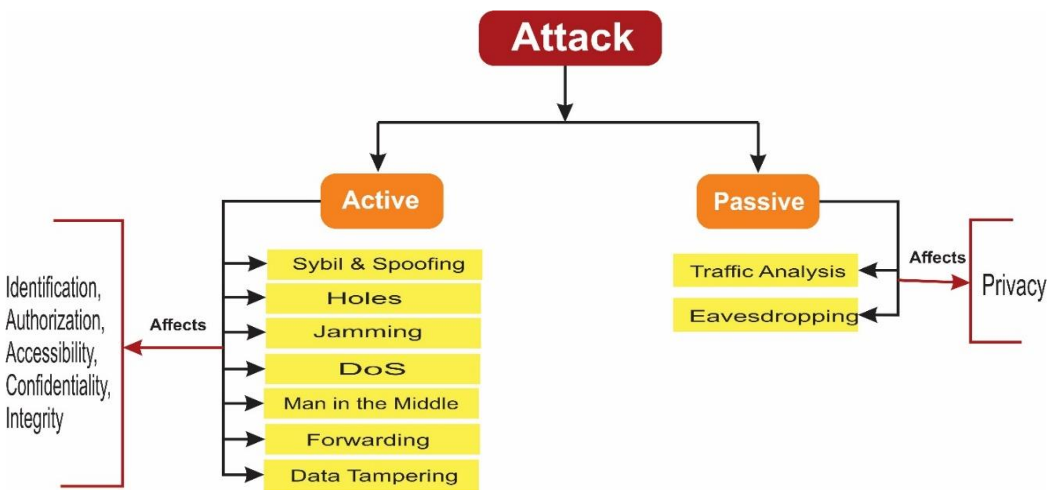

Fig. 5. Types of attacks and their effects

and anomaly types. Many different Internet of Things devices is the target of cyberattacks, which involve hacking into wireless networks and stealing, deleting, altering, or destroying user data.

Physical attacks destroy IoT devices. The gadget may be attacked without a network. Mobile devices, cameras, sensors, routers, etc., can also be attacked [38]. The following subsections focus on cyber-attacks based on their severity on active and passive IoT devices as shown in Figure 5.

5.1 Active IoT Attacks

An active assault is carried out by a network attacker who, after gaining access to the interface settings, then disconnects certain services from the IoT devices they target. Interruptions, interventions, and changes are all examples of active assaults that may occur in several different ways. Attacks such as denial of service, middle hand, Sybil and spoofing, hole attacks, jamming, selective forwarding, and data manipulation are shown in Figure 6 [39].

5.1.1 Denial of Service (DoS) Attacks

DoS attacks disable system services by sending repeated requests, as seen in Figure 5. The user cannot navigate or connect to the IoT device, which prevents them from making informed decisions. DoS attacks force Internet of Things devices to remain active, which causes battery drain. Repeated attacks from various IP addresses create multiple requests to overwhelm a server in a DDoS attack. It's tough to tell natural from hazardous traffic. An IoT botnet malware has been responsible for disruptive DDoS attacks in recent years [40].

5.1.2 Sybil and Spoofing Attacks

These exploits obtain unwanted access to IoT systems using user identification (RFID and MAC address). The TCP/IP lacks a comprehensive security protocol, making IoT devices vulnerable to phishing. These two attacks also launch man-in-the-middle and DoS attacks [41].

5.1.3 Jamming Attacks

Continuous wireless network communication by broadcasting undesired signals to IoT devices causes user issues by keeping the network busy (Figure 6). This exploit affects IoT system performance by requiring more memory, bandwidth, etc. [42].

5.1.4 Man in Middle Attacks

Network participants carry out man-in-the-middle attacks directly connected to another user interface. False information may easily disrupt conversations. Bad data to hack original data [43].

5.1.5 Forwarding Attacks

Figure 5 illustrates how a broadcast attack node may be dropped in the middle of a transmission, resulting in a networking system hole. Malicious inbound assaults include Trojans, rootkits, worms, adware, and viruses that may cause financial harm, power dissipation, and corrupt wireless network output [44]. This attack is difficult to detect.

5.1.6 Holes Attacks

Black Hole and Gray Hole attacks are active attacks since they influence network performance and create crashes [45].

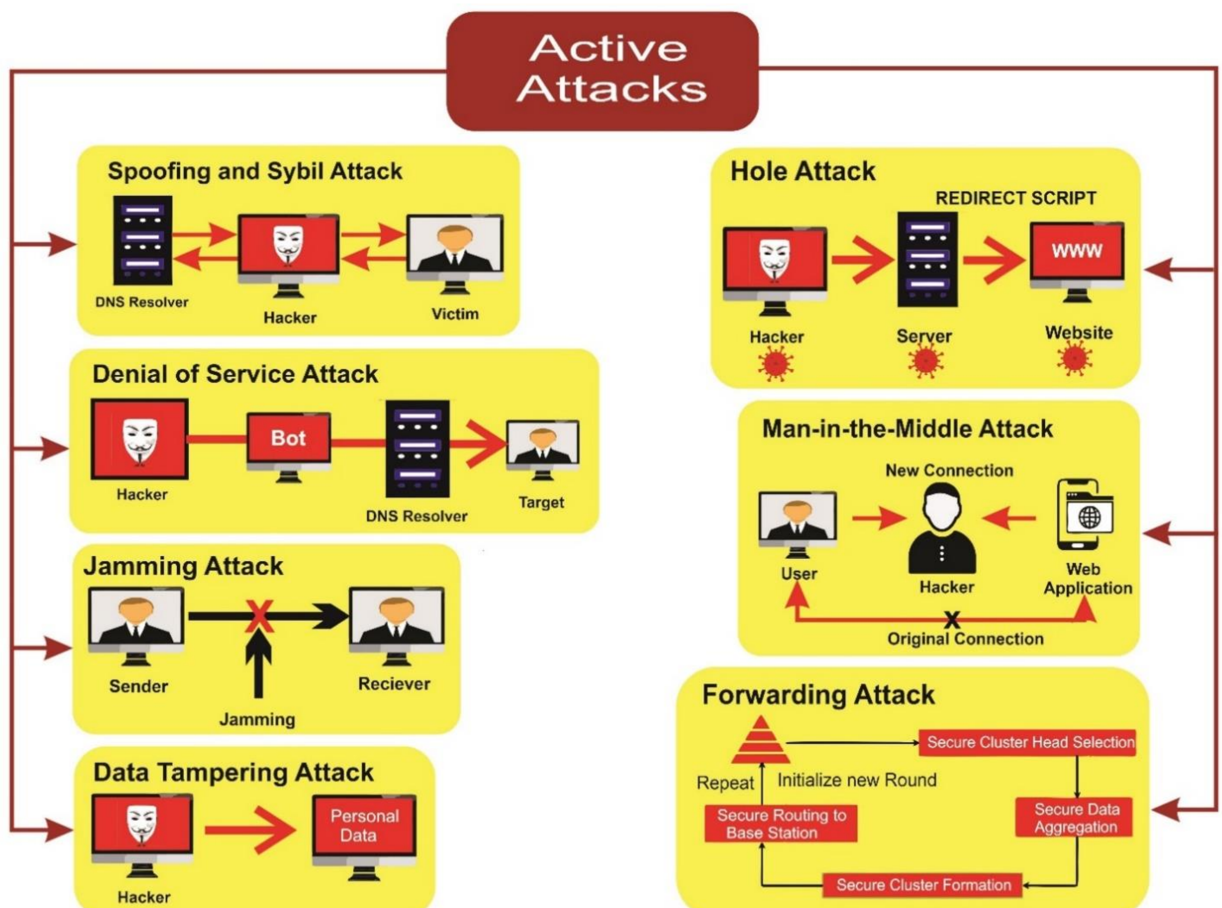

Fig. 6. Types of active attacks

5.1.7 Data Tampering Attacks

Data tampering threatens businesses, lives, and property. Companies must avoid such attacks and mitigate their harm [46].

5.2 Passive Attacks

Passive attacks capture user data without their awareness. Listening and traffic monitoring are prominent passive attack approaches [47].

- **Eavesdropping:** an attacker listens to two parties' messages. Attack works without encrypted traffic. The attacker can access unencrypted information, such as a password [48].
- **Traffic analysis:** the attacker analyses the traffic's metadata to learn about the traffic, such as the entities involved (speed, duration, etc.). Traffic analysis can lead to attacks if encrypted data is utilized, allowing an attacker to access decrypted information [49].

5.3 IoT Attacks Affect

IoT threats threaten network privacy, authentication, and authorization. Figure 6 lists the attacks and their consequences on IoT devices. When creating an IoT security protocol, consider the following.

5.3.1 Accessibility

Provides IoT device services to authorized users. DoS attacks and jamming make nonsensical requests and keep the network busy, undermining the IoT network. A solid security protocol is needed to keep IoT accessible to user clients [50].

5.3.2 Privacy

Privacy is the only IoT element attacked actively and passively. Today, secret papers, medical information, and national security data are securely encrypted and delivered over the Internet by various IoT devices. Hackers can follow the IoT computer's position and decode third-party data [51].

5.3.3 Integrity

To safeguard IoT data integrity, the recipient must verify that transferred or distributed messages have not been changed. Data integrity ensures that supplied data isn't altered. Even if intruders can't steal data, the network won't work if the susceptible nodes corrupt the delivered data. Insecure interaction channels can modify data without an attacker. Integrity check detects unintentional and purposeful message modifications [52].

5.3.4 Identification

Identification is essential for the authorization of IoT networks. Customers are required to register before they can connect to the Cloud Server. The commercialization of IoT and its resilience are both hindered by identification problems. Phishing and Sybil attacks lower the network's security level and allow unauthorized access to servers. Therefore, it's essential to find an efficient IoT system identification that offers excellent safety [53].

5.3.5 Authorization

Authorization is the user's IoT access. Authorized clients can enter, track, and use IoT data. Admins' directives are also performed. Preserving all user data and offering them information-based access is hard since users are sensors, devices, and services. Identification is IoT user authorization. Clients must register to use the cloud server. IoT trade-offs and resilience make detection challenging. Sybil and phishing attacks impair network security, and attackers get server access without proper identification. A suitable IoT system identification technique is essential to safeguard system restrictions [54]. User permission is accomplished by identification in the IoT. To utilize the cloud server, clients first need to register. The internet of things' resilience and trade-offs compound the detection challenges. Attacks such as spoofing and Sybil weaken the security of a network and make it easier for attackers to access a server without the necessary ID. When protecting system limits, having an appropriate identification method for IoT systems is vital [55].

5.4 IoT Anomaly Detection

There are unconventional real-world datasets. Identifying anomalies implies detecting unusual phenomena compared to typical nodes. Intrusion

Prevention Systems, Fraud Detection, and Data Leakage generate abnormalities. Smart cities, network security, and industries employ anomaly detection [56].

5.4.1 Detection of Intrusion

IoT devices are connected to the Internet and are nevertheless vulnerable to cyber-attacks. DoS and DDOS attacks, for example, do severe harm to the IoT network. Detecting and preventing these threats is the most challenging difficulty in IoT systems [57].

5.4.2 Detecting Fraud

During online logins or payments, IoT networks are vulnerable to intercepting credit card information, banking information, or other personal information [57].

5.4.3 Data Leakage

The disclosure of confidential information from databases, file servers, and other information sources by external entities may lead to the loss of data and jeopardize the confidentiality of the information. Such losses may be prevented using suitable encryption algorithms [56].

5.5 Anomalies Types

It can be identified as a contextual or communal point in the form [57].

5.5.1 Anomalies in Points

Anomalies are used to identify points that are considerably different from the rest of the data points when the evolution of the sequence is unexpected. Frequently used in the identification of fraud [57].

5.5.2 Anomalies in Groups

Many IoT devices exhibit typical time series patterns, such as recurring patterns or shapes. However, a joint audit and review are necessary if several delays occur in the supply chain [56].

5.5.3 Anomalies in Context

The kind of meaning of past information, such as the day of the week, is used to detect it. The circumstances practically cover the whole domain [56].

6. IOT SECURITY BASED ON MACHINE LEARNING

IoT systems must adopt a defensive posture while identifying the primary parameters in security protocols to adjust for dynamic and diverse networks as intelligent attacks and MLs become more common. This is a difficult endeavor since the IoT device's limited resources make it difficult to precisely estimate the current network and attack condition. Reinforcement learning supervised learning, and unsupervised learning are three machine learning approaches used to improve network security in the IoT. Through malware identification, downloaded anti-jamming, access control, and authentication, these strategies serve to increase security [58]. These methods are outlined below in Figure 7.

6.1 Reinforcement Learning

Deep Q networks, post-decision states, Dyna-Q, and Q-learning are examples of reinforcement learning approaches. Through trial and error, these strategies assist IoT devices in selecting security protocols and important parameters for various threats. Q-learning, for example, is utilized as a model-free approach to improve malware detection, downloaded anti-jamming, and authentication performance. Dyna-applicability Qs in malware detection and authentication can also be considered by IoT devices. Finally, malware is detected using the post-decision state [59].

6.2 Supervised Learning

Random Forest, Deep Neural Network (DNN), Neural Network, K-Nearest Neighbor (KNN), Naive Bayesian, and SVM (Support Vector Machine) are examples of supervised learning approaches [60]. To construct a classification or regression model, these approaches may be used to label application traces or network data from

IoT devices. SVM may be used by IoT devices to identify phishing attacks and network breaches, for example. A K-NN program to identify malware and network breaches may exist. Then, to identify DoS attacks and network breaches, neural networks are deployed. IoT systems may also employ naive Bayes to identify intrusions, and malware may be detected using the Random Forest Classifier [61]. Finally, DNNs may be used for phishing detection in IoT devices with enough memory and processing capability.

6.2.1 Role of Supervised Learning in IoT Security

Supervised learning approaches are led by a goal that creates a mathematical framework for datasets. This approach employs tagged data to train an algorithm that describes input data best. Inputs and outcomes are offered for learning. These datasets assist machines in discovering outputs for inputs [62]. Supervised learning performance may be achieved when particular targets are specified. For such understanding, it's vital to identify the machine's desired outputs and actual inputs [5]. It identifies rules from datasets and defines classes. Predict criteria, persons, and objects' class memberships. To identify network traffic in an IoT device, you must employ neural networks, KNN, Naive Bayes, and SVM [63]. Classification models can be used if a class or value category has few outputs. Regression can be utilized when the predicted output value is numeric. KNN can identify viruses and networks in IoT systems [64].

Supervised learning techniques use tagged data in IoT networks to solve location, security, adaptive filtering, channel estimation, and spectrum detection. This ML category uses regression and classification. Using classification, supervised learning predicts and models data sets. Regression predicts numerical variables reflecting trends [65]. Decision trees, random forest, naive Bayes, and SVM are classification algorithms. SVM utilizes a kernel to distinguish between classes. SVM models nonlinear decision boundaries. SVM naturally reflects memory intensity; therefore, choosing a kernel may be tricky. This complicates the modelling of massive datasets. IoT users prefer random forests to SVM [65]. Naive Bayes models issues like spam detection and text categorization. Random forest algorithms are naïve, and all input qualities are mutually free, making them better for simulating real-world matters [66]. Random Forest methods are readily developed and adaptable to dataset size. These algorithms demand more training time than Naive Bayes and SVM. It also improves prediction accuracy and precision in less time [66]. It's then linked to a graph with leaves and

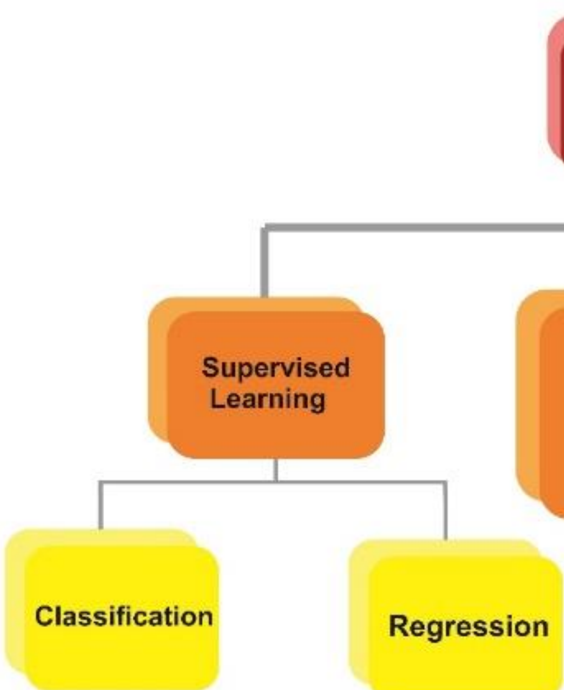

Fig.7. Machine Learning and Its Classification

branches to represent class and choice. A top-down technique traverses the tree to rate an event until a class-specific choice is made. Regression methods include logistic regression and ANN [66]. These are instance-based algorithms. These forecast fresh observations based on training data. Such methods are memory-intensive and perform poorly with substantial data sets.

6.3 Unsupervised Learning

There is no necessity for data labelling, unlike supervised learning. It examines the similarities between unlabeled data to categorize them [67]. IoT systems, for example, might use multivariate correlation analysis to identify DoS attacks. They could also enforce IGMM with PHY-based authentication with privacy protection [67]. While supervised learning focuses on document categorization in the IoT system, unsupervised learning ensures the grouping of documents in the IoT system to increase security. This is in contrast to unsupervised learning providing the set of records in the IoT system.

6.3.1 Role of Unsupervised Learning in IoT Security

Unsupervised learning trains algorithms with unlabeled data. Describing a pattern helps notice a way. If so, incoming data helps the algorithm uncover rules and patterns. Summarizing and combining key points provides meaning and clarity [68]. No output configuration. Unsupervised learning uses association and grouping methods. Clustering involves combining data sets and discovering similarities. This uses K-mean and PCA (principal component analysis). In unsupervised learning, the environment provides input without a purpose. Similarity searches may be done on untagged data. Data may be categorized. Unsupervised learning techniques handle unlabeled data heuristically. Balance loads, group cells, and identify intrusions, faults, and abnormalities. Clustering group data based on similarities and contrasts in unsupervised learning [68]. Unmonitored cluster development means no established performance procedures. Use the displayed data to assess the correctness of the results. If there's an incorrect or correct answer, dataset groupings may be pre-labelled. In this situation, classification methods are preferred. Hierarchical and K-mean clustering are prevalent [69]. K-means is a common technique for categorizing data based on geometric distinctions. Clusters must merge across centroids to become uniformly spherical.

Before clustering, define the cluster size. Clustering does not indicate competence and efficiency. Non-global clusters can cause poor clustering. Most IoT systems and applications use unsupervised learning with limited external environment knowledge. This resembles animal learning. Zero-day attacks on IoT networks are unknown [69].

7. COMPARATIVELY ANALYSIS OF ML ALGORITHMS USED FOR IDS

Table 1 shows that researchers employed ML algorithms and approaches to detect attacks and anomalies with high accuracy. In investigations [70-81], researchers utilized and compared different ML algorithms. The Random Forest (RF) method obtained the best results with 99.34 %, 99.5 %, 99.9 %, 99.59 %, and 99.9 % accuracy. DT and KNN outperformed the other methods. However, KNN takes longer to classify. In addition, combining RF and DT improved attack detection accuracy. RF and KNN obtained 99.9 % attack detection accuracy in experiments.

The evaluated study indicated that Random Forest ML provided the best attack and anomaly detection. ML is suited for IoT-specific challenges and general cybersecurity applications. ML-based systems balance IoT network risks depending on their speed and adaptability. All ML research is encouraged. ML's importance as an emerging technology is well-established.

8. IOT SECURITY LIMITATIONS OF THE ML APPROACH

Figure 8 shows the number of linked IoT devices, the worldwide IoT market, and forecast predictions through 2025. Since then, electrical and computer engineers have paid much attention to IoT development and security. Machine learning is used to safeguard IoT networks, but it has limits. Uncertainty, fluctuating speed, variety, and volume characterize IoT traffic. Traditional machine-learning approaches are not scalable enough for IoT data handling [9]. Major field modifications require a precondition. Limitations of ML in IoT networks include energy processing, and data analysis issues as shown in Figure 9.

8.1. Energy Processing

ML algorithms have a sample, computational, and memory complexity. Conventional ML algorithms aren't scalable for small tasks. Traditional ML algorithms aren't fit for resource-constrained IoT. Intelligent IoT devices need real-time data processing for applications. Traditional ML approaches can't handle real-time data streams [82-83].

8.2. Data Analysis

Communication and sensor devices and network-based information systems may generate wireless data. IoT systems value data. To extract sensitive data, do efficient analyses. IoT applications confront a severe issue in managing massive data. IoT data creation is semantical, format-, and type-diverse. Semantic and syntactic heterogeneity. These heterogeneities complicate IoT big data management [84].

9. CONCLUSION

The IoT can revolutionize the globe and solve global challenges. Thanks to innovative IoT services, everyone on the network may access, connect, and store information. While IoT improves our lives through smart gadgets that link us to the virtual world, security is a serious problem. This article reviews Machine Learning-based IoT security literature, encompassing IoT and its architecture, security risks, ML-based methods, and ML-based security solutions. This study focuses on built-in machine learning techniques for IoT security, giving an overview of threats and their implications. In addition, research has been done on machine learning algorithms to identify potential roadblocks, which may be helpful to future researchers as they

Table 1. Summary of Literature Review

Dataset	Feature Optimization Approach	Classifier	Accuracy	Reference
UCI's ML repository	Intrusion and attack detection for IoT Botnet.	SVM, Random Forest	99 %	[70]
IoT-23	ML-based detecting anomalies in IoT networks	Random Forest	99.50 %	[71]
BoT-IoT	Improving IoT Security by ML	Random Forest	99 %	[72]
NSL-KDD, DS2OS	ML Based prediction of attacks on IoT networks.	Random Forest	99.4 %	[73]
CICIDS-2017, Cyberattack	Detection of anomalous activities	Random Forest	99.9 %	[74]
IoT Network Intrusion Dataset	Enhance IoT security through ML methods on the IoT network	KNN	99 %	[75]
UCI	Detect Attacks in IoT devices	Decision Tree	99.20 %	[76]
UNSW-NB15	ML-based detection of attacks and anomalies in IoT	Random Forest + KNN	99 %	[77]
KDDCUP99	Improve the security IDS	KNN, Decision Tree	99.9 %	[78]
IoT-23	Anomaly Detections in IoT Networks.	Random Forest	99.50 %	[79]
UNSW-NB 15	Attack Detection in IoT Networks	Random Forest	99.5 %	[80]
Bot-IoT	Detecting IoT attacks	Random Forest	97.00 %	[81]

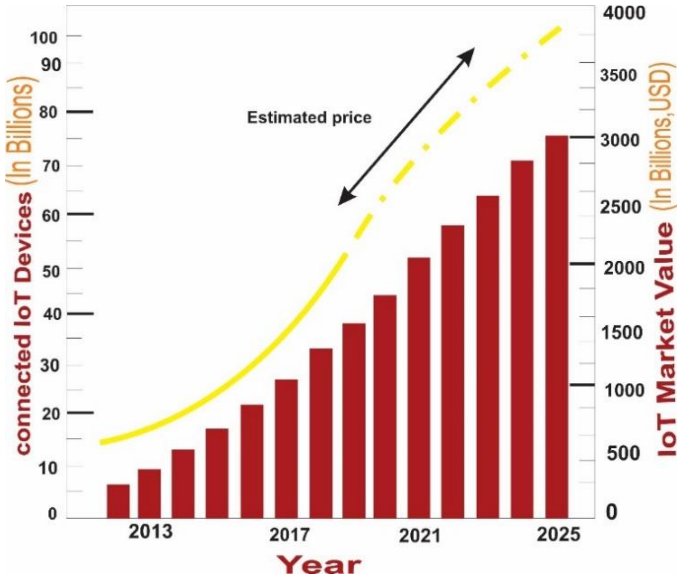

Fig. 8. Total Connected IoT Devices, Global IoT Market, and Future Forecast

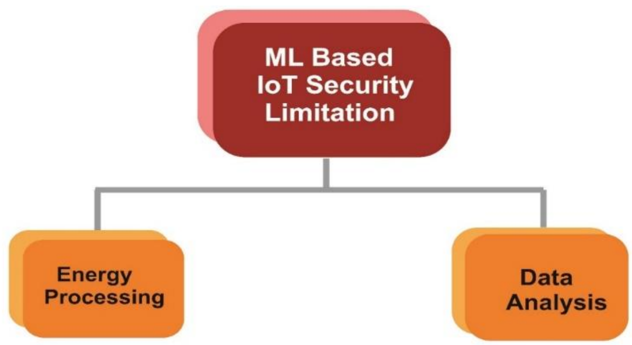

Fig. 9. Machine Learning-Based IoT Security Limitations

choose their ultimate goals.

10. ACKNOWLEDGEMENTS

The authors would like to thank the referees for their careful reading and for their comments, which significantly improved the paper. Additionally, thanks to Dr. Salman Qadri, (Associate Professor, Chairman Department of Computer Science, MNS University of Agriculture, Multan, Pakistan) and Dr. Farrukh Jamal, (Assistant Professor, Department of Statistics, The Islamia University of Bahawalpur, Pakistan) for his motivational support.

11. CONFLICT OF INTEREST

The authors declare no conflict of interest.

12. REFERENCES

1. S.T. Arzo, C. Naiga, F. Granelli, R. Bassoli, M. DevetsikIoTis, and F.H. Fitzek. A Theoretical Discussion and Survey of Network Automation for IoT: Challenges and Opportunity. *IEEE Internet of Things Journal* 8(15):12021-12045(2021).
2. D. Desai, and H. Upadhyay. Security and privacy consideration for internet of things in smart home environments. *International Journal of Engineering Research and Development* 10(11):73-83(2014).
3. M. Boland, F. Alam, and J. Bronlund. Modern technologies for personalized nutrition. *Trends in Personalized Nutrition* 195-222(2019).
4. R. Karthick, A.M. Prabaharan, and P. Selvaprasanth. Internet of things based high security border surveillance strategy. *Asian Journal of Applied Science and Technology* (AJAST) (3):94-100(2019).

5. T. Alam. IBchain: Internet of things and blockchain integration approach for secure communication in smart cities. *Informatica* 45(3)1-14(2021).
6. V. Chang, L. Golightly, P. Modesti, Q.A. Xu, L.M.T. Doan, K. Hall, ... and A. Kobusińska. A Survey on Intrusion Detection Systems for Fog and Cloud Computing. *Future Internet* 14(3):89(2022).
7. C. Butpheng, K.H. Yeh, and H. Xiong. Security and privacy in IoT-cloud-based e-health systems—A comprehensive review. *Symmetry* 12(7):1191(2020).
8. D. Ageyev, T. Radivilova, and O. Mohammed. Traffic Monitoring and Abnormality Detection Methods Analysis. IEEE International Conference on Problems of Infocommunications. *Science and Technology* (PIC SandT) 823-826(2020).
9. H.A. Abdul-Ghani, and D. Konstantas. A comprehensive study of security and privacy guidelines, threats, and countermeasures: An IoT perspective. *Journal of Sensor and Actuator Networks* 8(2):22(2019).
10. A. Abeshu, and N. Chilamkurti. Deep learning: the frontier for distributed attack detection in fog-to-things computing. *IEEE Communications Magazine* 56(2): 169-175(2018).
11. S. Shamshirband, M. Fathi, A.T. Chronopoulos, A. Montieri, F. Palumbo, and A. Pescapè. Computational intelligence intrusion detection techniques in mobile cloud computing environments: Review, taxonomy, and open research issues. *Journal of Information Security and Applications* 55:102582(2020).
12. P.R. Kumar, J.S. Raj, and S. Smys. Analysis of dynamic topology wireless sensor networks for the Internet of Things (IOT). *International Journal of Communication Systems* 34(17):315(2021).
13. I. Alrashdi, A. Alqazzaz, E. Aloufi, R. Alharthi, M. Zohdy, and H. Ming. Ad-IoT: Anomaly detection of IoT cyberattacks in smart city using machine learning. In *2019 IEEE 9th Annual Computing and Communication Workshop and Conference (CCWC)* 0305-0310(2019).
14. S.V.N. Santhosh Kumar, M. Selvi, and A. Kannan. A Comprehensive Survey on Machine Learning-Based Intrusion Detection Systems for Secure Communication in Internet of Things. *Computational Intelligence and Neuroscience* (2023).
15. W. Li, Y. Chai, F. Khan, S.R.U. Jan, S. Verma, V.G. Menon, and X. Li. A comprehensive survey on machine learning-based big data analytics for IoT-enabled smart healthcare system. *Mobile networks and applications* 26:234-252(2021).
16. H. Mliki, A.H. Kaceam, and L. Chaari. A comprehensive survey on intrusion detection-based machine learning for IOT networks. *EAI Endorsed Transactions on Security and Safety* 8(29):e3-e3(2021).
17. M. Imran, U. Zaman, J. Imtiaz, M. Fayaz, and J. Gwak. Comprehensive survey of IoT, machine learning, and blockchain for health care applications: A topical assessment for pandemic preparedness, challenges, and solutions. *Electronics* 10(20):2501(2021).
18. A. Gaurav, B.B. Gupta, and P.K. Panigrahi. A comprehensive survey on machine learning approaches for malware detection in IoT-based enterprise information system. *Enterprise Information Systems* 1-25(2022).
19. M. Zubair, A. Ali, S. Naeem, S. Anam. Traffic Video-Based Parking and Abandoned Object Event Detection. *Proceedings of the MOL2NET'22, Conference on Molecular, Biomedical and Computational Sciences and Engineering 8th ed.* 1–15(2023).
20. M. Zubair, A. Ali, S. Naeem, S. Anam, Image Processing Algorithm. P*roceedings of the MOL2NET'22, Conference on Molecular, Biomedical and Computational Sciences and Engineering 8th ed.* 1–15(2023).
21. M. Zubair, A. Ali, S. Anam. A DDDAS-Based Impact Area Simulation Study of Highway Abnormalities. *Proceedings of the MOL2NET'22, Conference on Molecular, Biomedical and Computational Sciences and Engineering 8th ed*. 1–15(2023).
22. M. Zubair, A. Ali, S. Naeem, S. Anam, Video Streams for The Detection of Thrown Objects from Expressways. P*roceedings of the MOL2NET'22, Conference on Molecular, Biomedical and Computational Sciences and Engineering 8th ed.* 1–15(2023).
23. A. Tewari, and B.B. Gupta. Security, privacy and trust of different layers in Internet-of-Things (IoTs) framework. *Future generation computer systems* 108: 909-920(2020).
24. S. Rekha, L. Thirupathi, S. Renikunta, and R. Gangula. Study of security issues and solutions in Internet of Things (IoT). *Materials Today: Proceedings* (2021).
25. H. HaddadPajouh, A. Dehghantanha, R.M. Parizi, M. Aledhari, and H. Karimipour. A survey on internet of things security: Requirements, challenges, and solutions. Internet of Things 14:100129(2021).
26. W.Z. Khan, M.H. Rehman, H.M. Zangoti, M.K.

Afzal, N. Armi, and K. Salah. Industrial internet of things: Recent advances, enabling technologies and open challenges. *Computers and Electrical Engineering* 81: 106522(2020).

27. M. Noura, M. Atiquzzaman, and M. Gaedke. Interoperability in internet of things: Taxonomies and open challenges. *Mobile networks and applications* 24(3):796-809(2019).
28. M. Lombardi, F. Pascale, and D. Santaniello. Internet of things: A general overview between architectures, protocols and applications. *Information* 12(2):87(2021).
29. M. Jangjou, and M.K. Sohrabi. A Comprehensive Survey on Security Challenges in Different Network Layers in Cloud Computing. *Archives of Computational Methods in Engineering* 1-22(2022).
30. D. Oliveira, M. Costa, S. Pinto, and T. Gomes. The future of low-end motes in the Internet of Things: A prospective paper. *Electronics* 9(1):111(2020).
31. Z. Shouran, A. Ashari, and T. Priyambodo. Internet of things (IoT) of smart home: privacy and security. *International Journal of Computer Applications* 182(39):3-8(2019).
32. L. Da Xu, Y. Lu, and L. Li. Embedding blockchain technology into IoT for security: A survey. *IEEE Internet of Things Journal* 8(13):10452-10473(2021).
33. G. Han, H. Wang, X. Miao, L. Liu, J. Jiang, and Y. Peng. A dynamic multipath scheme for protecting source-location privacy using multiple sinks in WSNs intended for IIoT. *IEEE Transactions on Industrial Informatics* 16(8):5527-5538(2019).
34. M.Z. Gunduz, and R. Das. Cyber-security on smart grid: Threats and potential solutions. *Computer networks* 169:107094(2020).
35. M. Arulprakash, and R. Jebakumar. People-centric collective intelligence: decentralized and enhanced privacy mobile crowd sensing based on blockchain. *The Journal of Supercomputing* 77(11):12582-12608(2021).
36. K. Kimani, V. Oduol, and K. Langat. Cyber security challenges for IoT-based smart grid networks. *International Journal of Critical Infrastructure Protection* 25:36-49(2019).
37. D.A.S. Resul, and M.Z. Gündüz. Analysis of cyberattacks in IoT-based critical infrastructures. *International Journal of Information Security Science* 8(4):122-133(2020).
38. C. Silpa, G. Niranjana, and K. Ramani. Securing Data from Active Attacks in IoT: An Extensive Study. In Proceedings of International Conference on Deep Learning, Computing and Intelligence, *Springer* 51-64(2022).
39. N.F. Syed, Z. Baig, A. Ibrahim, and C. Valli. Denial of service attack detection through machine learning for the IoT. *Journal of Information and Telecommunication* 4(4):482-503(2020).
40. Y. Tian, S. Chen, and L. Zhang. Unsupervised Detection of Sybil Attack in Wireless Networks. In *IOP Conference Series: Earth and Environmental Science* 693(1):012114(2021).
41. H. Pirayesh, and H. Zeng. Jamming attacks and anti-jamming strategies in wireless networks: A comprehensive survey. *IEEE Communications Surveys and Tutorials* (2022).
42. M. Thankappan, H. Rifà-Pous, and C. Garrigues. Multi-Channel Man-in-the-Middle Attacks Against Protected Wi-Fi Networks: A State-of-the-Art Review. *preprint arXiv*:2203.00579(2022).
43. A. Ali, S. Naeem, S. Anam, M. Zubair. Agile Software Development Processes Implementing Issues and Challenges with Scrum. P*roceedings of the MOL2NET'22, Conference on Molecular, Biomedical and Computational Sciences and Engineering 8th ed.* 1–15(2023).
44. A. TsIoTa, D. Xenakis, N. Passas, and L. Merakos. On jamming and black hole attacks in heterogeneous wireless networks. I*EEE Transactions on Vehicular Technology* 68(11):10761-10774(2019).
45. D. W. Huang, W. Liu, and J. Bi. Data tampering attacks diagnosis in dynamic wireless sensor networks. *Computer Communications* 172:84-92(2021).
46. K. Guha, S. Saha, and A. Chakrabarti. Bypassing Passive Attacks. In Self Aware Security for Real Time Task Schedules in Reconfigurable Hardware Platforms *Springer* 91-110(2021).
47. D. K. Jasim, and S. B. Sadkhan. The Eavesdropping Attack on Security tradeoff for Cognitive Radio Networks. In *2021 4th International Iraqi Conference on Engineering Technology and Their Applications (IICETA)* 223-229(2021).
48. L. Basyoni, N. Fetais, A. Erbad, A. Mohamed, and M. Guizani. Traffic analysis attacks on Tor: a survey. In *2020 IEEE International Conference on Informatics, IoT, and Enabling Technologies (ICIoT)* 183-188(2020).
49. P. K. Jena, S. Ghosh, and E. Koley, Design of a coordinated cyber-physical attack in IoT based smart grid under limited intruder accessibility. *International Journal of Critical Infrastructure Protection* 35:100484(2021).

50. M. M. Ogonji, G. Okeyo, and J. M. Wafula, A survey on privacy and security of Internet of Things. *Computer Science Review* 38:100312(2020).
51. H. Xu, W. Yu, X. Liu, D. Griffith, and N. Golmie. On data integrity attacks against industrial Internet of Things. In *2020 IEEE Intl Conf on Dependable, Autonomic and Secure Computing, Intl Conf on Pervasive Intelligence and Computing, Intl Conf on Cloud and Big Data Computing, Intl Conf on Cyber Science and Technology Congress (DASC/PiCom/CBDCom/CyberSciTech)* 21-28(2020).
52. S. Rizvi, R. J. Orr, A. Cox, P. Ashokkumar, and M.R. Rizvi. Identifying the attack surface for IoT network. *Internet of Things* 9:100162(2020).
53. Y. Zhao, J. Yang, Y. Bao, and H. Song. Trustworthy authorization method for security in Industrial Internet of Things. *Ad Hoc Networks* 121:102607(2021).
54. M.A. Ferrag, L. Maglaras, and A. Derhab. Authentication and authorization for mobile IoT devices using biofeatures: Recent advances and future trends. *Security and Communication Networks* (2019).
55. I. Alrashdi, A. Alqazzaz, E. Aloufi, R. Alharthi, M. Zohdy, and H. Ming. Ad-IoT: Anomaly detection of IoT cyberattacks in smart city using machine learning. In *2019 IEEE 9th Annual Computing and Communication Workshop and Conference (CCWC)* 0305-0310(2019).
56. A.A. Cook, G. Mısırlı, and Z. Fan. Anomaly detection for IoT time-series data: A survey. *IEEE Internet of Things Journal* 7(7):6481-6494(2019).
57. I.H. Sarker, A.I. Khan, Y.B. Abushark, and F. Alsolami. Internet of things (IoT) security intelligence: a comprehensive overview, machine learning solutions and research directions. *Mobile Networks and Applications* 1-17(2022).
58. A. Uprety, and D.B. Rawat. Reinforcement learning for IoT security: A comprehensive survey. IEEE Internet of Things Journal 8(11):8693-8706(2020).
59. V. Vijayalakshmi, and K. Venkatachalapathy. Comparison of predicting student's performance using machine learning algorithms. *International Journal of Intelligent Systems and Applications* 11(12):34(2019).
60. E. Toch, B. Lerner, E. Ben-Zion, and I. Ben-Gal. Analyzing large-scale human mobility data: a survey of machine learning methods and applications. *Knowledge and Information Systems* 58(3):501-523(2019).
61. F. Zantalis, G. Koulouras, S. Karabetsos, and D. Kandris. A review of machine learning and IoT in smart transportation. *Future Internet* 11(4):94(2019).
62. P. Linardatos, V. Papastefanopoulos, and S. Kotsiantis. Explainable ai: A review of machine learning interpretability methods. *Entropy* 23(1):18(2020).
63. A. Aldahiri, B. Alrashed, and W. Hussain. Trends in using IoT with machine learning in health prediction system. *Forecasting* 3(1):181-206(2021).
64. Y. Liu, J. Wang, J. Li, S. Niu, and H. Song. Machine Learning for the Detection and Identification of Internet of Things Devices: A Survey. *IEEE Internet of Things Journal* 9(1):298-320(2021).
65. E.G. Dada, J.S. Bassi, H. Chiroma, A.O. Adetunmbi, and O.E. Ajibuwa. Machine learning for email spam filtering: review, approaches and open research problems. *Heliyon* 5(6):e01802(2019).
66. G. Casolla, S. Cuomo, V.S. Di Cola, and F. Piccialli. Exploring unsupervised learning techniques for the Internet of Things. *IEEE Transactions on Industrial Informatics* 16(4):2621-2628(2019).
67. T.T. Nguyen, P. Krishnakumari, S.C. Calvert, H.L. Vu, and H. Van Lint. Feature extraction and clustering analysis of highway congestion. *Transportation Research Part C: Emerging Technologies* 100:238-258(2019).
68. H. Yang, R. Zeng, F. Wang, G. Xu, and J. Zhang. An unsupervised learning-based network threat situation assessment model for Internet of Things. *Security and Communication Networks* (2020).
69. S. Bagui, X. Wang, X. Wang, and S. Bagui. Machine learning based intrusion detection for IoT botnet. *International Journal of Machine Learning and Computing* 11(6):399-406(2021).
70. S.H. Haji, and S.Y. Ameen. Attack and anomaly detection in IoT networks using machine learning techniques: A review. *Asian journal of research in computer science* 9(2):30-46(2021).
71. T. Wang, M. Z. A. Bhuiyan, G. Wang, L. Qi, J. Wu, and T. Hayajneh. Preserving balance between privacy and data integrity in edge-assisted Internet of Things. *IEEE Internet of Things Journal* 7(4):2679-2689(2019).
72. A. Batool, B. N. Hashmi, A. Ali, S. Naeem, S. Anam. IoT based smart mirror. Proceedings of the MOL2NET'22, Conference on Molecular, *Biomedical and Computational Sciences and Engineering 8th ed.* 1–15 (2023).
73. N. Elmrabit, F. Zhou, F. Li, and H. Zhou. Evaluation of machine learning algorithms for anomaly detection. In *2020 International Conference on*

Cyber Security and Protection of Digital Services (Cyber Security) 1-8 (2020).
74. Z. Liu, N. Thapa, A. Shaver, K. Roy, X. Yuan, and S. Khorsandroo. Anomaly detection on IoT network intrusion using machine learning. In *2020 International Conference on Artificial Intelligence, Big Data, Computing and Data Communication Systems (icABCD)* 1-5(2020).
75. M.H. Aysa, A.A. Ibrahim, and A.H. Mohammed. IoT ddos attack detection using machine learning. In *2020 4th International Symposium on Multidisciplinary Studies and Innovative Technologies (ISMSIT)* 1-7(2020).
76. A. Batool, B. N. Hashmi, A. Ali, S. Naeem, M. H. Bukhari, M. M. Khan. The Smart Cradle System Basis on Internet of Things. *Proceedings of the MOL2NET'22, Conference on Molecular, Biomedical and Computational Sciences and Engineering 8th ed.* 1–15(2023).
77. D. Rani, and N.C. Kaushal. Supervised machine learning based network intrusion detection system for Internet of Things. In *2020 11th International Conference on Computing, Communication and Networking Technologies* (ICCCNT) 1-7(2020).
78. A. Ali, S. Naeem, S. Anam, and M.M. Ahmed. Entropy in Information Theory from Many Perspectives and Various Mathematical Models. *Journal of Applied and Emerging Sciences* 12(2):158-167(2022).
79. I. Alrashdi, A. Alqazzaz, E. Aloufi, R. Alharthi, M. Zohdy, and H. Ming. Ad-IoT: Anomaly detection of IoT cyberattacks in smart city using machine learning. In *2019 IEEE 9th Annual Computing and Communication Workshop and Conference (CCWC)* 0305-0310(2019).
80. J. Alsamiri, and K. Alsubhi. Internet of things cyber-attacks detection using machine learning. *International Journal of Advanced Computer Science and Applications* 10(12):232(2019).
81. S. Naeem, and A. Ali. Bees Algorithm Based Solution of Non-Convex Dynamic Power Dispatch Issues in Thermal Units. *Journal of Applied and Emerging Sciences* 12(1):35(2022).
82. A. Ali, and S. Naeem. The Controller Parameter Optimization for Nonlinear Systems Using Particle Swarm Optimization and Genetic Algorithm. *Journal of Applied and Emerging Sciences* 12(1):56(2022).
83. A. Bhargava, G. Salunkhe, S. Bhargava, and P. Goswami. A Comprehensive Study of IoT Security Risks in Building a Secure Smart City. *Digital Cities Roadmap: IoT-Based Architecture and Sustainable Buildings,* 401-448(2021).
84. D. Li, L. Deng, M. Lee, and H. Wang. IoT data feature extraction and intrusion detection system for smart cities based on deep migration learning. *International journal of information management* 49:533-545(2019).

Proceedings of the Pakistan Academy of Sciences: A Physical and Computational Sciences 59(3): 17-25 (2022)

ISSN (Print): 2518-4245; ISSN (Online): 2518-4253
https://doi.org/10.53560/PPASA(59-3)778

Pakistan Academy of Sciences

Research Article

Fractional Order Modeling of PWR Pressurizer Dynamics and Fractional Order Nonlinear H_∞ Controllers Design in LabVIEW

Arshad Habib Malik[1*], Aftab Ahmad Memon[2], Feroza Arshad[3], and Mehwish Shaikh[4]

[1]Department of Basic Training, Chashma Centre of Nuclear Training, Pakistan Atomic Energy Commission, Chashma, Pakistan
[2]Department of Telecommunication Engineering, Mehran University of Engineering and Technology, Jamshoro, Pakistan
[3]Department of Information System, Karachi Nuclear Power Generating Station, Pakistan Atomic Energy Commission, Karachi, Pakistan
[4]Department of Software Engineering, Mehran University of Engineering and Technology, Jamshoro, Pakistan

Abstract: The novel fractional order intelligent transient dynamics and advanced fractional order nonlinear robust control synthesis scheme of the Pressurized Water Reactor (PWR) pressurizer are addressed in this research work. The Graphical User Interface (GUI) is designed for closed-loop model-based PWR pressurizer dynamical studies in LabVIEW. Based on the demand for power, the reactor power and turbine power are predicted using a fractional order backpropagation algorithm in an open loop configuration. Using turbine power and heater power as input variables, pressurizer level, pressurizer pressure and coolant average temperature as output variables, the open loop multi-input multi-output (MIMO) dynamic model of pressurizer is estimated using fractional order artificial intelligence in LabVIEW. Four fractional order robust nonlinear H_∞ sub-controllers are designed for charging flow, spray flow, proportional heaters power and backup heaters power. All the dynamic controller models are in fractional order nonlinear H∞ framework and are designed in LabVIEW. The performance of the proposed design work is evaluated in closed loop configuration at 100 %, 75 % and 15 % in steady state conditions. Dynamic transient analysis is performed from 100 % to 90 % power reduction scenario and found satisfactory and within design limits and robust bounds.

Keywords: Fractional Order, Neural Estimation, PWR Pressurizer, Robust Controller, LabVIEW

1. INTRODUCTION

In this research work, the Pressurized Water Reactor (PWR)-type nuclear power plant of 340 MWe rating, operating in Pakistan is considered for closed-loop dynamic modeling and control design purposes. A non-equilibrium three-region analytical transient model of PWR pressurizer is developed by Baek *et al*. [1]. An analytical pressurizer model for 1a 200 MWe VVER type nuclear power plant is addressed by Sheta *et al*. [2] for simulation purposes. The dynamics of the 1200 MWe VVER pressurizer is investigated in detail using Modelica software by Rabie *et al.* [3] for parametric studies. A 300 MWe PWR is adopted by Takasuo *et al*. [4] for the analytical modeling of the pressurizer pressure system. A nuclear codes-based approach is considered by Xu *et al.* [5] which was implemented for PWR pressurizer dynamic modeling using APROS and TRACE nuclear codes. A VVER pressurizer model is identified using the system identification technique by Varga *et al*. [6] for data-driven modeling. PWR pressurizer insurge characteristics is modeled by Lin *et al.* [7] in 3D using transient analysis for the time-dependent studies. Sensitivity analysis of VVER 1000 PWR pressurizer level is performed by Groudev *et al.* [8]. PWR simulator is developed by Suryabrata *et al.* [9]

Received: June 2022; Accepted: September 2022
*Corresponding author: Arshad Habib Malik <engr.dr.arshad.habib.malik@gmail.com>

in MATLAB using linearized state space modeling for controller design purposes. A conventional permissive and interlocks-based PWR pressure control module is developed by Yu *et al*. [10] for condition-based logics developed using MATLAB. PID controller-based pressurizer pressure controller is designed by Zhang *et al*. [11] for closed loop model development for 900 MWe PWR nuclear power plant. A similar approach is adopted by Sheta *et al*. [12] for 1350 MWe PWR pressurizer pressure and level controllers using the PID algorithm. A fuzzy PID controller is designed by Victor *et al*. [13] for a PWR pressurizer for gray control synthesis and compared with PID controller performance. A fuzzy logic controller is synthesized by Victor *et al*.[14] for PWR pressurizer in detail using rule-based approach. A fuzzy PID controller is adopted by Sheta *et al*. [15] for VVER 1200 pressurizer. The fractional order PID controller is designed by Damayanti *et al*. [16] for the PWR pressurizer level controller which is different from pressure control logic. Fractional order neural transient modeling of the primary circuit of ACP1000 based nuclear power plant is carried out by Malik *et al*. [17] in LabVIEW for a generation-3 nuclear power plant. A fractional order nonlinear H_∞ controller is designed by Xue *et al*. [18] for the self-balancing system in dynamic mode. Such study is extended for advanced fractional order controllers design using artificial intelligence for PWR pressurizer dynamics. Finite-time synchronization of fractional order memristor-based neural networks with time delays are addressed by Velmurugan *et al*. [19] which is a class of fractional neural network.

In this research work, the new coupled pressurizer pressure and level dynamics are estimated using state-of-the-art fractional order intelligent neural network algorithm in LabVIEW.

Four new controllers are configured for charging flow control, spray control, proportional heaters power control and backup heaters power control using novel fractional order nonlinear H∞ control framework using intelligent control design algorithm in most modern graphical programming environments using LabVIEW. LabVIEW has been selected as a programming platform because it has a more powerful GUI than visual basic and MATLAB. Further, LabVIEW is a totally graphical programming environment with excellent and improved data flow and function control.

2. MATERIALS AND METHODS

2.1. PWR Pressurizer

The pressurizer is the main equipment of the reactor heat removal system in PWR and is used to regulate the pressure of the reactor coolant. The main function of the primary heat transport system is to remove heat from the reactor core to the steam generator. The primary loop consists of two loops designated as loop-A and loop-B. In the primary loop, there are two steam generators, one pressurizer, one reactor coolant pump and a piping structure. There are two loops in the primary system to accommodate two steam generators. So, the single loop cannot be used to achieve the dynamics of two steam generators.

The reactor coolant pressure is controlled by the pressurizer to prevent departure from nucleate boiling (DNB), which has adverse effects on heat transfer. Single pressurizer is used for two loop primary system so that the system pressure can be maintained at a single pressure else more pressurizers will try to create differential pressure in the primary circuit that will result in flow disturbance.

The reactor coolant pressure control is carried out by the action of electric heaters and spray valves. The spray system is fed from two cold legs and is connected to the pressurizer through the spray nozzle. A small continuous spray flow is provided through the flow-regulating valve. The electric heaters are installed at the bottom head of the pressurizer. Over-pressure protection is provided by two pressurizer safety valves and two pressurizer relief valves connected to the pressurizer.

The discharge of pressurizer safety and relief valves are joined to the relief header and then routed to the pressurizer relief tank. The relief tank also collects leak-off and discharges from valves of some other systems located inside the containment. The pressurizer relief tank is blanketed by nitrogen inside and equipped with an internal spray for cooling.

The pressurizer is a vertical, cylindrical vessel with hemispherical top and bottom heads. Electrical heaters are installed vertically in the bottom head. The surge line nozzle is located in the center of the bottom head, at the lowest point of the pressurizer. This surge line is connected at its other end to the Loop B hot leg. A retaining screen is located just above the inlet of the surge line to mix the surged water with the water contained in the pressurizer and to prevent the entrance of foreign matters into the reactor coolant system.

The top head receives the spray line nozzle and the pressurizer relief and safety valve nozzles. Spraying of cold water from the cold legs of the reactor coolant piping is achieved in a fog state through a spray nozzle located at the end of the spray line inside the pressurizer. Thus the spraying can be better mixed with the saturated steam in the pressurizer to achieve a better cooling effect and reduce the pressure of the pressurizer.

The pressurizer is used to accommodate positive and negative surges caused by load transient. During an insurge, the spray system condenses steam in the pressurizer to prevent the pressurizer pressure from reaching the set point of the relief valve. During an out surge, the flashing of water and generation of steam by automatic actuation of the electrical heaters keep the pressure of the pressurizer above low-pressure reactor trip set point. The pressurizer is designed to accommodate in and out surges caused by load transients. It provides a point in the reactor coolant system (SRC) system where liquid and vapor can be maintained in equilibrium under saturated conditions for pressure control purposes. Since there are continuous process pressure fluctuations in the reactor coolant system. So, spray flow is continuous which provides minor flow while heater logic is used to compensate spray flow.

2.2 Pressurizer Pressure and Level Control System

The pressurizer spray lines and valves are designed to provide the necessary spray rate selected to prevent the pressurizer pressure from reaching the opening set point of the pressurizer relief valve following a step-load reduction of the 10% of full load. The pressurizer spray is controlled by two automatically controlled, air-operated downstream of the spay valves to the spray line. The auxiliary spray path is used to provide auxiliary spray during reactor cool down when the reactor coolant pumps are out of service.

The pressurizer is equipped with 90 electric heaters in which 30 elements are proportional heaters, while the other 60 elements are reserved heaters. The heaters are direct immersion straight tubular sheath type. The tubular sheath is sealed at its upper end by a welded plug and at its lower end by a connection socket which remains leak proof even in the event of sheath failure. The heater, made of nickel-chrome alloy, is isolated from the sheath by compacted, magnesium oxide. The pressurizer electrical heater capacity is designed to heat the pressurizer water at the average rate of 45 0C / h taking into account the continuous spray flow rate. The conventional pressurizer pressure and level control system consist of modules which are designed based pressurizer pressure and level interlocks [1].

2.3 Fractional Order Pressurizer Control System

The fractional order pressurizer closed-loop control system consists of fractional order pressure intelligent modeling and four coupled fractional order controllers. Fractional order pressurizer intelligent modeling consists of coupled pressure and level dynamics of pressurizer while four fractional order advanced controllers are designed for charging flow control, pressurizer spray control, proportional heaters power control and back-up heaters power control as in Figure1.

Total heater power is the sum of proportional heaters power and backup heaters power. Proportional heaters work all the time in minor transients of spray flow while backup heaters work when 100 % proportional heater are used in transients [1].

2.4 Fractional Order Pressurizer Intelligent Modeling

2.4.1 Selection of Input and Output Variables

One pair of demanded power and turbine power is used as the first single input single output fractional-order neural network (FO-SISO-ANN1) while the

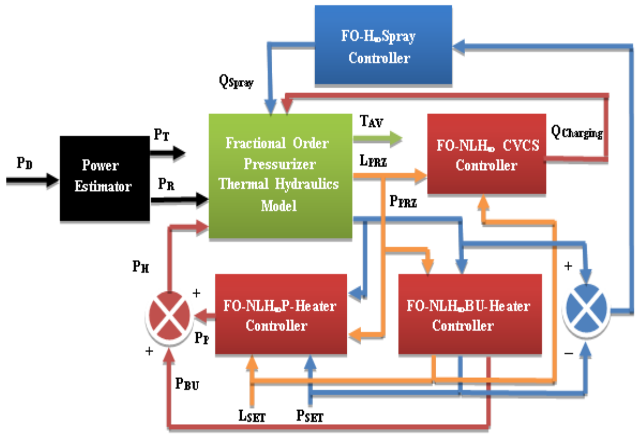

Fig. 1. Proposed closed loop pressurizer pressure and level control system.

second pair of demanded power and reactor power is used as the second single input single output fractional-order neural network (FO-SISO-ANN2). Third multi-input multi-output fractional-order neural network (FO-MIMO-ANN3) is comprised of reactor power and heater power as inputs while coolant average temperature, pressurizer pressure and pressurizer level as outputs.

2.4.2 Choice of Modeling Algorithm

In this research work, all three FO-SISO-ANN1, FO-SISO-ANN2 and FO-MIMO-ANN3 are modeled using the model developed in [17] for the new and modified formulation of the proposed work.

The output of FO-SISO-ANN1 is given as:

$$\widehat{P}_T(t_k) = \Delta_k^\alpha f\left[\sum_{n_q=1}^{q} w_{nq,nr}^{[1]} \Delta_k^\alpha f\left(\sum_{n_p=1}^{1} w_{np,nq} P_{Dn_p}^{[1]}(k)\right)\right]$$

The output of FO-SISO-ANN2 is given as:

$$\widehat{P}_R(t_k) = \Delta_k^\alpha f\left[\sum_{n_q=1}^{q} w_{nq,nr}^{[1]} \Delta_k^\alpha f\left(\sum_{n_p=1}^{1} w_{np,nq} P_{Dn_p}^{[1]}(k)\right)\right]$$

The output of FO-MIMO-ANN3 is given as:

$$\widehat{Y}_{n_r}(t_k) = \Delta_k^\alpha f\left[\sum_{n_q=1}^{q} w_{nq,nr}^{i} \Delta_k^\alpha f\left(\sum_{n_p=1}^{4} w_{np,nq} u_{n_p}^{i}(k)\right)\right]$$

Where symbols having their usual meanings.

2.5 Fractional Order Nonlinear Robust Controller

2.5.1 Problem Formulation

Since spray and heater are highly disturbing parameters. So, a robust H∞ framework is required for the pressurizer circuit.

If t = kT_s where T_s is the sample time and assuming v = 1,2,3,…..,n, z = 1,2,3,…..,n such that z_v, $A_z(.)$, $yc(t)$, $u_v(t)$, $d_v(t)$ and w_{vz} are positive constants, the nonlinear activation function of v-th neuron, controlled system output, control input of v-th neuron, unknown disturbance and memristive weights respectively, then controlled output of closed-loop control system in the continuous time domain is given as using [19]:

$$D_t^\alpha y_c(t) = -z_v y_c^v(t) + \sum_{z=1}^{n} w_{vz} y_c^z(t) A_z(y_c^z(t)) + u_v(t) \quad (4)$$

The performance index of fractional order nonlinear robust controller is given as:

$$\left\|T_{NLH_\infty}(s)\right\|_\infty < \gamma = \left(\frac{\sum_{v=1}^{n} e_v(t)^2}{\sum_{v=1}^{n} d_v(t)^2}\right) \quad (5)$$

Since there are four H∞ controllers for the pressurizer circuit, so there are four control design parameters (y_1, y_2, y_3 and y_4).

2.5.2 Configuration of Sub-Controllers

The charging flow controller is configured using pressurizer level dynamics. The spray controller is configured using pressurizer pressure dynamics. The proportional heaters power controller and backup heaters power controller are configured using pressurizer pressure and level dynamics using formulation developed in equations (4) and (5). All the four controllers work together in a parallel computing scheme using artificial intelligence.

3. RESULTS AND DISCUSSION

3.1 Development of Pressurizer and Control Flow Models in LabVIEW

All the modeling, analysis and simulation work is carried out in LabVIEW. The two-loop primary circuit process flow is shown in Figure 2. The PWR pressurizer pressure and level control flow diagram is shown in Figure 3.

3.2 Steady State and Transient Analysis of Closed Loop Simulation Model in LabVIEW

The dynamic closed loop of the pressurizer system is initialized at 100 % demanded power. In response to the initialization of the model and controllers at 100 % power, trends of various parameters of interest are simulated and tested at 100 % power condition of the plant as shown in Figure 5.

Now, the reactor power is reduced from 100 % power level to 75 % power level and trends of various parameters of interest are simulated for this power reduction transient condition and tested at 100% power condition as shown in Figure 6 and Figure 7.

The simulation shows that backup heaters are turned on in this simulation experiment as indicated by the red color.

Now, another large power transient is tested in which the reactor power is reduced from 100 % power level to 15 % power level and the simulation shows that proportional heaters are turned on in this simulation experiment as indicated by the red color as shown in Figure 8.

Now, in order to assess the parametric dynamic behavior of various parameters, the power transient is simulated, tested and visualized in which the reactor power is reduced from 100 % power level to 90 % power level and various parameters are analyzed on different time intervals as shown in Figure 8 to Figure 14.

In Figure 12, pressure flow is shown but in this scenario, it is very small and near zero on the fractional scale. However, it is clear and visible in Figure 9 which shows the initiation of the spray flow transient.

Since heater power is the primary side parameter while turbine power is the secondary side parameter. So its impact is very slowly transmitted

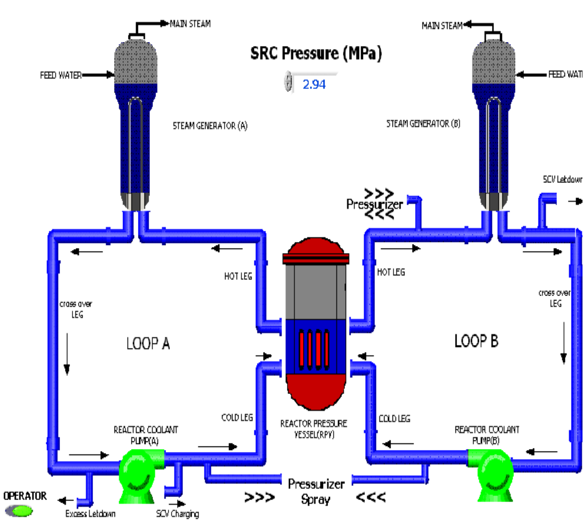

Fig. 2. Two loop primary circuit design of PWR in LabVIEW

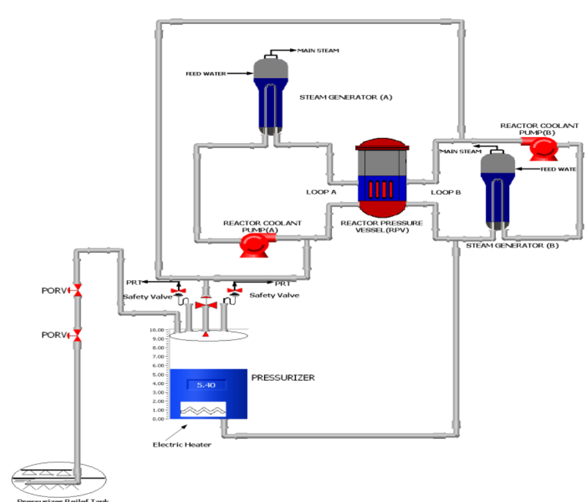

Fig. 3. Pressurizer pressure and level control system design of PWR in LabVIEW

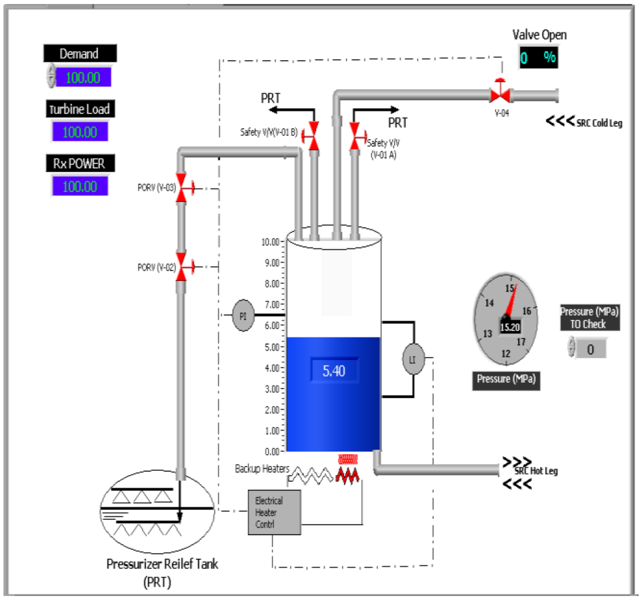

Fig. 4. Transient simulation model of pressurizer.

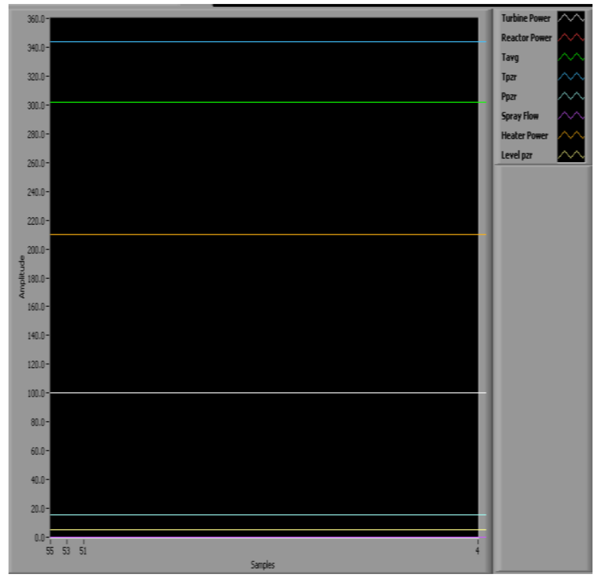

Fig. 5. Trends of pressurizer steady-state parameters at 100% steady state power

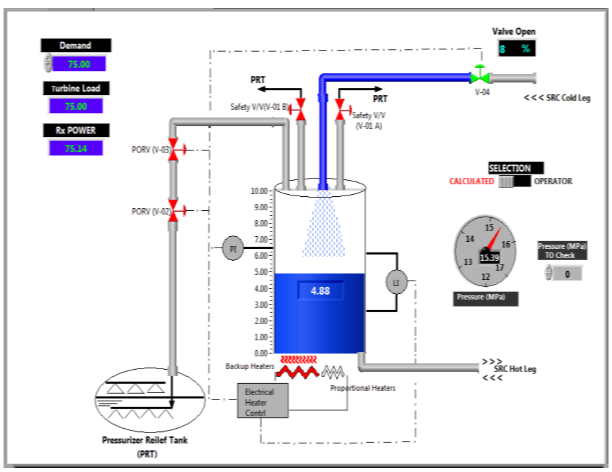

Fig. 6. Transient simulation model of pressurizer when reactor power level is reduced from 100 % to steady 75 %.

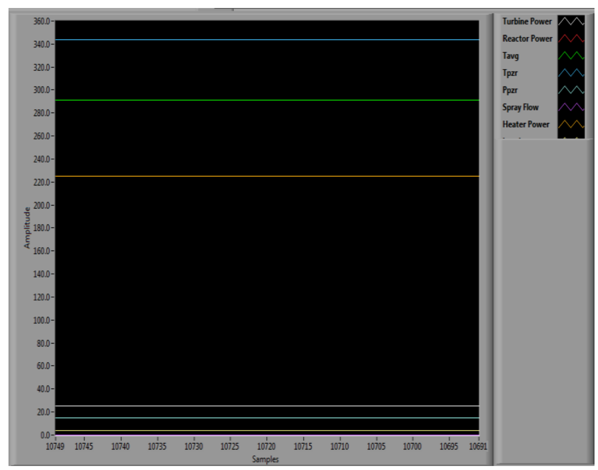

Fig. 7. Trends of pressurizer steady state parameters at 25 % steady state power.

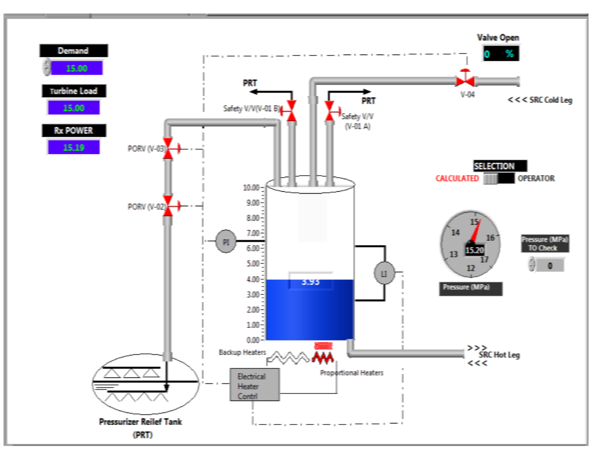

Fig. 8. Transient simulation model of pressurizer when reactor power level is reduced from 100 % to steady 15 %.

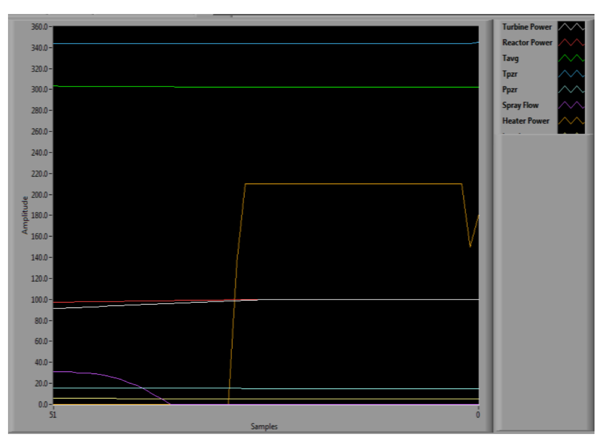

Fig. 9. Trends of pressurizer parameters from 100 % to 90 % power transient at 51st sample state.

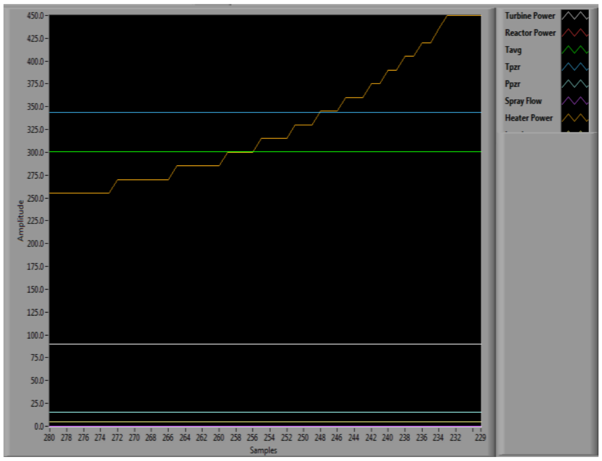

Fig. 10. Trends of pressurizer parameters from 100 % to 90 % power transient at 114th sample state.

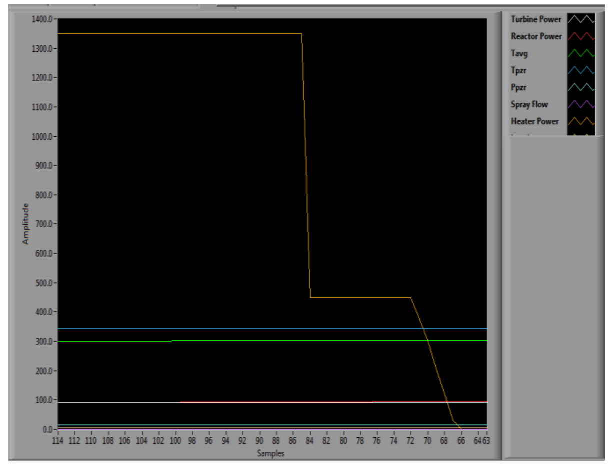

Fig. 11. Trends of pressurizer parameters from 100 % to 90 % power transient at 180th sample state

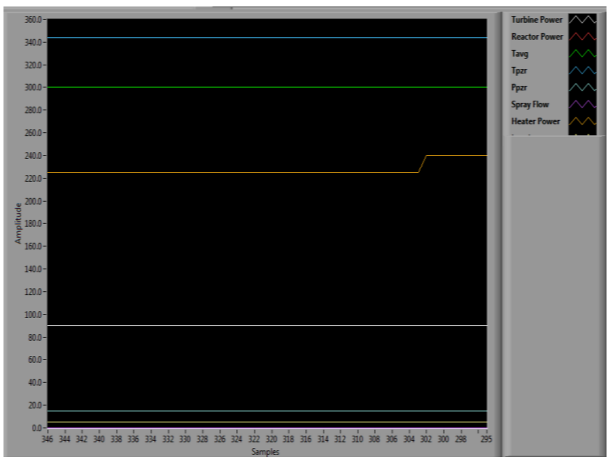

Fig. 12. Trends of pressurizer parameters from 100 % to 90 % power transient at 280th sample state

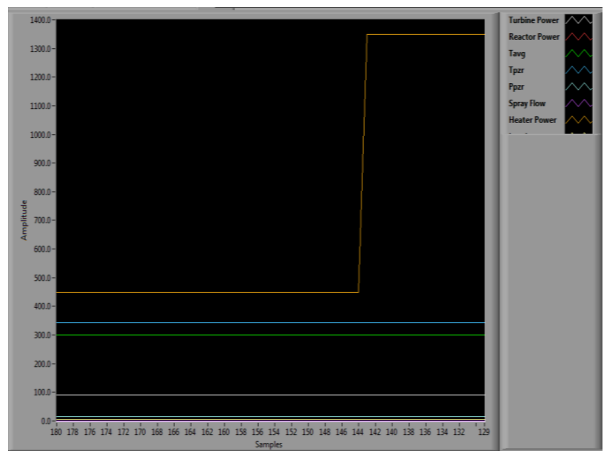

Fig. 13. Trends of pressurizer parameters from 100 % to 90 % power transient at 346th sample state.

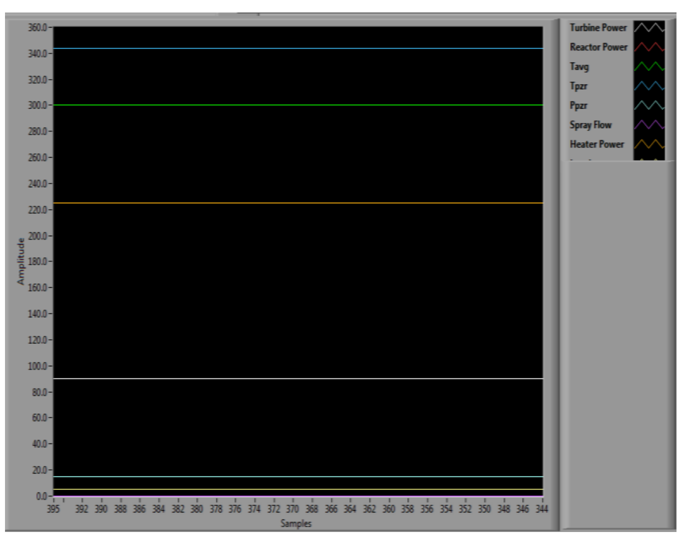

Fig. 14. Trends of pressurizer parameters from 100 % to 90 % power transient at 395th sample state

to the secondary side with process and system delay. However, in Figure 9, it is obvious that as heaters are turned OFF at the 25th sample, turbine power starts decreasing. Hence, this relationship is quite clear at the 25th sample of time.

Since FO MIMO is the combination of the FO SISO algorithm. Since the FO MIMO is a multivariable algorithm while FO SISO is a single variable algorithm, so the results are different.

This simulation experiment proves that dynamic transient analysis is excellent in tracking and parameters are settled after the transient is die out hence its performance is proved robust.

4. CONCLUSION

The nonlinear dynamics of the PWR pressurizer of 340 MWe PWR have been predicted in a graphical programming environment in LabVIEW. The model parameters have been estimated in a nonlinear open-loop MIMO framework. A graphical user interface has been developed for variable transfer and parametric display in LabVIEW. Four controllers have been synthesized for charging flow control, spray flow control, proportional heaters power control and backup heaters power control. All the four controllers have been configured with a pressurizer nonlinear dynamic model in fractional order nonlinear robust stabilizing H∞ framework. Controllers have been optimized in LabVIEW. The closed-loop performance of the PWR pressurizer has been studied in steady state and transient conditions. The fast convergence of parameters in transient conditions stabilizing at 90% demanded and turbine power proves that the robust performance of the proposed scheme is achieved. The presented design scheme can be used for other PWR systems and controllers and ever for different generations of PWRs in future.

5. ACKNOWLEDGEMENTS

The support of the Pakistan Atomic Energy Commission, Chashma Centre of Nuclear Training and Computer Development Division of KANUPP is gratefully acknowledged.

6. CONFLICT OF INTEREST

The authors declare no conflict of interest.

7. REFERENCES

1. S. M. Baek, H. C. No, and I. Y. Park. A nonequilibrium three-region model for transient analysis of pressurized water reactor pressurizer. *Nuclear Technology* 74: 260-266 (1986).
2. A. A. Sheta, E. A. Ali, R. M. Fikry, S. M. Elaraby, T. A. Mahmoud, and M. I. Mahmoud. A developed analytical model for pressurizer unit in nuclear power plants. *Journal Radiation Research and Applied Sciences* 14: 179-203 (2021).
3. M. A. Rabie, A. Elshahat, and M. H. Hassan. Investigation of VVER-1200 pressurizer dynamics by adopting modelica based modeling. *Progress in Nuclear Energy* 143: 01-17 (2022).
4. E. Takasuo. Modeling of pressurizer using APROS and TRACE thermal hydraulic codes. *VTT Technical Research Centre of Finland* 2339: 108 (2006).
5. Z. B. Xu, J. Wu, Z. T. Quan, X. S. Zhang, and X. Q. Ma. Model and simulation study on pressurizer pressure system. *International Conference Electrical, Automation and Mechanical*: 404-407 (2015).
6. I. Varga, G. Szederkenvi, and K. M. Hangos. Modeling and model identification of a pressurizer at the PAKS nuclear power plant. *14th IFAC Symposium on System Identification, Newcastle, Australia* 39: 678-683 (2006).
7. J. Lin, J. Zhang, J. Shi, and D. Li. Research of PWR pressurizer insurge characteristics on three-dimensional transient modeling. *Science and Technology of Nuclear Installations* 2018: 1-13 (2018).
8. P. P. Groudev, and M. P. Pavlova. Sensitivity calculations of PRZ water level during the natural circulation test at unit 6 of Kozloduy NPP. *Progress in Nuclear Energy* 49: 130-141 (2007).
9. A. G. Suryabrata, T. Mulyana, and D. Witarsyah. Pressurizer simulator. *Proceeding of International Conference on Electrical Engineering, Computer Science and Informatics, Palembang, Indonesia, Advances in Difference Equations*: 46-51 (2015).
10. M. Yu, X. Zhao, Y. Niu, and P. Yang. Modeling and simulation of pressure control logic module in pressurizer of nuclear power plant. *Advanced Material Research* 860: 2409-2414 (2014).
11. G. D. Zhang, X. H. Yang, S. Y. Qiao, and Y. J. Wu. Research on pressurizer pressure control of 900 MW pressurized water reactor nuclear power plant. *Advanced Material Research* 718: 1215-1220 (2013).
12. A. A. Sheta, E. H. Ali, R. m. Filry, T. A. Mahmoud,

S. M. El-Araby, and M. I. Mahmoud. Efficient linearized model of pressurizer system in pressurized water reactors for control purposes. *Journal of Physics* 1447: 01-12 (2019).

13. M. Victor, D. Oliveira, and J. C. S. Aleida. Modeling and control of a nuclear power plant using AI techniques. *International Nuclear Atlantic Conference, Brazil* 2013: 01-15 (2013).
14. M. Victor, D. Oliveira, and J. C. S. Aleida. Fuzzy control applied to nuclear power plant pressurizer system. *International Nuclear Atlantic Conference, Brazil* 2011: 01-15 (2011).
15. A. A. Sheta, E. H. Ali, R. m. Filry, T. A. Mahmoud, S. M. El-Araby, and M. I. Mahmoud. Intelligent control for pressurizer system in nuclear power. *Journal of Physics* 2128: 01-13 (2021).
16. R. Damayanti, A. Halim, and S. Nakhri. Control of air pressurizer levels on pressurized water reactor with fractional order PID control system. *Journal of Physical Science and Engineering* 05: 71-82 (2020).
17. A. H. Malik, A. A. Memon, and F. Arshad. Fractional order neural transient modeling of primary circuit of ACP1000 based nuclear power plant in LabVIEW. *Proceedings of Pakistan Academy of Sciences-A, Physical and Computational Sciences* 58: 17-26 (2021).
18. H. Xue, Q. Fang, J. Zhong, and Z. Shao. H∞ Time-delayed fractional order adaptive sliding mode control for two-wheel self-balancing vehicles. *Computational Intelligence and Neuroscience* 2020: 01-12 (2020).
19. G. Velmurugan, R. Rakkiyappan, and J. Cao. Finite time synchronization of fractional order memristor based neural networks with time delays. *Neural Networks* 73: 36-46 (2016).

Proceedings of the Pakistan Academy of Sciences: A Physical and Computational Sciences 59(3): 27-34 (2022)

ISSN (Print): 2518-4245; ISSN (Online): 2518-4253
https://doi.org/10.53560/PPASA(59-3)788

Pakistan Academy of Sciences

Research Article

Investigating the Impact of Technology Involvement in Education from Student's Perspective

Muhammad Khateeb Khan[1*], Kiran Sheraz[2], Umar Sultan[3], and Adil Mushtaq[4]

[1]Computing Department, Iqra University, Islamabad, Pakistan
[2]Education Department, National University of Modern Languages, Islamabad, Pakistan
[3]Computing Department, Riphah International University, Islamabad, Pakistan
[4]Software Department, University of Engineering and Technology, Taxila, Rawalpindi, Pakistan

Abstract: Technology is a great blessing from God as it makes life easier. It has various facets of life and has a strong impact on living organisms. Modern technologies have a strong impact on our education system. In our study, we investigated the impact of modern technologies in our academic era. A questionnaire was designed and gathered data from both male and female students in the education department of NUML University. There are more than 90 % of students who are interested to use technology to excel in their careers in academia. Students are highly interested to solve complex problems by using search engines including Google and YouTube. Based on our research, there are more than 90 % of students agreed that information technology (IT) helped them to solve problems and improve their grades and skills. Similarly, more than 80 % of students are well aware of the ethical use of online tools and information by providing the proper references to the source to avoid academic misconduct.

Keywords: Modern Technologies, Education, Learning Impact, Students Involvement, E-Learning, Tools and Techniques

1. INTRODUCTION

Technologies play a vital role in education for instant learning. The modern era is surrounded by with full of technologies for education, research and entertainment. Various kinds of techniques and algorithms are designed to improve the skills for education in an individual. With the help of technology, knowledge is disseminated and communicated more quickly. Various tools are designed that engaged the students and help them to learn during the class as a class activity and practical demonstrations. Technology has a strong contribution towards education development and involvement for students at the university level [1].

The impact of modern technologies is assessed through quick feedback from the students, teachers, administrations and parents. The students are more attracted and fascinated towards the technologies like the visual representation of facts and practical demonstrations of knowledge through online sources [2]. Different kinds of techniques (brainstorming) and visuals are used to involve the students and make their participation possible in the class. The education technology program provided computer access for both students and teachers and this technology was considered an apple classroom for tomorrow (ACOT) and the objective of ACOT was to promote the education context and the practicality of the theoretical concepts [3].

In addition, by applying abstract ideas to real-world situations, technology helps students to understand complex concepts. Through the use of online tools, self-learning and the competence level of the students are enhanced [4]. Technology also plays a significant role in teachers making their lectures and providing various sources to students for the same information to validate

Received: July 2022; Accepted: September 2022
*Corresponding author: Muhammad Khateeb Khan <m.khateeb231@gmail.com>

their arguments. There are also some techniques and algorithms developed which create automatic groups of students based on their performance as low, average and high. These groups increase the students' performance as knowledge and technical difficulties are communicated within the group and the low-performance students improve their learning with the help of these groups [5].

Collaborating learning is a significant technique in education as it also contributes to internal personal skills which is the prime requirement of the modern era. Collaborating learning improves the ability of critical thinking, and cognitive skills and provides help to solve complex problems analysis [6]. Group formation (which determines the high quality of group work) is the basic element to assess the quality of collaborative learning [7].

The purpose of this study is to 1) find the students' perceptions of technology involved in academia, and 2) describe the current use of general technologies and assistive technology in academia including students (those with documented learning disabilities). The objective of the study is to understand the need and importance of technology involved in education learning. By the use of modern technologies, we can motivate, encourage and involve the students in learning and use these technologies for the betterment of their upcoming careers.

2. METHODOLOGY

2.1 Research Design

In our research, we conducted a quantitative research design to evaluate the student's interest towards modern technologies for self-learning and personal development. A questionnaire was designed that contained various questions as shown in Table 1 regarding the online tools, ethical use of information, basic tools for education and IT infrastructures of the university. With the help of questionnaires, we collected the data from a selected population and analyzed the results based on these data as shown below in Figure 1.

2.2 Population

The study was conducted at the National University of Modern Languages (NUML), Islamabad and our targeted population was the students of M.A Education in the final semester. We selected 62 students from the final semester (both morning and evening). There were both male and female

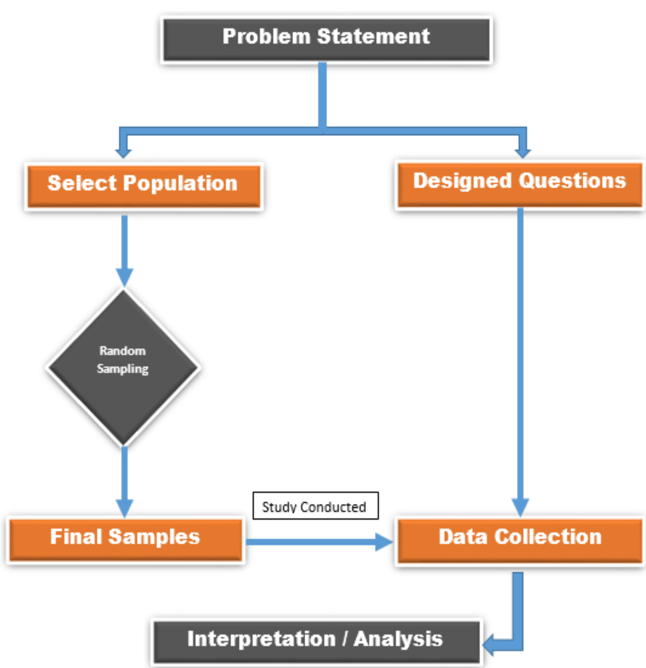

Fig. 1. Research Framework

students in our selected population with a specific proportion.

2.3 Sampling Technique

As our audience came from the same background and possessed similar kinds of technical skills and knowledge, the selection of any sample could contribute similarly. We used a simple random sampling technique to select the samples from the populations. As in random sampling, there remained an equal probability for all the samples being selected from the target population.

2.4 Sample Size

By using a random sampling technique, we selected 50 participants (male and female) from the target population. We informed the selected participants about the purpose of the study and then data was collected from the final selected samples.

2.5 Data Collection Instrument

We used questionnaires as tools for data collection purposes. We designed 15 questions apart from the participant's personal information. The 15 questions were based on various studies and tried to cover the very aspect of technologies impact on academia. As each question carried four options as either participant may strongly agree, agree, disagree or strongly disagree against each question as given in Table 1.

The data were collected in a controlled environment as we did not use any online tool for data collection like Google Forms. The designed questionnaire was provided to the selected students after random sampling techniques and collected the data. As the questions were designed based on some previous research and some questions were designed by keeping the view of the current situation of covid-19 as shown in Table 1. The questions are categorized based on training needs, ethical use, online tools, basic introductory courses and IT facilitations provided by the university as shown in Figure 3 and replicated in Table 1.

During Covid-19, both students and faculty faced a lot of problems while tackling the online tools and applications. There were a lot of technical difficulties to handle the students and made their involvement in class during online teaching.

3. RESULTS AND DISCUSSION

EThe experiment was performed and we collected the data from the participants and analyzed it to check the specific impact of modern technology on education. There were more than 60 % of students strongly agreed and 30 % of students agreed that technology helped them to solve complex problems and secure good grades. There were also 46 % and 42 % of students strongly agreed and agreed respectively that the online available resources helped them to solve and manage their work efficiently. 42 % of participants strongly Agreed and 40 % of students agreed with the use of basic IT tools like MS office (word, PowerPoint, excel).

As the legal aspects were concerned there were 60 % and 20 % of students strongly agreed and agreed that the ethical use and plagiarism issues of online resources to avoid academic misconduct. Participants were highly interested in basic computer training to excel in their academic careers. Based on our survey students were satisfied with the internet speed and fair IT infrastructure provided by the university. After performing the experiments and gathering data through questionnaires, it became the need to indulge the basic computer-based technology in our education system. As most students strongly agreed that modern technologies helped them to analyze, understand and solve complex problems. There were only a few students who disagreed that there was no impact of modern technologies on education.

As most of the participants agreed that grades were improved by using modern technologies. Participants agreed that modern technologies helped them out with subject understanding and task completion. No participant strongly disagreed that modern tools or applications did not contribute to learning purpose as shown in Figure 2.

As the survey was conducted and most of the participants agreed with fair internet speed at the university level. According to the survey, there were enough tools for educational learning in the targeted university i.e. NUML. There were a large number of students who strongly agreed that there must be

Table 1. Designed Questionnaires

Question Statements	Question Responses			
Technology helps me to get better results in my subjects.	Strongly Agree	Agree	Disagree	Strongly Disagree
Technology helps me to understand the subject's material more deeply.	Strongly Agree	Agree	Disagree	Strongly Disagree
Technology provides help to complete my assignments more conveniently.	Strongly Agree	Agree	Disagree	Strongly Disagree
Integrating the technologies in education increase the student's involvement in class.	Strongly Agree	Agree	Disagree	Strongly Disagree
There are many online tools to solve the complex problems more easily.	Strongly Agree	Agree	Disagree	Strongly Disagree
I am very familiar with some e-learning tools and applications.	Strongly Agree	Agree	Disagree	Strongly Disagree
I am familiar with basic education tools like MS Office (Word, PowerPoint, excel).	Strongly Agree	Agree	Disagree	Strongly Disagree
I am comfortable to search the relevant information from the internet.	Strongly Agree	Agree	Disagree	Strongly Disagree
I encourage the use of technology to complete class tasks / activities.	Strongly Agree	Agree	Disagree	Strongly Disagree
There is a need to integrate the basic computer course in education department.	Strongly Agree	Agree	Disagree	Strongly Disagree
There must be some IT related training to learn the basic academic technologies.	Strongly Agree	Agree	Disagree	Strongly Disagree
The university provides enough IT infrastructure in our education department.	Strongly Agree	Agree	Disagree	Strongly Disagree
There is a fair internet speed provided by university for all students.	Strongly Agree	Agree	Disagree	Strongly Disagree
I am aware with the copyright laws to use the resources from the internet.	Strongly Agree	Agree	Disagree	Strongly Disagree
There is need of reference to use the other work to avoid the academic misconduct.	Strongly Agree	Agree	Disagree	Strongly Disagree

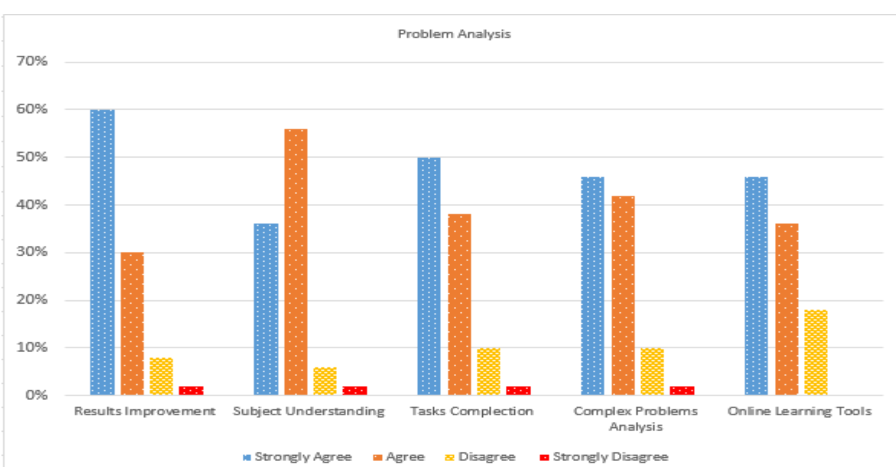

Fig. 2. Complex Problems and Technology Support

some IT-related training or integration of some IT course with the curriculum for career grooming as shown in Figure 3. There were very few participants showed resistance to the involvement of technology at the university level.

Most of the students strongly agreed that modern technologies helped them to analyze, understand and solve complex problems. There were only a few students who disagreed that there was no impact of modern technologies in the academic era.

Based on our experiments, we explored the overall acceptance and rejection ratio of technology involved in the education department. As we used the accumulated results of (strongly agree + agree) and (Strongly Disagree + Disagree) as shown in Figure 4. As there were more than 90 % of participants agreed that modern tools and technologies helped them to understand the subjects. Almost 90 % of participants strongly encouraged the technology to improve their academic results as shown in Figure 4.

By using the technology in education can increase the academic achievement both for students and educators. The technology based learning incorporated, analyzed and solved real-world complex problems both for students and educators [8]. There were a lot of online resources which provided help to understand subjects. The technology-based learning incorporates, analyses and solves real-world complex problems both for students and educators. [9]. There were a lot of academic resources including internet sources, WebCT, and YouTube which provided help to understand situations, and complex concepts and apply abstract ideas to the real world at the bachelor level [10].

All kinds of Technologies are fully integrated to daily life from cell phones with fingerprint scanners to cars with integrated GPS navigation. Modern technologies internet, chat boat and other online platforms were widely used in communication and information sharing [11]. The rapid growth of information and communication technology (ICT) including laptops, mobile, computers, and television completely changed the education era [12]. Students benefited by using online and offline technologies to solve their academic problems. With the help of software applications, students can easily access their records from remote areas as well.

According to the modern school day, students preferred to use technology and knew the impact of these technologies in their life. Augmented reality (AR) contributed well to education and helped to increase critical thinking, decision making and personal development [13]. Augmented reality applications were used to teach various subjects in higher education systems with visual impacts and had a strong positive influence on education [14]. There was another research conducted about the global universities partnerships and interaction was made about the technology transitions paradigm in education. The research emphasized the associations between education, technologies and continuous improvement in education by involving the technologies in education [15].

Another research was conducted which identified the number of software which have visual effects that attracted the students to the classroom for their participation [16]. There were some animations which were mapped on the learning modules and pedagogical community response to the information challenges. The model was developed with the name of the author's children's animations, which helped the preschool-age students thinking ability and modern information society [17]. There was also existed an innovative conceptual framework approach called the Students Career Assistance System (SCAS) which described the state-of-the-art education system. The smart education system was based on content analysis and evolved rapidly through the range of various technology applications [18].

There was a study conducted which depicted that students who used mobile phones more frequently performed better as compared to those students who avoided using phones [19]. It also depicted that communication through mobile phone among students which were primarily not for the class content but also contribute to students teaching [20]. There was a study, which correlated the methodological value and the importance of modern technologies in edutainment. The objective of this study was the determination

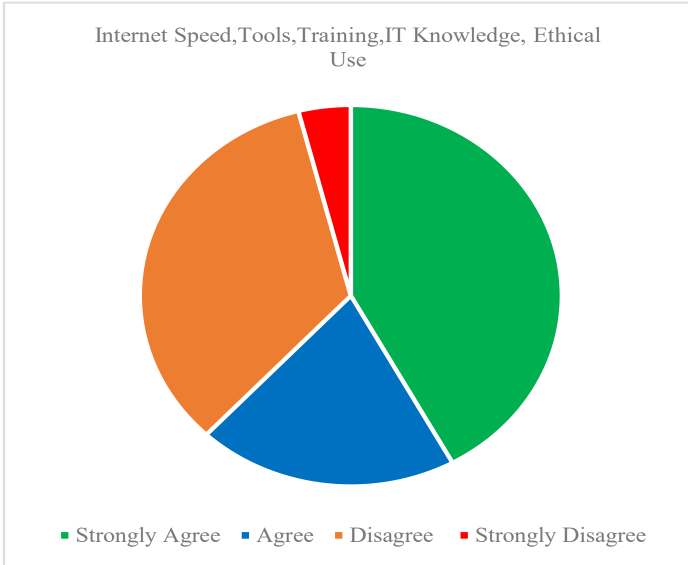

Fig. 3. Technology and Student Involvement

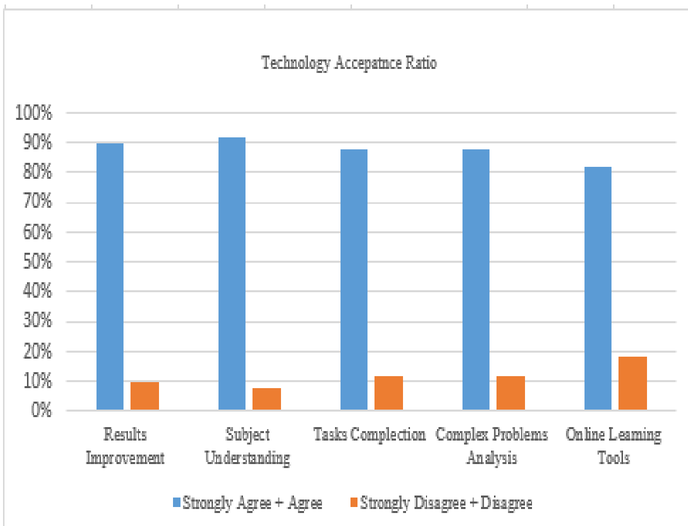

Fig. 4. Technology Acceptance Ratio

of methodological technology edutainment. As information volume grew rapidly became obsolete as time progressed and it became difficult to acquire useful knowledge. Rapidly developing technologies facilitate new leisure activities, and the time for obtaining information becomes smaller [21].

Based on the above results we determined the importance of technology in academia for the current era. Most of the students showed their interest towards technology involvement in education to excel in their careers. The students were happy with the IT infrastructure provided university and highly interested in IT-relevant training or integrating the IT course with the curriculum. Most of the students knew the basic ethical use of online information and the consequence of misuse of information as education misconduct.

4. CONCLUSION

Current technologies play a vital role in daily life and academic development. In our study, we investigated the impact of academic technologies on students' development and learning. We conducted a survey at NUML University with students from the education department. A questionnaire was designed and collected the data from a population of 62 students. The collected data were analyzed to find the students' concerns towards the technology involved in academia. The results have shown that the students were highly interested in the technology involved in education to learn and grow their future careers. As more than 90 % of students either strongly agreed or agreed that online resources helped them to understand their subjects and improve their academic results. Similarly, more than 85 % of students agreed that current tools and technologies helped them to complete their home tasks and solve their complex problems with proper analysis.

5. RECOMMENDATIONS

Based on this research, it is recommended that there is a need for computer-related training for students having no technical skills and abilities in IT so that they can use the tools and technologies more appropriately. Further, based on students there must be an introductory course on computers in non-computing departments including the education department.

6. CONFLICT OF INTEREST

The authors declare no conflict of interest.

7. REFERENCES

1. M. Masood, M. Asim, and S. Manzoor. Impact of Technology on the Behavior of Students Towards Learning in Pakistanl. *Psychology and Education* 58(2): 9111-9113(2021).
2. R. Nadia,W. Zhang and M. Iqbal. The use of technology for online classes during the global pandemic: Challenges encountered by the schoolteachers in Pakistan. *Liberal Arts and Social Sciences International Journal (LASSIJ)* 5(2): 193–208(2021).
3. E.L. Baker. The Apple Classrooms of Tomorrow. *The UCLA Evaluation Studies* 24 (1993).
4. A.L. Cloete. Technology and education: Challenges and opportunities. *HTS: Theological Studies* 73(3): 1-7 (2017).
5. C. Liang, R. Majumdar, and H. Ogata. Learning log-based automatic group formation: system design and classroom implementation study. *Research and Practice in Technology Enhanced Learning* 16(1): 14(2021).
6. F. Ramos-Quintana, M.D. Vargas-Cerdan, and J.R. Rojano-Cáceres. Towards an on-Line Student Assistant within a CSCL Framework. *Creative Education* 3(5): 1-19(2012).
7. E. Maina, R. Oboko, and W. Wagacha. Evaluation of Intelligent Grouping Based on Learners' Collaboration Competence Level in Online Collaborative Learning Environment. *International Review of Research in Open and Distance Learning* 17(2): (2016).
8. K. Ratheeswari. Information communication technology in education. *Journal of Applied and Advanced Research* 3(1): 45-47(2018).
9. Y.C. Hsu, H.N.J. Ho, C.C.Tsai, G.J.Hwang, H.C. Chu, C.Y. Wang, and N.S. Chen . Research trends in technology-based learning from 2000 to 2009: A content analysis of publications in selected journals. *Journal of Educational Technology & Society* 15(2): 354-370(2012).
10. R. Andika, C.T. Kao, C. Williams, Y.J. Lee, H. Al-Battah, and R. Alweis. YouTube as a source of information on the COVID-19 pandemic. *Journal of Community Hospital Internal Medicine Perspectives* 11(1): 39-41 (2021).
11. G. Hiremath, A. Hajare, P. Bhosale, R. Nanaware, and K.S. Wagh. Chatbot for education system. *International Journal of Advance Research, Ideas and Innovations in Technology* 4(3): 37-43(2018).
12. V. Vinu, P.C. Sherimon, and R. Krishnan. Towards pervasive mobile learning – the vision of 21st century. *Procedia - Social and Behavioral Sciences* 15:3067-3073 (2011).
13. M. Bower, C. Howe, N. McCredie, A. Robinson, and D. Grover. Augmented Reality in education – cases, places and potentials. *Educational Media International* 51(1): 1-15(2014).
14. A. Iatsyshyn, and K. Valeriia. Application of augmented reality technologies for education projects preparation. *Proceedings of the 7th Workshop on Cloud Technologies in Education (CTE)* 2643: (2020).
15. R.L. Sakhapov, and S.G. Absalyamova. The use of telecommunication technologies in education network. Proceedings of 2015 12th International *Conference on Remote Engineering and Virtual Instrumentation (REV), Bangkok, Thailand* (2015).
16. C. Buckley, and C. Nerantzi. Effective Use of Visual Representation in Research and Teaching within Higher Education. *International Journal of Management and Applied Research* 7(3): 196-214(2020).
17. F. Hamidi, M. Meshkat, M. Rezaee, and M. Jafari., Information Technologies in Education. *Procedia*

Computer Science 3(2): 369-373(2011).

18. H. Singh, and S.J. Miah. Smart education literature: A theoretical analysis. *Education and Information Technologies* 25(4): 3299–3328(2020).
19. M.S. Sarvestani, M. Mohammad, J. Afshin, and L. Raeisy S. Nouroozi. Students' Experiencesof E-Learning Challenges; a Phenomenological Study. *Interdisciplinary Journal of Virtual Learning in Medical Sciences* 10(3): 1-10(2019).
20. S. Zaheer, S.M. Butt, G.V. Anatolyevna, and H. Salmani. Do Mobile Technology in the Classroom Really Improve Learning Outcomes?. *International Journal of Evaluation and Research in Education* 7(3): 188-193(2018).
21. O.V. Anikina, and E.V. Yakimenko. Edutainment as a Modern Technology of Education. *Procedia - Social and Behavioral Sciences* 166(4): 475-479(2015).

Proceedings of the Pakistan Academy of Sciences: A Physical and Computational Sciences 59(3): 35-43 (2022)

ISSN (Print): 2518-4245; ISSN (Online): 2518-4253
https://doi.org/10.53560/PPASA(59-3)653

Pakistan Academy of Sciences

Research Article

An Improved Iterative Scheme using Successive Over-relaxation for Solution of Linear System of Equations

Zaheer Ahmed, Zubair Ahmed Kalhoro*, Abdul Wasim Shaikh, Muhammad Shakeel Rind Baloch, and Owais Ali Rajput

Institute of Mathematics and Computer Science, University of Sindh, Jamshoro, Pakistan

Abstract: To solve the system of linear equations is one of the hottest topics in iterative methods. The system of linear equations occurs in business, engineering, social and in sensitive research areas like medicine, therefore applying efficient matrix solvers to such systems is crucial. In this paper, an improved iterative scheme using successive overrelaxation has been constructed. The proposed iterative method converges well when a linear system's matrix is M-matrix, Symmetric positive definite with some conditions, irreducibly diagonally dominant, strictly diagonally dominant, and H-matrix. Such type of linear system of equations does arise usually from ordinary differential equations and partial differential equations. The improved iterative scheme has decreased spectral radius, improved stability and reduced the number of iterations. To show the effectiveness of the improved scheme, it is compared with the refinement of generalized successive over-relaxation and generalized successive over-relaxation method with the help of numerical experiments using MATLAB software.

Keywords: GSOR, RGSOR, Diagonally Dominant, Irreducibly Diagonally Dominant, Rate of Convergence

1. INTRODUCTION

The world of mathematics is surrounded by many mathematical problems. The efforts to find the solution to the system of linear equations are one of the most popular and interesting problems in the math world. A lot of people, apart from mathematicians, like computer scientists, chemists, biologists, physicists, engineers, social scientists, industry experts, economists etc, struggle to solve the system of linear equations in their fields [1-2]. The branch of mathematics which is devoted to developing a different algorithm for solving a system of linear equations is called Linear Algebra (LA) and the branch of LA that deals with the numerical solution of these linear systems, is called Numerical Linear Algebra (NLA). A linear equation system can be transformed into a matrix equation in the following form:

$$Ay=b \quad (1)$$

In equation 1, matrix A is an invertible square matrix whereas y and b are unknown and known column vectors respectively.

In NLA we search for the indirect or numerical solution of the linear system. The indirect methods are applied when the co-efficient matrices of matrix equations are large dimensional and sparse [3].

Improvements in the classical iterative techniques have been done earlier [11], however since the SOR outperforms all the other iterative techniques, an improvement in the SOR scheme will be highly effective. In this research work an iterative scheme namely "improved iterative scheme using successive overrelaxation (IIS)" is developed. This scheme is just an improved version of the generalized successive overrelaxation (RGSOR) refinement. Stability and Spectral Radius are used as comparative factors for checking the efficiency of the proposed algorithm. The IIS has decreased spectral radius, improved stability and

Received: July 2022; Accepted: September 2022
*Corresponding author: Zubair Ahmed Kalhoro <zubair.kalhoro@usindh.edu.pk>

the number of iterations. The convergence of IIS has been proved. Different types of numerical experiments are considered to demonstrate the efficiency of the IIS method.

2. MATERIALS AND METHODS

First, we decompose the matrix $\boldsymbol{A} = \boldsymbol{T_m} - \boldsymbol{L_m} - \boldsymbol{U_m}$. Let $\boldsymbol{A} = (\boldsymbol{\alpha_{ij}})$ be a nonsingular square matrix and $\boldsymbol{T_m} = \boldsymbol{t_{ij}}$ with bandwidth 2m+1 is be a banded matrix, defined as

$$\boldsymbol{t_{ij}} = \begin{cases} \boldsymbol{\alpha_{ij}}, |\boldsymbol{i}-\boldsymbol{j}| \le \boldsymbol{m} \\ \boldsymbol{0} \quad \textbf{otherwise} \end{cases} \qquad (1.1)$$

Where $\boldsymbol{L_m}$ and $\boldsymbol{U_m}$ are strictly lower part and strictly upper part, these matrices are defined as under

$$\boldsymbol{T_m} = \begin{bmatrix} \boldsymbol{\alpha_{1,1}} & \cdots & \boldsymbol{\alpha_{1,m+1}} & \\ \vdots & \ddots & \ddots & \boldsymbol{\alpha_{n-m,n}} \\ \boldsymbol{\alpha_{m+1,1}} & \ddots & \ddots & \vdots \\ & \boldsymbol{\alpha_{n,n-m}} & \cdots & \boldsymbol{\alpha_{n,n}} \end{bmatrix}$$

$$\boldsymbol{L_m} = \begin{bmatrix} -\boldsymbol{\alpha_{m+2,1}} & & \\ \vdots & \ddots & \\ -\boldsymbol{\alpha_{n,1}} & \cdots & -\boldsymbol{\alpha_{n-m-1,n}} \end{bmatrix}$$

$$\boldsymbol{U_m} = \begin{bmatrix} & -\boldsymbol{\alpha_{1,m+2}} & \cdots & -\boldsymbol{\alpha_{1,n}} \\ & & \ddots & \vdots \\ & & & -\boldsymbol{\alpha_{n-m-1,n}} \\ & & & \end{bmatrix}$$

Definition 1: [4-5] A square matrix $\boldsymbol{A} = (\boldsymbol{\alpha_{ij}})$ is known as diagonally dominant (DD) if

$$|\boldsymbol{\alpha_{ii}}| \ge \sum_{\substack{j=1 \\ j\neq 1}}^{n} |\boldsymbol{\alpha_{ij}}| \qquad (1.2)$$

Definition 2: [4-5] A square matrix $\boldsymbol{A} = (\boldsymbol{\alpha_{ij}})$ is known as strictly diagonally dominant (SDD) if

$$|\boldsymbol{\alpha_{ii}}| > \sum_{\substack{j=1 \\ j\neq 1}}^{n} |\boldsymbol{\alpha_{ij}}| \qquad (1.3)$$

Definition 3: [4-5] With satisfying the following four axioms a matrix $\boldsymbol{A}$ is called an $\boldsymbol{M}$-matrix.

i. $\boldsymbol{\alpha_{ii}} > \boldsymbol{0}$ for $\boldsymbol{i} = \boldsymbol{1, 2, 3, \dots, n}$

ii. $\boldsymbol{\alpha_{ij}} \le \boldsymbol{0}$ for $\boldsymbol{i} = \boldsymbol{1, 2, 3, \dots, n}$

iii. $\boldsymbol{A}$ must be a nonsingular

iv. $\boldsymbol{A^{-1}} > \boldsymbol{0}$

Definition 4: [4-5] If a square matrix $\boldsymbol{A}$ satisfies the following conditions then it is called symmetric positive definite.

i. $\boldsymbol{A^t} = \boldsymbol{A}$

ii. $\boldsymbol{y^t A y} > \boldsymbol{0}$

Definition.5: [4-5] Let $\boldsymbol{A}$ a square matrix and λ be its Eigen value then the equation $\boldsymbol{\rho(A)} = \mathbf{max}|\boldsymbol{\lambda}|$ is called spectral radius $\boldsymbol{A}$.

3. GENERALIZED SOR METHOD

The generalized SOR method for solving the system of linear equations is presented by Manideep Saha and Jahnvi Chakrabarty [6]. Using this method eq. (1) can be written as:

$$y^{(k+1)} = (T_m - \omega L_m)^{-1}\big((1-\omega)T_m + \omega U_m\big)y^{(k)} + (T_m - \omega E_m)^{-1}\omega b \qquad (2)$$

4. REFINEMENT OF GENERALIZED SOR METHOD

Hailu Muleta and Genanew Gofe proposed a refinement of the GSOR method [1]. Multiplying eq. (1) with $\boldsymbol{\omega}$ then substituting $\boldsymbol{A}$ with its splitting

$$\boldsymbol{\omega(T_m - L_m - U_m) = \omega y b} \qquad (2.1)$$

After simplification:

$$\boldsymbol{y = y + (T_m - \omega L_m)^{-1}(b - Ay)\omega} \qquad (2.2)$$

That is:

$$\boldsymbol{\tilde{y}^{(k+1)} = y^{(k+1)} + (T_m - \omega L_m)^{-1}(b - Ay^{(k+1)})\omega} \qquad (3)$$

Putting the values of $\mathbf{y^{(k+1)}}$ from Eq. (2) in Eq. (3) and after solving the refinement of the GSOR Scheme will be:

$$\boldsymbol{y^{(k+1)} = [(T_m - \omega L_m)^{-1}((1-\omega)T_m + \omega U_m)]^2 y^{(k)} + (T_m - \omega L_m)^{-1}[I + (T_m - \omega L_m)^{-1}((1-\omega)T_m + \omega U_m]\omega b} \qquad (4)$$

5. PROPOSED METHOD

Here we are presenting a second refinement of the GSOR Method. by using the equation $\tilde{y}^{(k+1)} = y^{(k+1)} + (T_m - \omega L_m)^{-1}(b - Ay^{(k+1)})\omega$ and Substituting value of $y^{(k+1)}$ form eq. (4) we get

$$\tilde{y}^{(k+1)} = [(T_m - \omega E_m)^{-1}(1-\omega)T_m + \omega F_m)]^2 y^{(k)} + \left[I + (T_m - \omega E_m)^{-1}(1-\omega)T_m + \omega F_m\right](T_m - \omega E_m)^{-1}b + (T_m - \omega E_m)^{-1}b\omega - \left(\omega A(T_m - \omega E_m)^{-1}\right)[(T_m - \omega E_m)^{-1}(1-\omega)T_m + \omega F_m)]^2 y^{(k)} + \left[I + (T_m - \omega E_m)^{-1}(1-\omega)T_m + \omega F_m\right](T_m - \omega E_m)^{-1}b \quad (5)$$

After rearranging and simplifying eq. (5) we get

$$\tilde{y}^{(k+1)} = \left[(T_m - \omega E_m)^{-1}\left((1-\omega)T_m + \omega F_m\right)\right]^3 y^{(k)} + \left[I + (T_m - \omega E_m)^{-1}\left((1-\omega)T_m + \omega F_m\right) + \left((T_m - \omega E_m)^{-1}\left((1-\omega)T_m + \omega F_m\right)\right)^2\right](T_m - \omega E_m)^{-1}\,\omega b \quad (6)$$

Equation (6) is the equation of IIS. For $m = 0$ IIS becomes SRSOR.

6. CONVERGENCE THEORY

Theorem 1: Let A be an SDD matrix then for any vector $y^{(0)}$, the RGSOR converges.

Proof: (see [1])

Theorem 2: Let A be a square matrix of dimension $n \times n$, where $m \le n$ and m belongs to a set of natural numbers then the RGSOR converges for any vector $\mathbf{y}^{(0)}$.

Proof: (see [1])

Theorem 3: A is an SPD matrix and if $\omega < 2$ then SOR converges for any vector $\mathbf{y}^{(0)}$.

Proof: (see [6])

Theorem 4: Let A be a square matrix of dimension $n \times n$, where $m \le n$ and m belongs to a set of natural numbers then the IIS converges for any vector $\mathbf{y}^{(0)}$.

Proof: Suppose Y be the exact solution of equation 1. Let us assume that A be the SDD so SOR, GSOR and RGSOR will converge, i.e.

$$y^{(k+1)} \to y$$

When:

$$y^{(k+1)} = [(T_m - \omega L_m)^{-1}((1-\omega)T_m + \omega U_m)]^2 y^{(k)} + (T_m - \omega L_m)^{-1}[I + (T_m - \omega L_m)^{-1}((1-\omega)T_m + \omega U_m)]\omega b \quad (6.1)$$

Also,

$$y^{(k+1)} = y^{(k+1)} + (T_m - \omega L_m)^{-1}(b\omega - \omega A y^{(k+1)})$$

$$\tilde{y}^{(k+1)} - Y = y^{(k+1)} - Y + (T_m - \omega L_m)^{-1}\left(b\omega - \omega A y^{(k+1)}\right) \quad (6.2)$$

Taking norm on both sides:

$$\left\|\tilde{y}^{(k+1)} - Y\right\| = \left\|y^{(k+1)} - Y + (T_m - \omega L_m)^{-1}(b\omega - \omega A y^{(k+1)})\right\|$$

$$\le \left\|y^{(k+1)} - Y\right\| + \left\|(T_m - \omega L_m)^{-1}(b\omega - \omega A y^{(k+1)})\right\|$$

$$\therefore \left\|y^{(k+1)} - Y\right\| \le \left\|y^{(k+1)} - Y\right\| + \omega\left\|(T_m - \omega L_m)^{-1}\right\|\left\|\left(b - A y^{(k+1)}\right)\right\|$$

$$\left\|\tilde{y}^{(k+1)} - Y\right\| \le \|Y - \| + \omega\left\|(T_m - \omega L_m)^{-1}\right\|\|(b - b)\|$$

$$\left\|\tilde{y}^{(k+1)} - Y\right\| \le 0 + \omega\left\|(T_m - \omega L_m)^{-1}\right\|0 = 0$$

Consequently $\left\|\tilde{y}^{(k+1)} - Y\right\| \to 0$

Then:

$$y^{(k+1)} \rightarrow Y$$

$$\Rightarrow \rho\left(\left[(T_m - \omega L_m)^{-1}\left((1-\omega)T_m + \omega U_m\right)\right]^3\right) = \left(\rho\left((T_m - \omega L_m)^{-1}\left((1-\omega)T_m + \omega U_m\right)\right)\right)^3 < 1 \quad (6.3)$$

Hence IIS is convergent.

Theorem 5: If be an M-matrix of order $n \times n$ and m$\leq$ $\mathbf{n}$ where m belongs to a set of natural numbers then the IIS converges for any initial vector $\mathbf{y}^{(0)}$.

Proof:
We have an M-matrix A; we try to produce that IIS is convergent. using the convergent theorem of GSOR, we have:

$$\rho\left(T_m - \omega L_m)^{-1}\left((1-\omega)T_m + U_m\right)\right) < 1 \quad (6.4)$$

We realize that,

$\mathbf{G_{IIS}} = [\boldsymbol{\rho}(\mathbf{G_{GSOR}})]^3$Where $\boldsymbol{\rho}(\mathbf{G_{GSOR}})$ and $\mathbf{G_{IIS}}$ are spectral radii of GSOR and IIS respectively. As $\boldsymbol{\rho}(\mathbf{G_{GSOR}}) < \mathbf{1}$, so $\boldsymbol{\rho}(\mathbf{G_{IIS}}) < \boldsymbol{\rho}(\mathbf{G_{GSOR}}) < \mathbf{1}$

Theorem 6: The IIS method converges for any SPD matrix A.

Proof:
Using theorem 3, We have $\rho\left((T_m - \omega L_m)^{-1}[(1-\omega)T_m + \omega L_m]\right) < 1$.

Let X be the actual solution of eq. 1. Now by using eq. 2 we can write equation 1 as

$$Y = \left[I - (T_m - \omega L_m)^{-1}\left((1-\omega)T_m + \omega U_m\right)\right]^{-1} b\omega (T_m - \omega L_m)^{-1} \quad (7)$$

Using IIS

$$\tilde{y}^{(k+1)} = \left[(T_m - \omega L_m)^{-1}\left((1-\omega)T_m + \omega U_m\right)\right]^3 y^{(k)} + \left[I + (T_m - \omega L_m)^{-1}\left((1-\omega)T_m + \omega U_m\right) + \left((T_m - \omega L_m)^{-1}\left((1-\omega)T_m + \omega U_m\right)\right)^2\right](T_m - \omega L_m)^{-1}\,\omega b \quad (8)$$

Now using eq.(8) and the exact solution Y, we have:

$$Y = \left[(T_m - \omega L_m)^{-1}\left((1-\omega)T_m + \omega U_m\right)\right]^3 y^{(k)} + \left[I + (T_m - \omega L_m)^{-1}\left((1-\omega)T_m + \omega U_m\right) + \left((T_m - \omega L_m)^{-1}\left((1-\omega)T_m + \omega U_m\right)\right)^2\right](T_m - \omega L_m)^{-1}\,\omega b$$

$$\Rightarrow Y = \left(1 - \left[(T_m - \omega L_m)^{-1}\left((1-\omega)T_m + \omega U_m\right)\right]^3\right)^{-1}\left[1 + (T_m - \omega L_m)^{-1}\left((1-\omega)T_m + \omega U_m\right) + \left((T_m - \omega L_m)^{-1}\left((1-\omega)T_m + \omega U_m\right)\right)^2\right](T_m - \omega U_m)^{-1}\omega b$$

$$Y = \left[1 + \left[(T_m - \omega L_m)^{-1}\left((1-\omega)T_m + \omega U_m\right)\right]^3 + \left[(1 - \omega L_m)^{-1}\left((1-\omega)T_m + \omega U_m\right)\right]^6 + \right]\left[I + (T_m - \omega L_m)^{-1}\left((1-\omega)T_m + \omega U_m\right) + \left((T_m - \omega L_m)^{-1}\left((1-\omega)T_m + \omega U_m\right)\right)^2\right](T_m - \omega U_m)^{-1}\omega b$$

Since $(1-M)^{-1}$=1+M+M^2+…

If $\rho(M) < 1$ and 1-M is singular.

$$\begin{aligned} \boldsymbol{Y} = \Big[& \mathbf{1} + (\boldsymbol{T_m} - \boldsymbol{\omega L_m})^{-1}\big((\mathbf{1}-\boldsymbol{\omega})\boldsymbol{T_m} + \boldsymbol{\omega U_m}\big) \\ & + \Big((\boldsymbol{T_m} - \boldsymbol{\omega L_m})^{-1}\big((\mathbf{1}-\boldsymbol{\omega})\boldsymbol{T_m} + \boldsymbol{\omega U_m}\big)\Big)^{2} \\ & + \Big((\boldsymbol{T_m} - \boldsymbol{\omega L_m})^{-1}\big((\mathbf{1}-\boldsymbol{\omega})\boldsymbol{T_m} + \boldsymbol{\omega U_m}\big)\Big)^{3} \\ & + \Big((\boldsymbol{T_m} - \boldsymbol{\omega L_m})^{-1}\big((\mathbf{1}-\boldsymbol{\omega})\boldsymbol{T_m} + \boldsymbol{\omega U_m}\big)\Big)^{3} \\ & + \cdots \Big] (\boldsymbol{T_m} - \boldsymbol{\omega U_m})^{-1}\boldsymbol{\omega b} \end{aligned}$$

$$\boldsymbol{Y} = \big[\mathbf{1} - (\boldsymbol{T_m} - \boldsymbol{\omega L_m})^{-1}((\mathbf{1}-\boldsymbol{\omega})\boldsymbol{T_m} + \boldsymbol{\omega U_m})\big]^{-1}(\boldsymbol{T_m} - \boldsymbol{\omega U_m})^{-1}\boldsymbol{\omega b} \quad (8.1)$$

As $(\mathbf{1}-\boldsymbol{M})^{-1} = \mathbf{1} + \boldsymbol{M} + \boldsymbol{M}^{2} + \cdots$

$\therefore \boldsymbol{Y} = \big[\mathbf{1} - (\boldsymbol{T_m} - \boldsymbol{\omega L_m})^{-1}((\mathbf{1}-\boldsymbol{\omega})\boldsymbol{T_m} + \boldsymbol{\omega U_m})\big]^{-1}(\boldsymbol{T_m} - \boldsymbol{\omega U_m})^{-1}\boldsymbol{\omega b}$ is consistent to GSOR.

Now examine the convergence of IIS for the SPD matrix.

$$\begin{aligned} \widetilde{\boldsymbol{y}}^{(\boldsymbol{k}+\mathbf{1})} = {} & [(\boldsymbol{T_m} - \boldsymbol{\omega L_m})^{-1}((\mathbf{1}-\boldsymbol{\omega})\boldsymbol{T_m} + \boldsymbol{\omega U_m})]^{3}\boldsymbol{y}^{(\boldsymbol{k})} \\ & + \Big[\boldsymbol{I} + (\boldsymbol{T_m} - \boldsymbol{\omega L_m})^{-1}\big((\mathbf{1}-\boldsymbol{\omega})\boldsymbol{T_m} + \boldsymbol{\omega U_m}\big) \\ & + \Big((\boldsymbol{T_m} - \boldsymbol{\omega L_m})^{-1}\big((\mathbf{1}-\boldsymbol{\omega})\boldsymbol{T_m} + \boldsymbol{\omega U_m}\big)\Big)^{2}\Big](\boldsymbol{T_m} - \boldsymbol{\omega L_m})^{-1}\boldsymbol{\omega b} \end{aligned}$$

$$\begin{aligned} \boldsymbol{y}^{(\boldsymbol{k}+\mathbf{1})} = {} & [(\boldsymbol{T_m} - \boldsymbol{\omega L_m})^{-1}((\mathbf{1}-\boldsymbol{\omega})\boldsymbol{T_m} + \boldsymbol{\omega U_m})]^{6}\boldsymbol{y}^{(\boldsymbol{k}-\mathbf{1})} \\ & + \Big[\boldsymbol{I} + (\boldsymbol{T_m} - \boldsymbol{\omega L_m})^{-1}\big((\mathbf{1}-\boldsymbol{\omega})\boldsymbol{T_m} + \boldsymbol{\omega U_m}\big) \\ & + \Big((\boldsymbol{T_m} - \boldsymbol{\omega L_m})^{-1}\big((\mathbf{1}-\boldsymbol{\omega})\boldsymbol{T_m} + \boldsymbol{\omega U_m}\big)\Big)^{2} \\ & + \Big((\boldsymbol{T_m} - \boldsymbol{\omega L_m})^{-1}\big((\mathbf{1}-\boldsymbol{\omega})\boldsymbol{T_m} + \boldsymbol{\omega U_m}\big)\Big)^{3} \\ & + \Big((\boldsymbol{T_m} - \boldsymbol{\omega L_m})^{-1}\big((\mathbf{1}-\boldsymbol{\omega})\boldsymbol{T_m} + \boldsymbol{\omega U_m}\big)\Big)^{4} \\ & + \Big((\boldsymbol{T_m} - \boldsymbol{\omega L_m})^{-1}\big((\mathbf{1}-\boldsymbol{\omega})\boldsymbol{T_m} + \boldsymbol{\omega U_m}\big)\Big)^{5}\Big](\boldsymbol{T_m} - \boldsymbol{\omega L_m})^{-1}\,\boldsymbol{\omega}\mathbf{b} \end{aligned}$$

$$\begin{aligned} \widetilde{\boldsymbol{y}}^{(\boldsymbol{k}+\mathbf{1})} = {} & [(\boldsymbol{T_m} - \boldsymbol{\omega L_m})^{-1}((\mathbf{1}-\boldsymbol{\omega})\boldsymbol{T_m} + \boldsymbol{\omega U_m})]^{9}\boldsymbol{y}^{(\boldsymbol{k}-\mathbf{1})} \\ & + \Big[\boldsymbol{I} + (\boldsymbol{T_m} - \boldsymbol{\omega L})^{-1}\big((\mathbf{1}-\boldsymbol{\omega})\boldsymbol{T_m} + \boldsymbol{\omega U_m}\big) \\ & + \Big((\boldsymbol{T_m} - \boldsymbol{\omega L_m})^{-1}\big((\mathbf{1}-\boldsymbol{\omega})\boldsymbol{T_m} + \boldsymbol{\omega U_m}\big)\Big)^{2} \\ & + \Big((\boldsymbol{T_m} - \boldsymbol{\omega L_m})^{-1}\big((\mathbf{1}-\boldsymbol{\omega})\boldsymbol{T_m} + \boldsymbol{\omega U_m}\big)\Big)^{3} \\ & + \Big((\boldsymbol{T_m} - \boldsymbol{\omega L_m})^{-1}\big((\mathbf{1}-\boldsymbol{\omega})\boldsymbol{T_m} + \boldsymbol{\omega U_m}\big)\Big)^{4} \\ & + \Big((\boldsymbol{T_m} - \boldsymbol{\omega L_m})^{-1}\big((\mathbf{1}-\boldsymbol{\omega})\boldsymbol{T_m} + \boldsymbol{\omega U_m}\big)\Big)^{5} \\ & + \Big((\boldsymbol{T_m} - \boldsymbol{\omega L_m})^{-1}\big((\mathbf{1}-\boldsymbol{\omega})\boldsymbol{T_m} + \boldsymbol{\omega U_m}\big)\Big)^{6} \\ & + \Big((\boldsymbol{T_m} - \boldsymbol{\omega L_m})^{-1}\big((\mathbf{1}-\boldsymbol{\omega})\boldsymbol{T_m} + \boldsymbol{\omega U_m}\big)\Big)^{7} \\ & + \Big((\boldsymbol{T_m} - \boldsymbol{\omega L_m})^{-1}\big((\mathbf{1}-\boldsymbol{\omega})\boldsymbol{T_m} + \boldsymbol{\omega U_m}\big)\Big)^{8}\Big](\boldsymbol{T_m} - \boldsymbol{\omega L_m})^{-1}\boldsymbol{\omega b} \end{aligned}$$

$$\begin{aligned} \boldsymbol{y}^{(\boldsymbol{k}+\mathbf{1})} = {} & [(\boldsymbol{T_m} - \boldsymbol{\omega L_m})^{-1}((\mathbf{1}-\boldsymbol{\omega})\boldsymbol{T_m} + \boldsymbol{\omega U_m})]^{3\boldsymbol{k}+3}\boldsymbol{y}^{(\mathbf{0})} \\ & + \Big[\boldsymbol{I} + (\boldsymbol{T_m} - \boldsymbol{\omega L_m})^{-1}\big((\mathbf{1}-\boldsymbol{\omega})\boldsymbol{T_m} + \boldsymbol{\omega U_m}\big) \\ & + \Big((\boldsymbol{T_m} - \boldsymbol{\omega L_m})^{-1}\big((\mathbf{1}-\boldsymbol{\omega})\boldsymbol{T_m} + \boldsymbol{\omega U_m}\big)\Big)^{2} \\ & + \Big((\boldsymbol{T_m} - \boldsymbol{\omega L_m})^{-1}\big((\mathbf{1}-\boldsymbol{\omega})\boldsymbol{T_m} \end{aligned}$$

$$+\omega U_m)\big)^3 + \cdots\cdots\Big((T_m-\omega L_m)^{-1}\big((1-\omega)T_m+\omega U_m\big)\Big)^{3k+2}\Big](T_m-\omega L_m)^{-1}\,\omega b \qquad (8.2)$$

If A is SPD then:

$$\rho\Big((T_m-\omega L_m)^{-1}\big((1-\omega)T_m+\omega U_m\big)\Big)<1$$

$$\therefore \lim_{k\to\infty}\big[(T_m-\omega L_m)^{-1}\big((1-\omega)T_m+\omega U_m\big)\big]^{3k+3}=0$$

$$\Rightarrow \lim_{k\to\infty} y^{(k+1)} = \lim_{k\to\infty}\big[(T_m-\omega L_m)^{-1}\big((1-\omega)T_m+\omega U_m\big)\big]^{3k+3}\sum_{k=0}^{\infty}\big[(T_m-\omega L_m)^{-1}\big((1-\omega)T_m+\omega U_m\big)\big]^{k}(T_m-\omega L_m)^{-1}\,\omega b$$

$$=0+[I-(T_m-\omega L_m)^{-1}((1-\omega)T_m+\omega L_m)]^{-1}b\omega(T_m-\omega L_m)^{-1}\to Y$$

$$\Rightarrow \rho[((T_m-\omega L_m)^{-1}((1-\omega)T_m+\omega U_m))^3]=\Big(\rho(T_m-\omega L_m)^{-1}\big((1-\omega)T_m+\omega U_m\big)\Big)^3<1 \qquad (8.3)$$

Theorem 7: If the SOR method converges then the IIS will converge more rapidly than GSOR and RGSOR.

Proof: The GSOR, RGSOR and IIS can be written respectively as,

$$y^{(k+1)}=Sy^{(k)}+I \qquad (8.4)$$

$$y^{(k+1)}=S^2y^{(k)}+J \qquad (8.5)$$

$$y^{(k+1)}=S^3x^{(k)}+K \qquad (8.6)$$

Where $S=(T_m-\omega L_m)^{-1}[(1-\omega)T_m+\omega U_m)$

$$I=\omega(T_m-\omega L_m)^{-1}\mathrm{b}$$

$$J=[I+(T_m-\omega L_m)^{-1}((1-\omega)T_m+\omega U_m)](T_m-\omega L_m)^{-1}b,$$

$$\mathrm{K}=[I+(T_m-\omega L_m)^{-1}\big((1-\omega)T_m+\omega U_m\big)+((T_m-\omega L_m)^{-1}((1-\omega)T_m+\omega U_m))^2](T_m-\omega l_m)^{-1}\omega b$$

Let the exact solution of eq (1) is X

$\Rightarrow Y=SY+I,\ Y=S^2Y+J$ and $Y=S^3Y+K$

let $k=0,1,2,\ldots$ are nonnegative integer.

Let's consider the GSOR method

$$y^{(k+1)}=Sy^{(k)}+I$$

$$\Rightarrow y^{(k+1)}-Y=Sy^{(k)}-Y+I$$

$$\Rightarrow y^{(k+1)}-Y=Sy^{(k)}-Y+I+SY-SY$$

$$\Rightarrow y^{(k+1)}-Y=S(y^{(k)}-Y)+SY+I-Y$$

$$\Rightarrow y-Y=S(y^{(k)}-Y)+Y-Y$$

$$\Rightarrow y^{(k+1)}-Y=S(y^{(k)}-Y)$$

$$\Rightarrow \|y^{(k+1)}-Y\|=\|S(y^{(k)}-Y)\| \le \|S\|\|(y^{(k)}-Y)\| \le \|S^2\|\|(y^{(k-1)}-Y)\|\le\cdots \le \|S^k\|\|(y^{(1)}-Y)\|$$

$$\Rightarrow \|y^{(k+1)}-Y\|\le\|S^k\|\|(y^{(1)}-Y)\|\le \|S\|^k\|y^{(1)}-Y\| \qquad \text{(a)}$$

Similarly, consider the refinement of GSOR and IIS.

$$\Rightarrow \|y^{(k+1)}-Y\|\le\|S^{2k}\|\|(y^{(1)}-Y)\|\le \|S\|^{2k}\|(y^{(1)}-Y)\| \qquad \text{(b)}$$

and

$$\Rightarrow \|y^{(k+1)}-Y\|\le\|S^{3k}\|\|(y^{(1)}-Y)\|\le \|S\|^{3k}\|(y^{(1)}-Y)\| \quad \text{(c)}$$

Using the inequalities, a, b and c, since $\|S\|<1$ we conclude that the IIS converges faster than GSOR and RGSOR if SOR converges.

7. RESULTS AND DISCUSSION

In this section some numerical examples have been experimented with. The comparative analysis of the proposed scheme is done with GSOR and RGSOR by using spectral radius and stability.

The below example 1, 2, 3 and 4 are referred from previously conducted studies [6-13]. Also, the results are depicted in tables 1-4 and figure 1 and 2.

Example 1:

$$A=\begin{bmatrix} 5 & -1 & 0 & 0 & -1 & 0 & 0 & -1 \\ -1 & 5 & -1 & 0 & 0 & 0 & -1 & -1 \\ 0 & -1 & 5 & -1 & 0 & -1 & -1 & 0 \\ 1 & 0 & -1 & 5 & -1 & 0 & 0 & -1 \\ -1 & -1 & 0 & 0 & 5 & -1 & 0 & -1 \\ 0 & 0 & -1 & -1 & 0 & 5 & 1 & -1 \\ -1 & 0 & 0 & 0 & -1 & 0 & 5 & -1 \\ -1 & 0 & -1 & 0 & -1 & 0 & -1 & 5 \end{bmatrix}; b=\begin{bmatrix} -2 \\ -1 \\ 4 \\ 13 \\ 4 \\ 2 \\ 9 \\ 12 \end{bmatrix}$$

Example 2:

$$A=\begin{bmatrix} 7 & -1 & 0 & -1 & 0 & -1 & 0 & -1 & 0 & 0 \\ -1 & 7 & -1 & 0 & -1 & 0 & -1 & 0 & -1 & 0 \\ 0 & -1 & 7 & -1 & 0 & -1 & 0 & -1 & 0 & -1 \\ 1 & 0 & -1 & 7 & -1 & 0 & -1 & 0 & -1 & 0 \\ 0 & -1 & 0 & -1 & 7 & -1 & 0 & -1 & 0 & -1 \\ -1 & 0 & -1 & 0 & -1 & 7 & -1 & 0 & -1 & 0 \\ 0 & -1 & 0 & -1 & 0 & -1 & 7 & -1 & 0 & -1 \\ -1 & 0 & -1 & 0 & -1 & 0 & -1 & 7 & -1 & 0 \\ 0 & -1 & 0 & -1 & 0 & -1 & 0 & -1 & 7 & -1 \\ 0 & 0 & -1 & 0 & -1 & 0 & -1 & 0 & -1 & 7 \end{bmatrix}; b=\begin{bmatrix} 7 \\ 3 \\ 2 \\ 2 \\ 2 \\ 2 \\ 2 \\ 2 \\ 2 \\ 2 \end{bmatrix}$$

Example 3:

$$A=\begin{bmatrix} -4 & 1 & 0 & 1 & 0 & 0 & 0 & 0 & 0 \\ 1 & -4 & 1 & 0 & 1 & 0 & 0 & 0 & 0 \\ 0 & 1 & -4 & 0 & 0 & 1 & 0 & 0 & 0 \\ 1 & 0 & 0 & -4 & -1 & 0 & 0 & 0 & -1 \\ 0 & 1 & 0 & 1 & -5 & -1 & 0 & 0 & -1 \\ 0 & 0 & 1 & 0 & 1 & -4 & 0 & 0 & 1 \\ 0 & 0 & 0 & 1 & 0 & 0 & -4 & 1 & 0 \\ 0 & 0 & 0 & 0 & 1 & 0 & 1 & -4 & 1 \\ 0 & 0 & 0 & 0 & 0 & 1 & 0 & 1 & -4 \end{bmatrix}; b=\begin{bmatrix} 1/512 \\ 4/512 \\ 9/512 \\ 4/512 \\ 16/512 \\ 36/512 \\ 9/512 \\ 36/512 \\ 81/512 \end{bmatrix}$$

Example 4:

$$A=\begin{bmatrix} 2 & -3 & 0 & 0 & 0 & 0 \\ -1 & 4 & -1 & 0 & -1 & 0 \\ 0 & -1 & 4 & 0 & 0 & -1 \\ 0 & 0 & 0 & 2 & -3 & 0 \\ 0 & -1 & 0 & -1 & 4 & -1 \\ 0 & 0 & -1 & 0 & -1 & 4 \end{bmatrix}; b=\begin{bmatrix} -5/3 \\ 2/3 \\ 3 \\ -4/3 \\ -1/3 \\ 5/3 \end{bmatrix}$$

Fig. 1. The spectral radius of the improved method in comparison to other schemes.

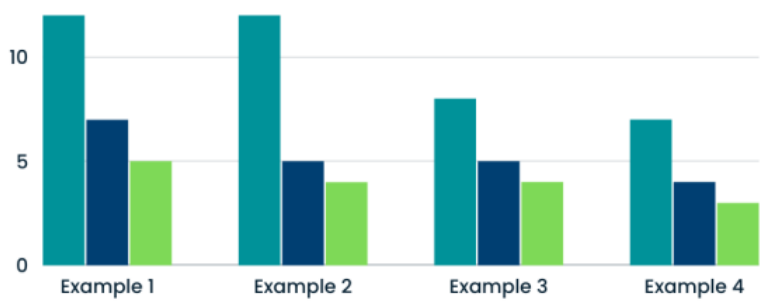

Fig. 2. The number of iterations taken by the improved method in comparison to other schemes.

Table 1. Numerical Results from example 1.

Methods	No of iterations	Spectral Radius	Stability (infinity norm) set up to 4th iteration
GSOR	12	0.1319	0.0372
RGSOR	07	0.0174	0.0004
IIS	05	0.0022	0.000003

Table 2. Numerical Results from example 2.

Methods	No of iterations	Spectral Radius	Stability (infinity norm) set up to 4^{th} iteration
GSOR	12	0.1460	0.02777
RGSOR	05	0.0350	0.00024
IIS	04	0.0066	0.000009

Table 3. Numerical Results from example 3.

Methods	No of iterations	Spectral Radius	Stability (infinity norm) set up to 4^{th} iteration
GSOR	08	0.1617	0.00099
RGSOR	05	0.0261	0.000013
IIS	04	0.0042	0.00000044

Table 4. Numerical Results from example 4.

Methods	No of iterations	Spectral Radius	Stability (infinity norm) set up to 4^{th} iteration
GSOR	07	0.5954	0.0589
RGSOR	04	0.3546	0.0005
IIS	03	0.2111	0.000003

The null vector is used as an initial approximation with a tolerance of 0.00001. The value of ω is taken optimally. In example 01, The coefficient matrix A is SDD and SPD with m=1 and ω=1.0695. In example 02, A is SDD and an M-matrix with m=1 and ω=1.099. In the example, 03 A is an SDD matrix with m=1 and ω=1.1617. In example 4, A is an M matrix with m=1 and ω=1.098.

8. CONCLUSION

An improved iterative scheme using successive over-relaxation for the solution of a linear system of equations is presented in this paper. The convergence of IIS for M-matrix, SPD and SDD, is examined and four numerical examples are presented using MATLAB version R2014b (8.4.0.150421). In aspects of the number of iterations and error analysis, all results obtained by IIS are compared to the first refinement of generalized SOR and generalized SOR, as shown in tables 1, 2, 3 and 4. The evolution of the result shows that the IIS converges faster than the GSOR and RGSOR.

The presented method works efficiently, however, it is only applicable to M-matrix, SPD and SDD matrices, Future work can be done in the application of similar improvement techniques to methods that are more robust and can handle a large variety of matrices.

9. CONFLICT OF INTEREST

The authors declare no conflict of interest.

10. REFERENCES

1. H. Muleta, and G. Gofe. Refinement of generalized accelerated over relaxation method for solving system of linear equations based on the Nekrassov-Mehmke1-method. *Ethiopian Journal of Education and Sciences* 13: 1-18 (2018).
2. Y. Saad. Iterative methods for sparse linear systems. *Society for Industrial and Applied Mathematics USA* (2003).
3. V.K. Vatti, and G.G. Gonfa. Refinement of generalized Jacobi (RGJ) method for solving system of linear equations. *International Journal of Contemporary Mathematical Sciences* 6: 109-116 (2011).
4. F. Mohammed, and M. Rivaie. Jacobi–Davidson, Gauss–Seidel and successive over-relaxation for solving systems of linear equations. *Applied Mathematics and Computational Intelligence* 6: 41-52 (2017).
5. F. Hailu, G.G. Gonfa, and H.M. Chemeda. Second Degree Generalized Successive Over Relaxation

Method for Solving System of Linear Equations. *Momona Ethiopian Journal of Science* 12: 60-71 (2020).
6. M. Saha, and J. Chakrabarty. On generalized jacobi, gauss-seidel and SOR methods. arXiv, *Cornell University* 1806.07682 (2018).
7. G.G. Gonfa. Refined Iterative Method for Solving System of Linear Equations. *American Journal of Computational and Applied Mathematics* 6: 144–47 (2016).
8. R.A. Horn, and C. R. Johnson. Matrix Analysis. Cambridge University Press, Cambridge, England MR0832183 (1985).
9. B.N. Datta. Numerical Linear Algebra and Applications. *Society for Industrial and Applied Mathematics, Philadelphia, USA* (2010).
10. R.L. Burden, and J.D. Faires. Numerical Analysis. *Cengage Learning* (2015).
11. M.S.R. Baloch, Z.A. Kalhoro, M.S. Khalil, and A.W. Shaikh. A New Improved Classical Iterative Algorithm for Solving System of Linear Equations. Proceedings of the Pakistan Academy of Sciences: *A. Physical and Computational Sciences* 58: 69-81 (2021).
12. G. Dessalew, T. Kebede, G. Awgichew, and A. Walelign. Generalized Refinement of Gauss-Seidel Method for Consistently Ordered 2-Cyclic Matrices. *Abstract and Applied Analysis* 2021: 8343207 (2021).

Proceedings of the Pakistan Academy of Sciences: A Physical and Computational Sciences 59(3):45-53 (2022)

ISSN (Print): 2518-4245; ISSN (Online): 2518-4253
https://doi.org/10.53560/PPASA(59-3)654

Pakistan Academy of Sciences

Research Article

Determination of Temperature Distribution of Rohri, Sindh using Artificial Neural Network and Regression Analysis

Adeel Tahir[1*], Muhammad Ashraf[1], Zaheer Uddin[2], Muhammad Sarim[3], and Syed Masood Raza[1]

[1]Department of Physics, Federal Urdu University of Arts Science and Technology, Karachi, Pakistan
[2]Department of Physics, University of Karachi, Karachi, Pakistan
[3]Department of Computer Science, Federal Urdu University of Arts Science and Technology, Karachi. Pakistan

Abstract: As time passes, the world is facing the problem of global warming, which results in a rise in average daily temperature. Proper knowledge of temperature distribution and future prediction may help to cope with the situation in the near future. Climate forecasting has gone through various faces; in the early days' people used to predict the behavior qualitatively. Now environmental scientists have developed a quantitative method for forest climate behavior with certain uncertainties. Empirical models have been developed based on regression analysis to estimate temperature distribution. Two models, linear and non-linear, use dew point temperature and relative humidity as independent variables. In addition to regression analysis, Artificial Neural Network (ANN) has been utilized to predict the average daily temperatures of Rohri Sindh, a city in Pakistan in the Sindh province. Both empirical models and ANN estimates are in good agreement with the known values of average daily temperatures.

Keywords: Artificial Neural Network, Estimated Model, Temperature Distribution, Forecasting, Rohri

1. INTRODUCTION

People have been forecasting climate changes manually since ancient times. Today, daily climate information can be recorded automatically due to technological developments. Once the data is recorded, it is projected to forecast the climatic information for the future. But the chaotic state of climate still causes forecast errors which makes the forecast prediction unreliable for a long time period. Therefore, further investigation is required to address the challenges in predicting the weather forecast. Reliable weather forecast is beneficial for humans in different aspects and they can prepare themselves to face the challenges in upcoming disasters. Although the researchers have developed various tools and made a significant contribution to metrology, it still requires further studies to overcome the existing challenges in weather forecasts [1].

Changing climate is the World's first environmental issue that presents a risk to humans. Industries are highly influential in causing this issue and the recent global warming that the planet has experienced. Extreme changes in air temperature can harm plants and animals, so knowing the variability of ambient temperature is critical in agriculture [2,3]. Temperature plays a vital role in routine life. The prediction of temperature for the respective region highly depends on the accurate data observed. Forecasting air temperature helps determine the probability of tornadoes and floods in a given region [4]. Soil temperature, energy load consumption, and solar radiation also depend on accurate forecasting of temperature [2]. Artificial neural networks are powerful techniques, which do not require any mathematical expressions to solve complex non-linear problems [5]. ANN model was designed to predict the highest winter temperature in Tehran (Iran) which consists of three input

Received: July 2022; Accepted: September 2022
*Corresponding author: Adeel Tahir <adeel.tahir@fuuast.edu.pk>

layers, nine hidden layers with hyperbolic tangent function, and one output layer. The estimated statistical parameters were found in the acceptable range [6]. A temperature prediction model is proposed based on the long short-term memory (LSTM) neural network. The model also refines the missing data and may forecast the temperature time series up to 14 days [7]. Another model based on (LSTM) NN may forecast the short-term temperature of Bandung (capital of West Java) with high accuracy by using the long period data [8]. During the period 1998 to 2000, a neural network estimated Saudi Arabia's solar radiation by using temperature and relative humidity [9]. Sea surface temperature (SST) and numerical estimations by ANN were combined with a special wavelet neural network to study the forecast of six different locations in the Indian Ocean over three-time scales (daily, weekly, and monthly). The performance was assessed by statistical error analyses, which showed satisfactory results [10]. A statistical post-processing method was proposed based on the Land-Atmosphere Modeling Package Weather Research and Forecasting model, which uses a Generalized Linear model and parameter correction to increase the accuracy of numerical weather prediction (NWP). The spatial distribution of temperature and wind speed (July and January, East Asia) was analyzed to show their consistent relation [11]. The method is based on the Geographically Weighted Kigring Regression model, which was applied to forecast Poland's spatial distribution of air temperature. It extends Hengl's decision tree to select the suitable prediction model for varying temperature and environmental predictors. The Local Geographically Weighted regression model was chosen to model the deterministic part of spatial variation. Sixty-nine air temperature cases (with time aggregation from daily to mean annual temperature) were analyzed. The author claimed local prediction models for air temperature were better fitted in spatial distribution irrespective of data aggregation [12]. The daily max and min temperature series (1887 to 2019) were constructed and homogenized by Tianjin Meteorological Archive to estimate the warning trends (0.154 ± 0.013 °C per decade) for the last 130 years [13]. A physical model was developed to predict the runway surface temperature at Oslo Airport, Norway. A Now-casting model was designed to estimate the surface temperature for the next three hours. The predictions were more satisfactory at the beginning of winter [14]. A polynomial fitting technique for computing the mean daytime and a double-cosine method was introduced to estimate daily ambient temperature profiles for any place in Europe using a spatially continuous database [15]. Based on daily data set from more than 5000 meteorological stations all over the World concluded that during the last century, the mean temperature, the maximum and minimum temperature increased by 0.5 °C, 0.050 °C, and 0.018 °C, respectively. Also observed is that rate of increase in minimum temperature is greater than maximum temperature [16]. From 1977 to 1994, the air temperature of high-altitude regions such as the Middle Mountains and the High Himalayas of Nepal was studied. The mean temperature per year increases by 0.06 °C. In the Terai and Siwalik areas, a significant decreasing trend was found. In addition, relative to other seasons, winter was found to be warm [17]. In Nepal, during 30 years (1975-2005), an increasing trend of mean temperature was observed by a factor of around 0.04 °C [18]. From 1950 to 2004 period, analyzed maximum temperature of 4280 stations, minimum temperature of 4284 stations and Diurnal temperature change (DTR) of 4157 stations of the entire World and found an increase of 0.296 °C, 0.287 °C, and 0.296 °C per decade for mean, maximum and minimum temperatures respectively [19].

This paper presents the work to forecast the air temperature using an Artificial neural network and multi-regression models of Rohri, Sindh based on two independent parameters, namely relative humidity and dew point.

2. STUDY AREA

The study area namely "Rohri" is situated on the east bank of the river Indus. It is one of the famous cities of Sindh province (Pakistan). It is also the Taluka of the Sukkur district. Rohri is a metropolitan city with a population of around 70,000 people. The area of this ancient city is 1,318 km^2.

Its geographical location (see Figure 1) lies at 27° 27′ 18″ N latitude, 68° 55′ 53″ E longitude and an altitude of 66 m. Rohri has a tropical desert like weather with scorching summers and chill winters. It remains hot and dry all over the summer. The temperature usually falls between 46 °F to 111 °F in a year, with temperatures rising above 117 °F and rarely falling below 40 °F [20,21].

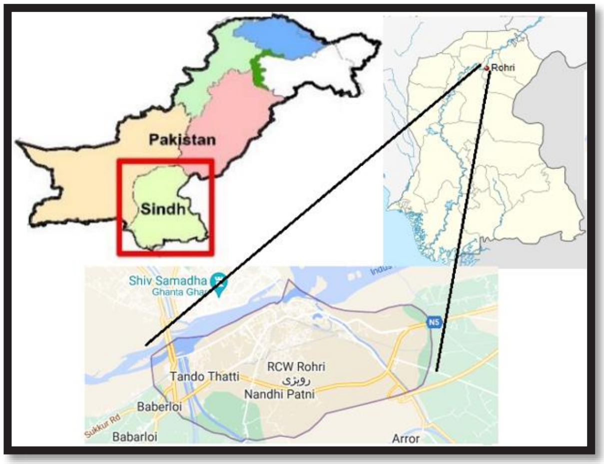

Fig. 1. Geographical location of Rohri, Sindh

3. MATERIALS AND METHODS

First weather parameters data was collected from the Pakistan Meteorological Department, Government of Pakistan, then two different models were designed to forecast the air temperature of Rohri (Sindh).

3.1 Artificial Neural Network

Artificial neural networks (ANN) are powerful mathematical tools developed from the inception of the human brain. They are widely used to solve complex problems involving non-linear behavior. ANN structure is based on three layers: the input layer, the hidden layer, and the out layer. The input layer receives data, which is then transferred to hidden layers, where the desired task is solved based on mathematical models internally designed on independent input variables. The result of hidden layers proceeds to the output layer [22]. The complete procedure involves two steps: First, an ANN is trained until it emulates according to the data provided; then, the network is used to predict the inputs not included in training data [23]. In this study, the designed ANN model is shown in Figure 2, which was utilized to estimate the mean daily temperature of Rohri city.

In this work, a feed-forward network model was constructed in MATLAB. The model predicts the temperature by taking in the dew point and relative humidity. It consists of three layers named as the input layer, hidden layer and output layer, where the input layer consists of two neurons, the hidden layer of ten neurons and the output layer of one neuron respectively. The non-linear complex mathematical model in the hidden layers was designed with a sigmoidal transfer function.

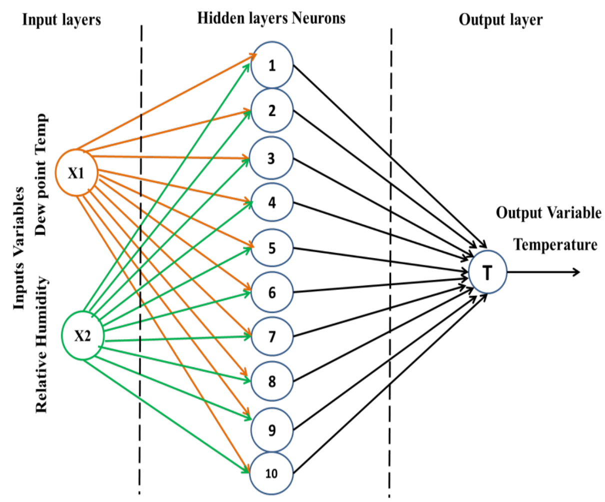

Fig. 2. 3 layered Feed-forward neural network

The output layer with one neuron contains the linear transfer function. The forecasted temperature T is given by

$$T = \sum_{i=1}^{10} \omega_i N_i + \beta \qquad (1)$$

Where bias β= 1.9578 and weights ωi are given in Table I.

Here, Ni can be calculated by the following equation

$$N_i = \frac{1}{1 + e^{-\Upsilon i}} \qquad (2)$$

ϒi can be calculated using the following formula,

$$\Upsilon i = \omega_{1i}\,\chi_1 + \omega_{2i}\,\chi_2 + b_i \qquad (3)$$

Where ωji indicates the jth synaptic link weight for ith neuron, bi the bias for that hidden neuron, χ_1 the dew point, and χ_2 the humidity.

3.2 Linear and Non-Linear Regression Models

The proposed linear and non-linear regression models are presented in the equations 4 and 5, where the bivariate functions give the daily mean temperature. Dew point and relative humidity are taken as independent input parameters.

The regression models in equation 4 are linear.

$$T = a + bT_d + c\,R_h \qquad (4)$$

Where regression coefficients are indicated by a, b and c respectively, R_h the relative humidity, while T and Td the daily mean temperature, and dew point respectively.

The regression models in equation 5 are non-linear.

$$T = a_o + a_1T_d + a_2R_h + a_3\left(\frac{{T_d}^2}{{R_h}^2}\right) \qquad (5)$$

where regression coefficients are indicated by a_o,a_1,a_2 and a_3 respectively, R_h the relative humidity, while T and Td the daily mean temperature, and dew point respectively.

3.3 Statistical Measurements for Authentication of Designed Models

By using statistical techniques including coefficient of determination R^2, Mean Absolute Percent Error (MAPE), Mean Absolute Error (MABE) and Mean Square Error (MSE), we have calculated the accuracy of our designed models.

$$MSE = \frac{1}{n}\sum_{k=1}^{n}(T_{c.k} - T_{m.k})^2 \qquad (6)$$

$$MABE = \frac{1}{n}\sum_{k=1}^{n}|T_{c.k} - T_{m.k}| \qquad (7)$$

$$MAPE = \frac{1}{n}\sum_{k=1}^{n}\left|\frac{(T_{c.k} - T_{m.k})}{T_{m.k}}\right| x100 \qquad (8)$$

$$R^2 = \left[1 - \frac{\sum_{k=1}^{n}(T_{c.k} - T_{m.k})^2}{\sum_{k=1}^{n}(T_{c.k} - \overline{T_m})^2}\right] \qquad (9)$$

4. RESULTS AND DISCUSSION

In this article, the temperature distribution for one of the cities (Rohri) province Sindh, Pakistan, has been investigated through two different directions, i.e., ANN and multiple regression analysis.

In ANN, the Levenberg–Marquardt algorithm with 10 hidden layers was used to train the network from 2015 - 2017 based on variables i.e dew point, relative humidity, and mean daily temperature. 70% data of this period were used to train, whereas the remaining 30% equally divide for validation and testing, respectively. As the network was trained, based on independent variable dew point and relative humidity, the mean daily temperature was forecasted for 2018 - 2020. Graphical analysis of actual and forecasted mean daily temperature with errors was found, shown in Figure 3. The ω1i and ω2i were the weights of neurons of input variables, whereas ωi represented the weights of hidden layers of neurons. The biases bi were also determined and represent all values in Table 1.

Furthermore, two empirical models, multilinear regression (model 2) and multi non-linear regression (model 3) were designed to forecast the mean daily temperature distribution. To determine regression coefficients, the related weather data from 2015 - 2017 was used to design the empirical models. The equations (see equations 10 and 11) for both models are formed by substituting equations 4 and 5, respectively. By these equations, the temperature-distribution for 2018-2020 (see Figure 4) is forecasted using dew point and relative humidity as independent input variables. To confirm the validation and performance of ANN and empirical models, statistical errors such as Mean Square Error (MSE), Mean Absolute Error (MABE), Mean Absolute Percent Error (MAPE), and R^2 were estimated. The best model was identified by comparing these calculated statistical errors.

$$T = 49.102658 + 1.061672\,T_d \\ -0.628384\,R_h \qquad (10)$$

$$T = 40.764341 + 0.939534\;T_d - 0.420574\,R_h \\ + 2.988233\left(\frac{{T_d}^2}{{R_h}^2}\right) \qquad (11)$$

It has observed the statistical errors calculated for ANN model result having lowest values than both estimated (linear and non-linear regression) models as shown in Table 2. The maximum root mean square error was 4.35 ^{o}F 2.85 ^{o}F, and 1.47 ^{o}F in 2018, 2019 and 2020 by a linear model. Since the weather is unpredictable due to complexity and non-linearity, our estimated non-linear model 3 showed a better result than estimated linear model 2. The minimum errors less than 0.5 ^{o}F from 2018-2020 have been observed in non-linear model 3. The ANN model shows the more reliable results for Rohri city.

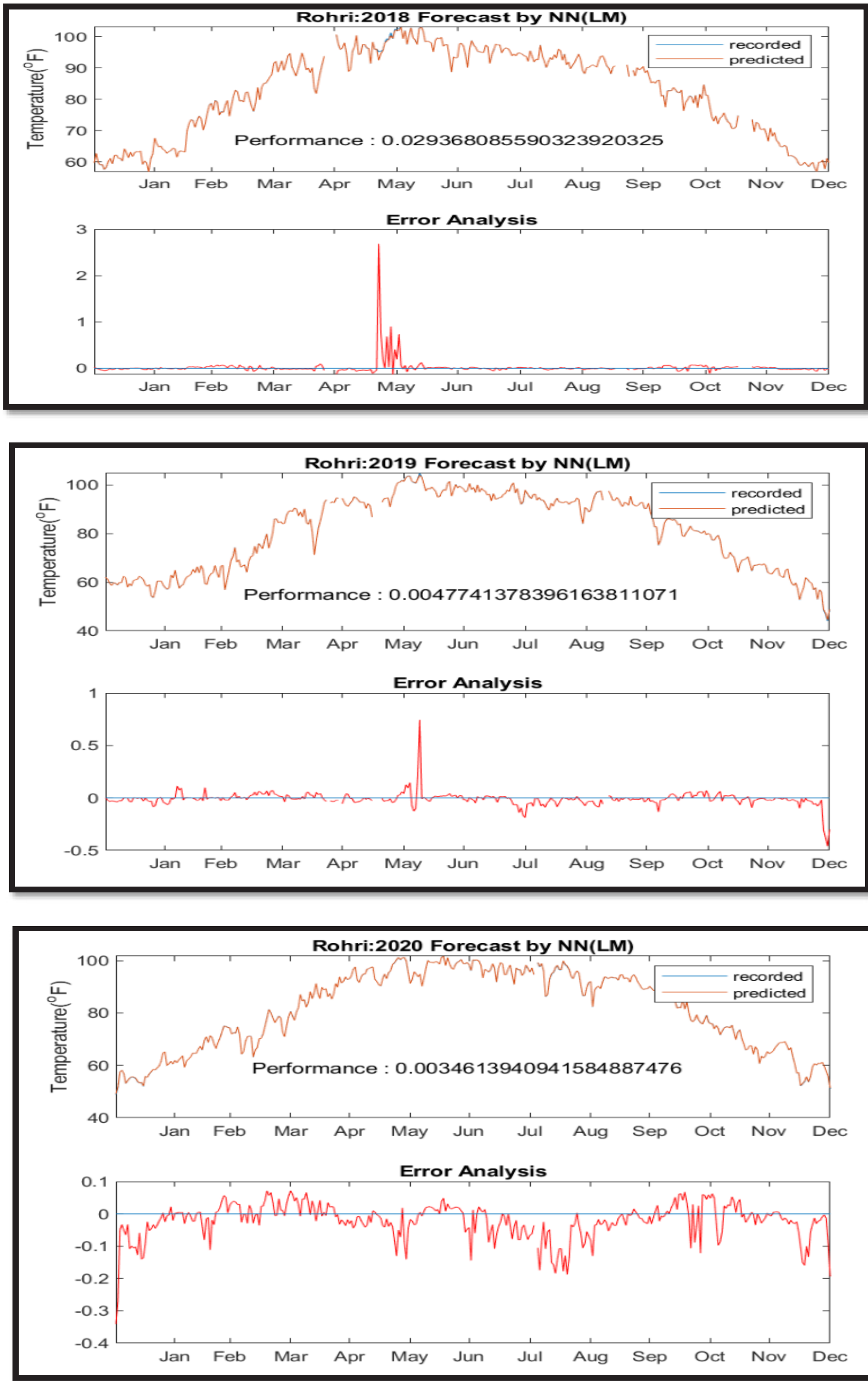

Fig. 3. Graphical analysis of recorded and predicted mean daily temperature of Rohri (2018-2020)

Table 1. Hidden layer neurons syanptic weights with biases

I	ω_{1i}	ω_{2i}	ω_i	b_i
1	-6.7467	-0.4713	3.5673	-7.7792
2	7.9793	0.0062	0.9250	-6.5946
3	0.7358	0.0290	-3.6938	2.7148
4	0.3354	-0.7788	-1.0415	-2.0080
5	-1.3409	0.5959	0.0524	-1.1601
6	0.1757	-3.3364	-0.3609	0.5331
7	-1.1484	0.0538	2.3892	1.1018
8	3.3007	0.0072	-2.6706	-1.9695
9	-4.1774	-0.0075	-4.6420	-3.4720
10	5.7911	-0.1191	-0.7732	4.9713

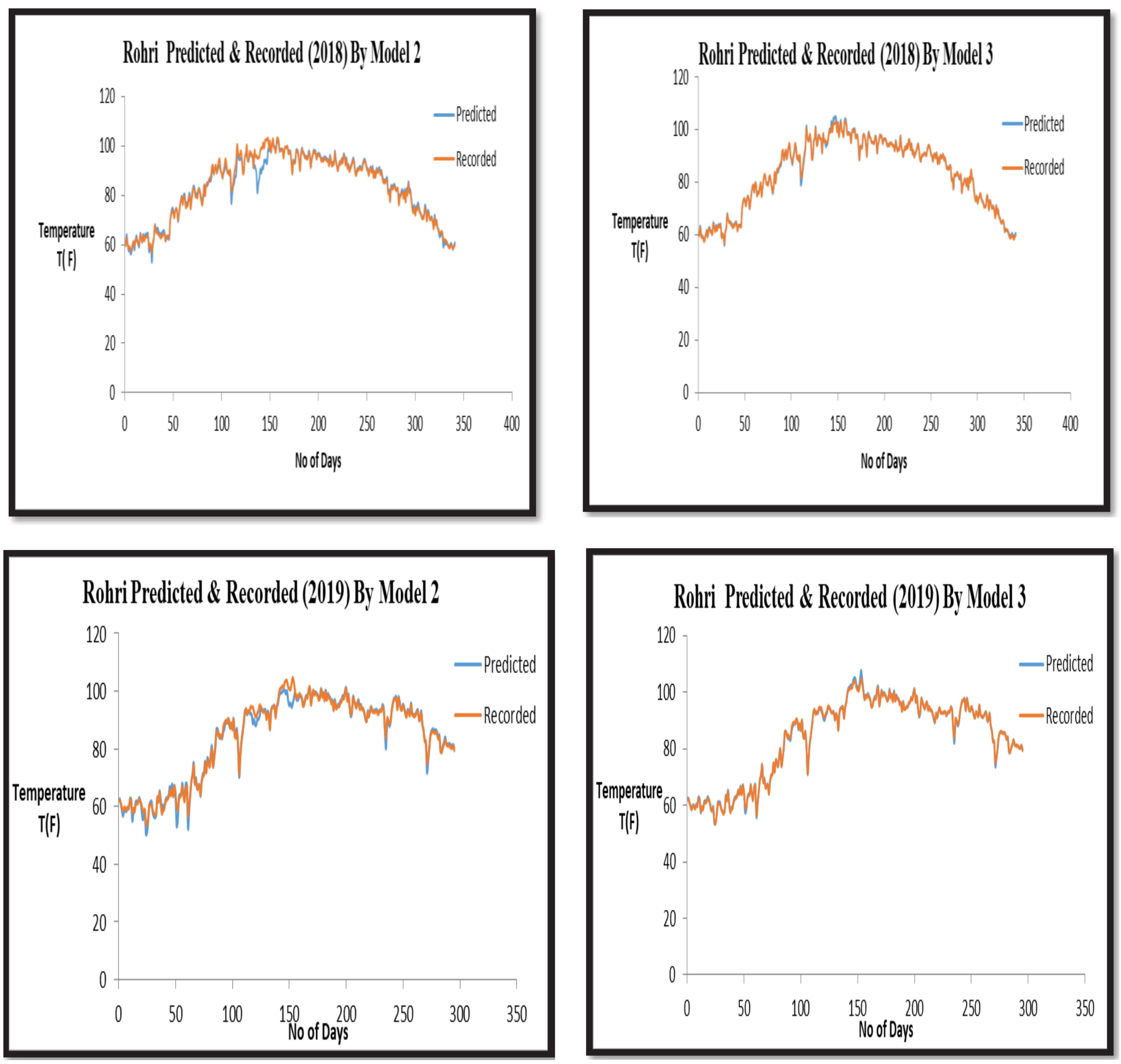

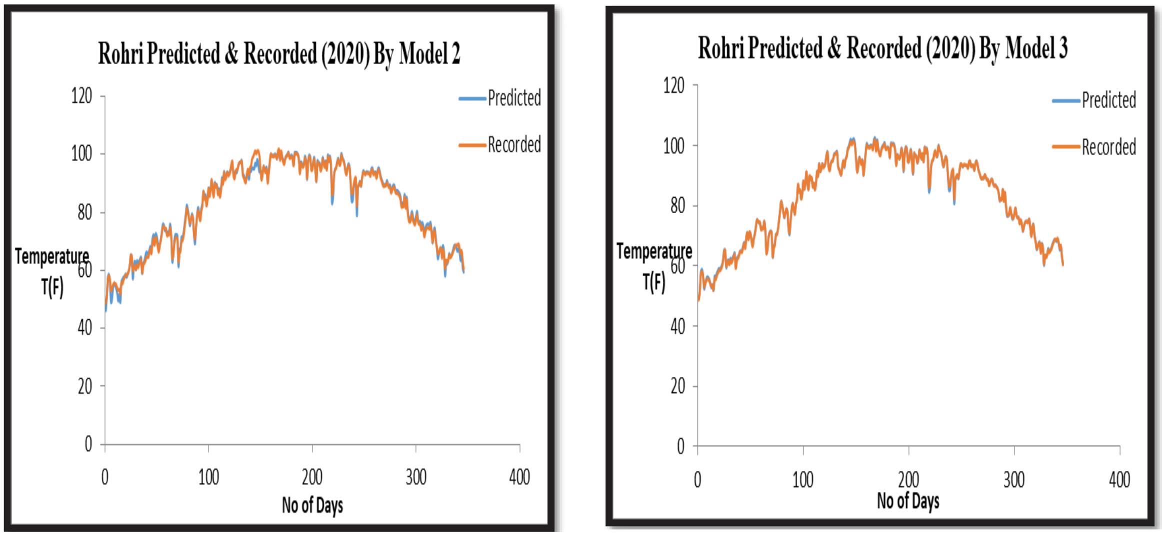

Fig. 4. The comparative analysis of temperature distribution (2018 – 2020) (a) model 2 (linear) and (b) model 3 (non-linear)

Table 2. Statistical Errors calculated between actual and forecasted temperature distribution (2018-2020) by ANN, Linear Regression, and Non-Linear Regression

Model	Year	MSE	MABE	MAPE	R^2
Model 1	2018	0.029368	0.04386	0.05016	0.99984
ANN	2019	0.00477	0.03492	0.04688	0.99997
	2020	0.00346	0.04029	0.05326	0.99998
Model 2	2018	4.3541594	1.14461	1.35716	0.97667
Linear Regression	2019	2.8494416	1.08434	1.46396	0.98886
	2020	1.4693335	0.87636	1.1713	0.99369
Model 3	2018	0.2549779	0.31374	0.38892	0.99866
Non Linear Regression	2019	0.2408168	0.32869	0.43837	0.99902
	2020	0.128415731	0.265981	0.35649	0.999484

5. CONCLUSION

This study was conducted to forecast the mean daily temperature distribution for Rohri, Sindh, Pakistan, based on three designed models including ANN model, a multi linear regression model and a non-linear multi regression. The ANN model takes in relative humidity and dew point as the input independent variables, and returns mean daily temperature as the output dependent variable. It consists of three layers including input, hidden and the output layers. We trained the machine to determine the temperature based on two independent variables, i.e., dew point and relative humidity, for the duration 2015-2017. As the machine trained, weights and bias were obtained, which were used to forecast the mean daily temperature for the next three years, 2018 - 2020. An excellent forecast was received and observed by ANN model 1. The statistical errors were less than ±0.1 for the years 2018- 2020.

Further, two estimation models were designed, multilinear regression (model 2) and non-linear multi regression (model 3). Three years 2015-2017, weather data were used to estimate the regression coefficients. During estimation, MABE for the linear and non-linear models were found ±1.07 and ±0.44, respectively. These coefficients are then employed for models 2 and 3 for forecasting temperatures for the years 2018-2020 on dew point and relative humidity.

To investigate the correlation between actual and forecasted mean daily temperature, the coefficient of determination R^2 was calculated. In all three models, R^2 determined close to 1, which shows a high correlation between them.

To see the authenticity of ANN and estimated multi regression models, statistical errors MSE, MABE, and MAPE were calculated. In ANN, the MSE, MABE, and MAPE were in the lowest range (between 0 and 0.1) as compared to non-linear model 3 (between 0.1 and 0.3) and linear model 2 (between 1.4 and 4.4).

All the model's actual and forecasted mean daily temperature distribution graphs were highly overlapped (see figure 3,4). So, we can conclude that for the Rohri city, non-linear regression model 3 showed better results to forecast the temperature than the linear regression model. Thus, it was proved that the ANN model forecast the temperature seemed more accurate than estimated empirical models.

6. ACKNOWLEDGEMENT

The metrological weather parameters data are gathered from the Pakistan Meteorological Department, Government of Pakistan. Data can be verified from website. https://en.tutiempo.net/climate/ws-417250.html.

7. CONFLICT OF INTEREST

The authors declare no conflict of interest.

8. REFERENCES

1. M. Hayati, and Z. Mohebi. Application of artificial neural networks for temperature forecasting. World Academy of Science, Engineering and Technology 28: 275-279 (2007).
2. Ö.A. Dombaycı, and M. Gölcü. Daily means ambient temperature prediction using artificial neural network method: A case study of Turkey. Renewable Energy 34: 1158-1161 (2009).
3. B.A. Smith, G. Hoogenboom, and R.W. McClendon. Artificial neural networks for automated year-round temperature prediction. Computers and Electronics in Agriculture 68: 52-61 (2009).
4. I. Tasadduq, S. Rehman, and K. Bubshait. Application of neural networks for the prediction of hourly mean surface temperatures in Saudi Arabia. Renewable Energy 25: 545-554 (2002)
5. M. Kumar , N. S. Raghuwanshi, R. Singh, W. W. Wallender, and W. O. Pruitt. Estimating evapotranspiration using artificial neural network. Journal of Irrigation and Drainage Engineering 128: 224-233 (2002).
6. E. F. Nezhad, G. F. Ghalhari, and F. B. Forecasting maximum seasonal temperature using artificial neural networks "Tehran case study". Asia-Pacific Journal of Atmospheric Sciences 55: 145-153 (2019).
7. I. Park, H.S. Kim, J. Lee, J.H. Kim, C.H. Song, and H.K. Kim. Temperature prediction using the missing data refinement model based on a long short-term memory neural network. Atmosphere 10: 718 (2019).
8. S. Zahroh, Y. Hidayat, R. S. Pontoh, A. Santoso, Sukono, and A. T. Bon. Modeling and forecasting daily temperature in bandung. Proceedings of the International Conference on Industrial Engineering and Operations Management Riyadh, Saudi Arabia 406-412 (2019).
9. S. Rehman, and M. Mohandes. Artificial neural network estimation of global solar radiation using air temperature and relative humidity. Energy Policy 36: 571-576 (2008).
10. K. Patil, M.C. Deo, and M. Ravichandran. Prediction of sea surface temperature by combining numerical and neural techniques. Journal of Atmospheric and Oceanic Technology 33: 1715-1726 (2016).
11. J. Jeong, and S.J. Lee. A statistical parameter correction technique for WRF medium-range prediction of near-surface temperature and wind speed using generalized linear model. Atmosphere 9: 291 (2018).
12. M. Szymanowski, M. Kryza, and W. Spallek. Regression-based air temperature spatial prediction models: an example from Poland. Meteorologische

Zeitschrift 22: 577-585 (2013).

13. P. Si, Q. Li, and P. Jones. Construction of homogenized daily surface air temperature for the city of Tianjin during 1887–2019. Earth System Science Data 13: 2211-2226 (2021).
14. A.D.W. Nuijten. Runway temperature prediction, a case study for Oslo Airport, Norway. Cold Regions Science and Technology 125: 72-84 (2016).
15. T.A. Huld, M. Šúri, E.D. Dunlop, and F. Micale. Estimating average daytime and daily temperature profiles with in Europe. Environmental Modeling & Software 21: 1650-1661 (2006).
16. D.R. Easterling, B. Horton, P.D. Jones, T.C. Peterson, T.R. Karl, D.E. Parker, M.J. Salinger, V. Razuvayev, N. Plummer, P. Jamason, and C. Folland. Maximum and minimum temperature trends for the globe. Science 277: 364-367 (1997).
17. A.B. Shrestha, C.P. Wake, P.A. Mayewski, and J. E. Dibb. Maximum temperature trends in the Himalaya and its vicinity: an analysis based on temperature records from Nepal for the period 1971–94. Journal of climate 12: 2775-2786 (1999).
18. K.L. Shrestha. Global change impact assessment for Himalayan mountain regions for environmental management and sustainable development. Global Environmental Research-English Edition 9: 69 (2005).
19. R.S. Vose, D.R. Easterling, and B. Gleason. Maximum and minimum temperature trends for the globe: An update through 2004. Geophysical Research Letters 32: (2005).
20. M. Ali, and M. J. Iqbal. Extreme rainfall incidents over Sindh province, against different return periods. Proceedings of the Pakistan Academy of Sciences 50: 159-166 (2013).
21. K. Aftab, and S. A. Jilani. Sunspots Influence on Climatic Variability of Karachi and Rohri: Sunspots Influence on Climatic of Karachi. Pakistan Journal of Scientific & Industrial Research Series A: Physical Sciences 64: 52-58 (2021).
22. S. Mehdizadeh. Assessing the potential of data-driven models for estimation of long-term monthly temperatures. Computers and Electronics in Agriculture 144: 114-125 (2018).
23. J. Cifuentes, G. Marulanda, A. Bello, and J. Reneses. Air temperature forecasting using machine learning techniques: a review. Energies 13: 4215 (2020).

Proceedings of the Pakistan Academy of Sciences: A Physical and Computational Sciences 59(3): 55-67 (2022)

ISSN (Print): 2518-4245; ISSN (Online): 2518-4253
https://doi.org/10.53560/PPASA(59-3)609

Pakistan Academy of Sciences

Research Article

Some Studies of Multi-Polar Fuzzy Ideals in LA-Semigroups

Fareeha Pervaiz*, Muhammad Shabir, and Muhammad Aslam

Department of Mathematics, Quaid-i-Azam University Islamabad, Pakistan

Abstract: This article's main goal is to investigate the concept of multi-polar fuzzy sets (MPF-sets) in LA-semigroups, which is an extension of bi-polar fuzzy sets (BPF-sets) in LA-semigroups. The main objective of this research is to extend certain significant BPF-set results to MPF-sets results. This article introduces the concepts of multi-polar fuzzy sub LA-semigroups, multi-polar fuzzy quasi-ideals, multi-polar fuzzy bi-ideals, multi-polar fuzzy generalized bi-ideals, and multi-polar fuzzy interior ideals in LA-semigroups. This article also discusses a number of fundamental aspects of multi-polar fuzzy ideals, and we use these aspects to define regular LA-semigroups.

Keywords: Multi-Polar Fuzzy Sub LA-semigroups, Multi-Polar Fuzzy Generalized Bi-Ideals, Multi-Polar Fuzzy Bi-Ideals, Multi-Polar Fuzzy Quasi-Ideals, Multi-Polar Fuzzy Interior Ideals

1. INTRODUCTION

Over the course of the field's evolution, various types of fuzzy set expansions have been developed. The theory of fuzzy sets is well known and has a large variety of applications in many different fields, including decision-making issues, neural networks, artificial intelligence, social sciences, and many more. The use of innovative ideas related to m-polar spherical fuzzy sets for medical diagnosis is investigated by Riaz *et al.* [16]. In the field of multi-criteria decision-making, researchers have recently introduced hybrid structures of MPF-sets to better model uncertainties. The idea of F-set was first represented by Zadeh [13-14]. The structure of fuzzy group is defined by Rosenfeld [12]. Mordeson *et al.* [8] and Kuroki [4] have examined fuzzy semigroups. The application of BPF-sets in decision making is examined by Malik *et al.* [7]. The membership function only ranged over the closed interval [0,1], it is hard to demonstrate the distinctness of irrelevant elements with the contradictory elements in a F-set. On the basis of these observations, the notion of BPF-set was introduced by Lee [5]. The BPF-set is actually an expansion of a F-set whose membership degree lies within the range [-1,1]. In a BPF-set, the associate degree 0 denotes that an element is unrelated to the correlative property, the associate degree from [0,1] denotes that the element partially fulfills the property to a bit extent, and the associate degree from [-1,0] denotes that the element completely fulfills the contrary property to a bit extent [5-6].

A 2-polar -sets and BPF-sets are two algebraic structures. Actually, BPF-set and 2-polar F-set have a natural one-to-one relationship. The BPF-sets can be expanded to MPF-sets by utilizing the concept of a one-to-one relationship. Sometimes, different things have occasionally been observed in various ways. This prompted research into MPF-set. The idea behind this interpretation is predicated on the fact that the given collection contains multi-polar information. MPF-sets have been successful in assigning membership degrees to multiple objects in the context of multi-polar information. In this case, it is important to note that MPF-sets only provide positive degrees of membership for each element, and no negative membership degrees are assumed [1]. Numerous real-world issues involving multiple factors, multiple indices, multiple items, and multiple polarities can be solved using multi-polar F-sets. Multi-polar F-sets can be used for diagnostic data, cooperative games, and decision-making.

A MPF-set can be written as m distinct F-sets, just like the BPF-sets can. As a consequence, every input is expressed by an m-dimensional vector whose entries belongs to [0,1], each represents a degree of confidence. Assume that the collection of context is N = {1,2,3,...,m}. Then, MPF-set will indicate the fulfillment degree of an element with regard to n^{th} context for each $n \in N$ [2]. For example, the F-set "brilliant" can have different interpretations among students in a particular class.

Received: March 2022; Accepted: September 2022
*Corresponding author: Fareeha Pervaiz <fareeha5531@yahoo.com>

We will give an example to demonstrate it.

Let $Z = \{z_1, z_2, z_3, z_4, z_5\}$ be the collection of 5 students. We shall grade them by a 4-polar F-set based on the following four qualities given below in Table 1.

Table 1. 4 polar fuzzy set

	IQ	Sports	Punctual	Discipline
z_1	1	0	0.8	0.9
z_2	1	0.8	0.5	0.5
z_3	0.5	1	1	0.8
z_4	0.8	0.5	1	0.8
z_5	1	0.5	0.9	0.8

Consequently, we get a 4-polar F-subset $\hat{g} : Z \rightarrow [0,1]^4$ of Z such that

$$\hat{g}(z_1) = (1, 0, 0.8, 0.9)$$

$$\hat{g}(z_2) = (1, 0.8, 0.5, 0.5)$$

$$\hat{g}(z_3) = (0.5, 1, 1, 0.8)$$

$$\hat{g}(z_4) = (0.8, 0.5, 1, 0.8)$$

$$\hat{g}(z_5) = (1, 0.5, 0.9, 0.8).$$

Here 1 stands for positive comments, 0.5 for average, and 0 for negative remarks.

In current paper, we define multi-polar fuzzy sub LA-semigroup (MPF-sub LA-semigroup) and multi-polar fuzzy ideals (MPF-ideals) of an LA-semigroup. Besides this, the characterization of regular LA-semigroups by MPF-ideals are presented.

2. PRELIMINARIES

We now illustrate some basic definitions and initial results centred on LA-semigroups that are significant in and of themselves. For the parts that follow, these are necessary. In the present paper, $\hat{S}$ will be denoting an LA-semigroup, unless stated otherwise. The concept of LA-semigroups, was first studied by Kazim and Naseerudin in 1972 [3]. Later on, Yusuf and Mushtaq worked on locally associative LA-semigroups in 1979 [10].

Definition 2.1 If an algebraic structure $(\hat{S},\bullet)$ holds the equation $(r\bullet s)\bullet t = (t\bullet s)\bullet r$ for each r, s, t $\in \hat{S}$, then it is a left almost semigroup (or LA-semigroup) [3].

Some basic definitions which are widely used in LA-semigroup as described below.

If for each $a \in \hat{S}$, $ea = a$, then e in $\hat{S}$ is a left identity. The left identity $e \in \hat{S}$ is unique [9]. Furthermore, if $e \in \hat{S}$, then $\hat{S} = \hat{S}e = e\hat{S}$ and $\hat{S}^2 = \hat{S}$. A left ideal (L-ideal) over $\hat{S}$ is a subset $\hat{I}$ that satisfies $\hat{S}\hat{I} \subseteq \hat{I}$ and right ideal (R-ideal) over $\hat{S}$ if $\hat{I}\hat{S} \subseteq \hat{I}$. $\hat{I}$ is simply termed an ideal (or two-sided) over $\hat{S}$ if $\hat{I}$ is a L-ideal and R-ideal over $\hat{S}$ [11]. A subset $\hat{I}$ over $\hat{S}$ which is non-empty is a sub LA-semigroup over $\hat{S}$ if $\hat{I}^2 \subseteq \hat{I}$. A subset $\hat{I}$ over $\hat{S}$ which is non-empty is a generalized bi-ideal (GB-ideal) over $\hat{S}$ if $(\hat{I}\hat{S})\hat{I} \subseteq \hat{I}$. A sub LA-semigroup $\hat{I}$ over $\hat{S}$ is a bi-ideal (B-ideal) over $\hat{S}$ if $(\hat{I}\hat{S})\hat{I} \subseteq \hat{I}$. A subset $\hat{I}$ over $\hat{S}$ which is non-empty is a quasi-ideal (Q-ideal) over $\hat{S}$ if $\hat{I}\hat{S} \cap \hat{S}\hat{I} \subseteq \hat{I}$. A sub LA-semigroup $\hat{I}$ over $\hat{S}$ is an interior ideal (I-ideal) over $\hat{S}$ if $(\hat{S}\hat{I})\hat{S} \subseteq \hat{I}$.

Definition 2.2 A function $\hat{g} : \hat{S} \rightarrow [0,1]$ from $\hat{S}$ into the interval [0,1] is a fuzzy subset (F-subset) of a universe $\hat{S}$.

Some important definitions in F-sets are defined below.

Let $\hat{g}$ be a F-subset over $\hat{S}$. Then the set $\hat{g}_t = \{s \in \hat{S} \mid \hat{g}(s) \geq t\}$ for all $t \in (0,1]$, is named as a level subset over $\hat{S}$.

Let $\hat{g}$ and $\hat{h}$ be any two F-subsets over $\hat{S}$, then $\hat{g} \leq \hat{h}$ means that $\hat{g}(s) \leq \hat{h}(s)$ for each $s \in \hat{S}$. The F-subsets $\hat{g} \wedge \hat{h}$ and $\hat{g} \vee \hat{h}$ of $\hat{S}$ is described as

$(\hat{g} \wedge \hat{h})(s) = \hat{g}(s) \wedge \hat{h}(s)$ and

$(\hat{g} \vee \hat{h})(s) = \hat{g}(s) \vee \hat{h}(s)$ for all $s \in \hat{S}$.

The product $\hat{g} \circ \hat{h}$ is defined as

$$(\hat{g}\circ\hat{h})(s) = \begin{cases} \bigvee_{s=pq}\{\hat{g}(p) \wedge \hat{h}(q)\}, \text{if } \exists\ p, q \in \hat{S} \text{ such that } s = pq \\ 0 \qquad\qquad\qquad\qquad\qquad\qquad otherwise \end{cases}$$

for all $s \in \hat{S}$.

A F-subset $\hat{g}$ over $\hat{S}$ is a fuzzy sub LA-semigroup (F-Sub LA-semigroup) over $\hat{S}$ if for every $p, q \in \hat{S}$, $\hat{g}(pq) \geq \hat{g}(p) \wedge \hat{g}(q)$ [15].

For every p, q ∈ $\hat{S}$, a F-subset $\hat{g}$ over $\hat{S}$ is classified as a fuzzy left ideal (FL-ideal) over $\hat{S}$ if $\hat{g}$(pq) ≥ $\hat{g}$(q) [15].

For every p, q ∈ $\hat{S}$, a F-subset $\hat{g}$ over $\hat{S}$ is classified as a fuzzy right ideal (FR-ideal) over $\hat{S}$ if $\hat{g}$(pq) ≥ $\hat{g}$(p) [15].

If F-subset $\hat{g}$ is both a FL-ideal and a FR-ideal over $\hat{S}$, so it is a fuzzy ideal (F-ideal) over $\hat{S}$.

A F-subset $\hat{g}$ over $\hat{S}$ is a fuzzy quasi-ideal (FQ-ideal) over $\hat{S}$ if $(\hat{g} \circ \delta) \wedge (\delta \circ \hat{g}) \leq \hat{g}$. Here, δ is the F-subset over $\hat{S}$ which maps each element of $\hat{S}$ on 1, that is δ is the characteristic function over $\hat{S}$ [15].

A F-subset $\hat{g}$ over $\hat{S}$ is a fuzzy generalized bi-ideal (FGB-ideal) over $\hat{S}$ if $\hat{g}$((pq)r) ≥ $\hat{g}$(p) ∧ $\hat{g}$(r) for each p, q, r ∈ $\hat{S}$ [15].

A F-Sub LA-semigroup $\hat{g}$ over $\hat{S}$ is known as a fuzzy bi-ideal (FB-ideal) over $\hat{S}$ if $\hat{g}$((pq)r) ≥ $\hat{g}$(p) ∧ $\hat{g}$(r) for each p, q , r ∈ $\hat{S}$ [15].

A F-Sub LA-semigroup $\hat{g}$ over $\hat{S}$ is a fuzzy interior-ideal (FI-ideal) over $\hat{S}$ if for all p, q, r ∈ $\hat{S}$, $\hat{g}$((pq)r) ≥ $\hat{g}$(q) [15].

3. RESULTS AND DISCUSSION

Now, we define some notions and present our main results regarding multi-polar fuzzy ideals in $\hat{S}$.

Definition 3.1 [1] Multi-polar fuzzy subset over $\hat{S}$ is a mapping $\hat{g} : \hat{S} \to [0,1]^m$.

MPF-set is represented by the m-tuple $\hat{g}$ = ($\hat{g}_1$,$\hat{g}_2$,...,$\hat{g}_m$), consists of mappings $\hat{g}_n : \hat{S} \to [0,1]$ for each n ∈ {1,2,3,...,m}. The collection of all MPF-subsets of $\hat{S}$, is represented as m($\hat{S}$). We define a relation ≤ on m($\hat{S}$) in the following manner:

For any two MPF-subsets $\hat{g}$ = ($\hat{g}_1$,$\hat{g}_2$,...,$\hat{g}_m$) and $\hat{h}$ = ($\hat{h}_1$,$\hat{h}_2$,...,$\hat{h}_m$) of an LA-semigroup $\hat{S}$, $\hat{g} \leq \hat{h}$ means that $\hat{g}_n(s) \leq \hat{h}_n(s)$ for each s ∈ $\hat{S}$ and n ∈ {1,2,3,...,m}.

The symbols $\hat{g} \wedge \hat{h}$ and $\hat{g} \vee \hat{h}$ denotes the following MPF-subsets over $\hat{S}$.

$(\hat{g} \wedge \hat{h})(s) = \hat{g}(s) \wedge \hat{h}(s)$ and $(\hat{g} \vee \hat{h})(s) = \hat{g}(s) \vee \hat{h}(s)$ that is $(\hat{g}_n \wedge \hat{h}_n)(s) = \hat{g}_n(s) \wedge \hat{h}_n(s)$ and $(\hat{g}_n \vee \hat{h}_n)(s) = \hat{g}_n(s) \vee \hat{h}_n(s)$ for each s ∈ $\hat{S}$ and n ∈ {1,2,3,...,m}.

Let $\hat{g}$ = ($\hat{g}_1$,$\hat{g}_2$,...,$\hat{g}_m$) and $\hat{h}$ = ($\hat{h}_1$,$\hat{h}_2$,...,$\hat{h}_m$) be any two MPF-subsets over $\hat{S}$.

The product $\hat{g} \circ \hat{h}$ = ($\hat{g}_1 \circ \hat{h}_1$, $\hat{g}_2 \circ \hat{h}_2$,..,$\hat{g}_n \circ \hat{h}_n$) is defined as

$(\hat{g}_n \circ \hat{h}_n)$ =

$$\begin{cases} \bigvee_{s=pq}\{\hat{g}_n(p) \wedge \hat{h}_n(q)\}, \text{if } s = pq \text{ for some } p, q \in \hat{S} \\ 0 \qquad\qquad\qquad\qquad otherwise \end{cases}$$

for every n ∈ {1,2,3,...,m}.

For m = 3, the following example illustrates the product of MPF-subsets $\hat{g}$ and $\hat{h}$ over $\hat{S}$.

Example 3.1 Let the LA-semigroup $\hat{S}$ = {u, v, w} with the binary operation "·" is defined as (Table 2):

Table 2. LA-semigroup

•	U	v	W
U	U	u	U
V	U	u	U
w	V	v	U

We define 3-polar fuzzy subsets $\hat{g}$ = ($\hat{g}_1$,$\hat{g}_2$,$\hat{g}_3$) and $\hat{h}$ = ($\hat{h}_1$,$\hat{h}_2$,$\hat{h}_3$) of $\hat{S}$ as follows:

$\hat{g}$(u) = (0.1,0.2,0.1), $\hat{g}$(v) = (0,0,0), $\hat{g}$(w) = (0.2,0.3,0.4)

and

$\hat{h}$(u) = (0,0,0), $\hat{h}$(v) = (0,0.1,0.2), $\hat{h}$(w) = (0.3,0,0.4).

By definition,

$(\hat{g}_1 \circ \hat{h}_1)$(u) = 0.2, $(\hat{g}_1 \circ \hat{h}_1)$(v) = 0, $(\hat{g}_1 \circ \hat{h}_1)$(w) = 0

$(\hat{g}_2 \circ \hat{h}_2)$(u) = 0.1, $(\hat{g}_2 \circ \hat{h}_2)$(v) = 0.1, $(\hat{g}_2 \circ \hat{h}_2)$(w) = 0

$(\hat{g}_3 \circ \hat{h}_3)$(u) = 0.4, $(\hat{g}_3 \circ \hat{h}_3)$(v) = 0.2, $(\hat{g}_3 \circ \hat{h}_3)$(w) = 0

So, the product of $\hat{g}$ = ($\hat{g}_1$,$\hat{g}_2$,$\hat{g}_3$) and $\hat{h}$ = ($\hat{h}_1$,$\hat{h}_2$,$\hat{h}_3$) is defined by

$(\hat{g} \circ \hat{h})$(u) = (0.2,0.1,0.4),

$(\hat{g} \circ \hat{h})$(v) = (0,0.1,0.2)

$(\hat{g} \circ \hat{h})$(w) = (0,0,0).

Definition 3.2 Consider $\hat{g}$ = ($\hat{g}_1$,$\hat{g}_2$,...,$\hat{g}_m$) be a MPF-subset over $\hat{S}$.

(1) Let $\hat{g}_t$ = {x ∈ Ŝ | $\hat{g}$(x) ≥ t} be defined for each t and t = (t_1,t_2,...,t_m) ∈ $(0,1]^m$, such that $\hat{g}_n(x) \geq t_n$ for each n ∈ {1,2,3,...,m}. We name $\hat{g}_t$ a t-cut or sometimes a level set. This means $\hat{g}_t$ = $\cap_{k=1}^{m}(\hat{g}_n)t_n$.

Definition 3.3 A multi-polar fuzzy subset $\hat{g}$ = *($\hat{g}_1$,$\hat{g}_2$,...,$\hat{g}_m$)* over $\hat{S}$ is a multi-polar fuzzy sub LA-semigroup (MPF-sub LA-semigroup) over $\hat{S}$ if $\hat{g}$(xy) ≥ min{$\hat{g}$(x), $\hat{g}$(y)} for every x,y ∈ $\hat{S}$, that is $\hat{g}_n$(xy) ≥ min{$\hat{g}_n$(x), $\hat{g}_n$(y)} for each n ∈ {1,2,3,...,m}.

Definition 3.4 A multi-polar fuzzy subset $\hat{g}$ = ($\hat{g}_1$,$\hat{g}_2$,...,$\hat{g}_m$) over $\hat{S}$ is a multi-polar fuzzy left ideal (MPFL-ideal) over $\hat{S}$ if for each x, y ∈ $\hat{S}$, $\hat{g}$(xy) ≥ $\hat{g}$(y), that is $\hat{g}_n$ (xy) ≥ $\hat{g}_n$(y) and multi-polar fuzzy right ideal (MPFR-ideal) over $\hat{S}$ if for each x, y ∈ $\hat{S}$, $\hat{g}$(xy) ≥ $\hat{g}$(x), that is $\hat{g}_n$(xy) ≥ $\hat{g}_n$(x) for each n ∈ {1,2,3,...,m}.

A MPF-subset $\hat{g}$ over $\hat{S}$ is considered a MPF-ideal over $\hat{S}$ if it satisfies the conditions of being a multi-polar fuzzy left ideal (MPFL-ideal) and a multi-polar fuzzy right ideal (MPFR-ideal) over $\hat{S}$.

The next example is of 3-polar fuzzy two-sided ideal over $\hat{S}$.

Example 3.2 Consider $\hat{S}$ = {r,s,t,u,v} be an LA-semigroup under the binary operation"·" defined below in Table 3.

Table 3. LA-semigroup

•	R	s	t	u	v
R	R	r	r	r	r
S	R	s	s	s	s
T	R	s	u	v	t
U	R	s	t	u	v
V	R	s	v	t	u

We define a 3-polar fuzzy subset $\hat{g}$ = ($\hat{g}_1$,$\hat{g}_2$,$\hat{g}_3$) of $\hat{S}$ as follows:

$\hat{g}$(r) = (0.8,0.8,0.7), $\hat{g}$(s) = (0.7,0.6, 0.5),

$\hat{g}$(t) = (0.6,0.4, 0.2), $\hat{g}$(u) = (0.6, 0.4,0.2) and

$\hat{g}$(v) = (0.6, 0.4, 0.2).

Clearly, $\hat{g}$ = ($\hat{g}_1$,$\hat{g}_2$,$\hat{g}_3$) is both a 3-polar FL-ideal and a 3-polar FR-ideal over $\hat{S}$. Hence $\hat{g}$ is a 3-polar fuzzy two-sided ideal over $\hat{S}$.

Definition 3.5 Let φ ≠ $\hat{A} \subseteq \hat{S}$, where $\hat{S}$ be an LA-semigroup. Subsequently, the multi-polar characteristic function

$\hat{C}_{\hat{A}}$: X →$[0,1]^m$ of $\hat{A}$ is described as

$$\hat{C}_{\hat{A}}(x) = \begin{cases} (1,1,\ldots,1)\ m-\text{tuple for } x \in \hat{A} \\ (0,0,\ldots,0)\ m-\text{tuple for } x \notin \hat{A} \end{cases}$$

Lemma 3.1 For any two subsets $\hat{A}$ ≠ φ and $\hat{B}$ ≠ φ of an LA-semigroup $\hat{S}$. The subsequent equalities are hold.

(1) $\hat{C}_{\hat{A}} \wedge \hat{C}_{\hat{B}} = \hat{C}_{\hat{A}\cap\hat{B}}$.

(2) $\hat{C}_{\hat{A}} \vee \hat{C}_{\hat{B}} = \hat{C}_{\hat{A}\cup\hat{B}}$

(3) $\hat{C}_{\hat{A}} \circ \hat{C}_{\hat{B}} = \hat{C}_{\hat{A}\hat{B}}$

Proof. (1) Let $\hat{A}$ ≠ φ and $\hat{B}$ ≠ φ be two subsets over $\hat{S}$. We examine the four cases as below,

Case 1: Consider x ∈ Â ∩ B̂. Then, $\hat{C}_{\hat{A}\cap\hat{B}}$(x) = (1,1,...,1). Also x ∈ Â ∩ B̂ implies x ∈ Â and x ∈ $\hat{B}$. Hence, $\hat{C}_{\hat{A}}$(x) = (1,1,...,1) and $\hat{C}_{\hat{B}}$(x) = (1,1,...,1). This implies that $(\hat{C}_{\hat{A}}\wedge\hat{C}_{\hat{B}})$(x) = $\hat{C}_{\hat{A}}(x)\wedge\hat{C}_{\hat{B}}(x)$ = (1,1,...,1). Thus, $\hat{C}_{\hat{A}}\wedge\hat{C}_{\hat{B}} = \hat{C}_{\hat{A}\cap\hat{B}}$.

Case 2: Consider x ∉ Â ∩ B̂. Then $\hat{C}_{\hat{A}\cap\hat{B}}$(x) = (0,0,...,0). As x ∉ Â ∩ $\hat{B}$ thus x ∉ Â or x ∉ $\hat{B}$. As a result, it follows that $\hat{C}_{\hat{A}}$(x) = (0,0,...,0) or $\hat{C}_{\hat{B}}$(x) = (0,0,...,0). Thus, $(\hat{C}_{\hat{A}} \wedge \hat{C}_{\hat{B}})(x) = \hat{C}_{\hat{A}}(x) \wedge \hat{C}_{\hat{B}}(x)$ = (0,0,...,0). Therefore $\hat{C}_{\hat{A}} \wedge \hat{C}_{\hat{B}} = \hat{C}_{\hat{A}\cap\hat{B}}$.

(2) Consider $\hat{A}$ and $\hat{B}$ denote non-empty subsets of $\hat{S}$.

Case 1: Let x ∈ Â ∪ $\hat{B}$. Then, $\hat{C}_{\hat{A}\cup\hat{B}}$(x) = (1,1,...,1). Since x ∈ Â ∪ $\hat{B}$ implies x ∈ Â or x ∈ $\hat{B}$. Hence, $\hat{C}_{\hat{A}}$(x) = (1,1,...,1) or $\hat{C}_{\hat{B}}$ (x) = (1,1,...,1). As a result, it follows that $(\hat{C}_{\hat{A}} \vee \hat{C}_{\hat{B}})(x) = \hat{C}_{\hat{A}}(x) \vee \hat{C}_{\hat{B}}(x)$ = (1,1,...,1). Thus, $\hat{C}_{\hat{A}} \vee \hat{C}_{\hat{B}} = \hat{C}_{\hat{A}\cup\hat{B}}$.

Case 2: Let x ∉ Â ∪ $\hat{B}$. Then $\hat{C}_{\hat{A}\cup\hat{B}}$(x) = (0,0,...,0). Since x ∉ Â ∪ $\hat{B}$, we get x ∉ Â and x ∉ B. This implies that $\hat{C}_{\hat{A}}$(x) = (0,0,...,0) and $\hat{C}_{\hat{B}}$(x) = (0,0,...,0). Thus, $(\hat{C}_{\hat{A}} \vee \hat{C}_{\hat{B}})(x) = \hat{C}_{\hat{A}}(x) \vee \hat{C}_{\hat{B}}(x)$ = (0,0,...,0). Hence $\hat{C}_{\hat{A}} \vee \hat{C}_{\hat{B}} = \hat{C}_{\hat{A}\cup\hat{B}}$.

(3) Let $\hat{A}$ ≠ φ and $\hat{B}$ ≠ φ be subsets over $\hat{S}$.

Case 1: Let x ∈ $\hat{A}\hat{B}$, which implies that x = ab for a ∈ $\hat{A}$ and b ∈ $\hat{B}$. Thus $\hat{C}_{\hat{A}\hat{B}}$(x) = (1,1,...,1). Since a ∈ $\hat{A}$ and b ∈ $\hat{B}$, we have $\hat{C}_{\hat{A}}$(a) = (1,1,...,1) and $\hat{C}_{\hat{B}}$(b) = (1,1,...,1). Now,

$$(\hat{C}_{\hat{A}}\circ\hat{C}_{\hat{B}})(x) = \vee_{x=uv}\{\hat{C}_{\hat{A}}(u)\wedge\hat{C}_{\hat{B}}(v)\}$$
$$\geq \hat{C}_{\hat{A}}(a)\wedge\hat{C}_{\hat{B}}(b)$$
$$= (1,1,...,1)$$

Thus, $\hat{C}_{\hat{A}} \circ \hat{C}_{\hat{B}} = \hat{C}_{\hat{A}\hat{B}}$.

Case 2: Let x ∉ $\hat{A}\hat{B}$. This implies that $\hat{C}_{\hat{A}\hat{B}}$(x) = (0,0,...,0). Because x ≠ ab for each a ∈ $\hat{A}$ and b ∈ $\hat{B}$. So, $(\hat{C}_{\hat{A}}\circ\hat{C}_{\hat{B}})$(x)= $\vee_{x=ab}\{\hat{C}_{\hat{A}}(a)\wedge\hat{C}_{\hat{B}}(b)\}$ = (0,0,...,0).

Hence $\hat{C}_{\hat{A}} \circ \hat{C}_{\hat{B}} = \hat{C}_{\hat{A}\hat{B}}$.

Lemma 3.2 Consider $\hat{L} \neq$ φ be a subset of $\hat{S}$. So the subsequent assertions hold.

(1) $\hat{L}$ is a sub LA-semigroup over $\hat{S}$ iff $\hat{C}_{\hat{L}}$ is a multi-polar fuzzy sub LA-semigroup over $\hat{S}$.

(2) $\hat{L}$ is a left (right, two-sided) ideal over $\hat{S}$ iff $\hat{C}_{\hat{L}}$ is a multi-polar fuzzy left (right, two-sided) ideal over $\hat{S}$.

Proof. (1) Consider $\hat{L}$ is a sub LA-semigroup over $\hat{S}$. We claim that

$\hat{C}_{\hat{L}}$(xy) ≥ $\hat{C}_{\hat{L}}$(x) ∧ $\hat{C}_{\hat{L}}$(y) for every x, y ∈ $\hat{S}$. We examine the four cases as below,

Case 1 : Let x, y ∈ $\hat{L}$. So, $\hat{C}_{\hat{L}}$(x) = $\hat{C}_{\hat{L}}$(y) = (1,1,...,1). Since $\hat{L}$ is a sub LA-semigroup over $\hat{S}$, so xy ∈ $\hat{L}$ it follows that $\hat{C}_{\hat{L}}$(xy) = (1,1,...,1). Hence $\hat{C}_{\hat{L}}$(xy) ≥ $\hat{C}_{\hat{L}}$(x) ∧ $\hat{C}_{\hat{L}}$(y).

Case 2 : Consider x ∈ $\hat{L}$, y ∉ $\hat{L}$. Then, $\hat{C}_{\hat{L}}$(x) = (1,1,...,1) and $\hat{C}_{\hat{L}}$(y) = (0,0,...,0). So, $\hat{C}_{\hat{L}}$x) ∧ $\hat{C}_{\hat{L}}$(y) = (0,0,...,0). But $\hat{C}_{\hat{L}}$(xy) ≥ (0,0,...,0). Thus $\hat{C}_{\hat{L}}$(xy) ≥ $\hat{C}_{\hat{L}}$(x) ∧$\hat{C}_{\hat{L}}$(y).

Case 3 : Consider x, y ∉ $\hat{L}$. Then, $\hat{C}_{\hat{L}}$(x) = $\hat{C}_{\hat{L}}$(y) = (0,0,...,0). Clearly, $\hat{C}_{\hat{L}}$(xy) ≥ (0,0,...,0) = $\hat{C}_{\hat{L}}$(x) ∧ $\hat{C}_{\hat{L}}$(y).

Case 4 : Consider x ∉ $\hat{L}$, y ∈ $\hat{L}$. Then, $\hat{C}_{\hat{L}}$(x) = (0,0,...,0) and $\hat{C}_{\hat{L}}$(y) = (1,1,...,1). Clearly, $\hat{C}_{\hat{L}}$(xy) ≥ (0,0,...,0) = $\hat{C}_{\hat{L}}$(x) ∧ $\hat{C}_{\hat{L}}$(y).

Conversely, let $\hat{C}_{\hat{L}}$ is a MPF-sub LA-semigroup over $\hat{S}$ and x, y ∈ $\hat{L}$. Then, $\hat{C}_{\hat{L}}$(x) = $\hat{C}_{\hat{L}}$y) = (1,1,...,1). By definition, $\hat{C}_{\hat{L}}$(xy) ≥ $\hat{C}_{\hat{L}}$(x) ∧$\hat{C}_{\hat{L}}$(y) = (1,1,...,1) ∧ (1,1,...,1) = (1,1,...,1), we have $\hat{C}_{\hat{L}}$(xy) = (1,1,...,1). This implies that xy ∈ $\hat{L}$, that is $\hat{L}$ is a sub LA-semigroup over $\hat{S}$.

(2) Suppose that $\hat{L}$ is a L-ideal over $\hat{S}$. We show that $\hat{C}_{\hat{L}}$(xy) ≥ $\hat{C}_{\hat{L}}$(y) for every x,y ∈ $\hat{S}$. We examine the two cases as below,

Case 1 : Consider y ∈ $\hat{L}$ and x ∈ $\hat{S}$. Then, $\hat{C}_{\hat{L}}$(y) = (1,1,...,1). As $\hat{L}$ is a L-ideal over $\hat{S}$, so xy ∈ $\hat{L}$ implies that $\hat{C}_{\hat{L}}$(xy) = (1,1,...,1). Hence $\hat{C}_{\hat{L}}$(xy) ≥ $\hat{C}_{\hat{L}}$(y).

Case 2 : Let y ∉ $\hat{L}$ and x ∈ $\hat{S}$. Then, $\hat{C}_{\hat{L}}$(y) = (0,0,...,0). Clearly, $\hat{C}_{\hat{L}}$(xy) ≥ $\hat{C}_{\hat{L}}$(y).

Conversely, let $\hat{C}_{\hat{L}}$ is a MPFL-ideal over $\hat{S}$. Consider that x ∈ $\hat{S}$ and y ∈ $\hat{L}$. Thus, $\hat{C}_{\hat{L}}$(y) = (1,1,...,1). By definition, $\hat{C}_{\hat{L}}$(xy) ≥ $\hat{C}_{\hat{L}}$(y) = (1,1,...,1), we get

$\hat{C}_{\hat{L}}$(xy) = (1,1,...,1). So xy ∈ $\hat{L}$, as a result $\hat{L}$ is a L-ideal over $\hat{S}$.

Likewise, we can demonstrate that $\hat{L}$ is a R-ideal over $\hat{S}$ iff $\hat{C}_{\hat{L}}$ is a MPFR-ideal over $\hat{S}$. Thus $\hat{L}$ is a two-sided ideal over $\hat{S}$ iff $\hat{C}_{\hat{L}}$ is a multi-polar fuzzy two-sided ideal over $\hat{S}$.

Lemma 3.3 Consider $\hat{g} = (\hat{g}_1,\hat{g}_2,...,\hat{g}_m)$ be a MPF-subset over $\hat{S}$. Then the subsequent assertions hold.

(1) $\hat{g}$ is a MPF-sub LA-semigroup over $\hat{S}$ iff

$\hat{g} \circ \hat{g} \leq \hat{g}$.

(2) $\hat{g}$ is a MPFL-ideal over $\hat{S}$ iff

$\delta \circ \hat{g} \leq \hat{g}$.

(3) $\hat{g}$ is a MPFR-ideal over $\hat{S}$ iff

$\hat{g} \circ \delta \leq \hat{g}$.

(4) $\hat{g}$ is a multi-polar fuzzy two sided over $\hat{S}$

iff $\delta \circ \hat{g} \leq \hat{g}$ and $\hat{g} \circ \delta \leq \hat{g}$.

Here, δ represents the MPF-subset over $\hat{S}$ that maps every element of $\hat{S}$ to (1,1,...,1).

Proof. (1) Consider that $\hat{g} = (\hat{g}_1,\hat{g}_2,...,\hat{g}_m)$ be a MPF-sub LA-semigroup over $\hat{S}$, i.e. $\hat{g}_n$(xy) ≥ $\hat{g}_n$(x) ∧ $\hat{g}_n$(y) for all n ∈{1,2,3,...,m}. Let a ∈ $\hat{S}$. If a ≠ bc for any b, c ∈ $\hat{S}$, so that $(\hat{g} \circ \hat{g})$(a) = 0. Hence, $(\hat{g} \circ \hat{g})$(a) ≤ $\hat{g}$(a). But if a = xy for x,y ∈ $\hat{S}$, then

$(\hat{g}_n \circ \hat{g}_n)(a) = \bigvee_{a=xy}\{\hat{g}_n(x) \wedge \hat{g}_n(y)\}$

$\leq \bigvee_{a=xy}\{\hat{g}_n(xy)\}$

$= \hat{g}_n(a)$ for every $n \in \{1,2,3,...,m\}$.

Therefore $\hat{g} \circ \hat{g} \leq \hat{g}$.

Conversely, assume that $(\hat{g} \circ \hat{g}) \leq \hat{g}$ and $x,y \in \hat{S}$. Then

$\hat{g}_n(xy) \geq (\hat{g}_n \circ \hat{g}_n)(xy)$

$= \bigvee_{xy=uv}\{\hat{g}_n(u) \wedge \hat{g}_n(v)\}$

$\geq \hat{g}_n(x) \wedge \hat{g}_n(y)$ for each $n \in \{1,2,3,...,m\}$.

Hence $\hat{g}(xy) \geq \hat{g}(x) \wedge \hat{g}(y)$. Thus $\hat{g}$ is a MPF-sub LA-semigroup over $\hat{S}$.

(2) Let $\hat{g} = (\hat{g}_1,\hat{g}_2,...,\hat{g}_m)$ be a MPFL-ideal over $\hat{S}$, i.e. $\hat{g}_n(xy) \geq \hat{g}_n(y)$ for every $x,y \in \hat{S}$ and $n \in \{1,2,3,...,m\}$. Consider $a \in \hat{S}$. If $a \neq bc$ for $b,c \in \hat{S}$, therefore

$(\delta\circ\hat{g})(a) = 0$. Hence, $\delta\circ\hat{g} \leq \hat{g}$. But if $a = xy$ for $x, y \in \hat{S}$, then

$(\delta_n \circ \hat{g}_n)(a) = \bigvee_{a=xy}\{\delta_n(x) \wedge \hat{g}_n(y)\}$

$= \bigvee_{a=xy}\{\hat{g}_n(y)\}$

$\leq \bigvee_{a=xy}\hat{g}_n(xy)$

$= \hat{g}_n(a)$ for all $n \in\{1,2,3,...,m\}$.

Thus $\delta \circ \hat{g} \leq \hat{g}$.

Conversely, assume that $(\delta \circ \hat{g}) \leq \hat{g}$ and $x,y \in \hat{S}$. Then

$\hat{g}_n(xy) \geq (\delta_n \circ\hat{g}_n)(xy)$

$= \bigvee_{xy=uv}\{\delta_n (u) \wedge \hat{g}_n(v)\}$

$\geq \{\delta_n (x) \wedge \hat{g}_n(y)\}$

$= \hat{g}_n(y)$ for all $n \in \{1,2,3,...,m\}$.

Hence $\hat{g}(xy) \geq \hat{g}(y)$. Thus $\hat{g}$ is a MPFL-ideal over $\hat{S}$.

(3) It can be proved on the same lines of (2).

(4) This can be proved by using equations (2) and (3).

Lemma 3.4 The subsequent statements hold for an LA-semigroup $\hat{S}$.

(1) Consider that $\hat{g} = (\hat{g}_1,\hat{g}_2,...,\hat{g}_m)$ and $\hat{h} = (\hat{h}_1,\hat{h}_2,...,\hat{h}_m)$ be two MPF-sub LA-semigroups over $\hat{S}$. Thus $\hat{g} \wedge \hat{h}$ is also a MPF-sub LA-semigroup over $\hat{S}$.

(2) Consider that $\hat{g} = (\hat{g}_1,\hat{g}_2,...,\hat{g}_m)$ and $\hat{h} = (\hat{h}_1,\hat{h}_2,...,\hat{h}_m)$ be two multi-polar fuzzy left (right, two-sided) ideals over $\hat{S}$. Then $\hat{g} \wedge \hat{h}$ is also a multi-polar fuzzy left (right, two-sided) ideal over $\hat{S}$.

Proof. Assume that $\hat{g} = (\hat{g}_1,\hat{g}_2,...,\hat{g}_m)$ and $\hat{h} = (\hat{h}_1,\hat{h}_2,...,\hat{h}_m)$ be two MPF-sub LA-semigroups over $\hat{S}$. Then

$(\hat{g}_n \wedge \hat{h}_n)(xy) = \hat{g}_n(xy) \wedge \hat{h}_n(xy)$

$\geq (\hat{g}_n(x) \wedge \hat{g}_n(y)) \wedge (\hat{h}_n(x) \wedge \hat{h}_n(y))$

$= (\hat{g}_n(x) \wedge \hat{h}_n(x)) \wedge (\hat{g}_n(y) \wedge \hat{h}_n(y))$

$= (\hat{g}_n \wedge \hat{h}_n)(x) \wedge (\hat{g}_n \wedge \hat{h}_n)(y)$

for each $n \in \{1,2,3,...,m\}$.

Thus, $\hat{g} \wedge \hat{h}$ is a MPF-sub LA-semigroup over $\hat{S}$.

Similar methods can be applied to prove other cases.

Proposition 3.1 Suppose that $\hat{g} = (\hat{g}_1,\hat{g}_2,...,\hat{g}_m)$ be a MPF-subset over $\hat{S}$. Then $\hat{g}$ is a MPF-sub LA-semigroup (left, right, two-sided ideal) over $\hat{S}$ iff $\hat{g}_t = \{x \in \hat{S} \mid \hat{g}(x) \geq t\} \neq \varphi$ is a sub LA-semigroup (left, right, two-sided ideal) over $\hat{S}$ for every $t = (t_1,t_2,...,t_m) \in (0,1]^m$.

Proof. Suppose $\hat{g}$ is a MPF-sub LA-semigroup over $\hat{S}$.Consider $x, y \in \hat{g}_t$. Then $\hat{g}_n(x) \geq t_n$ and $\hat{g}_n(y) \geq t_n$ for each $n \in \{1,2,3,...,m\}$. As $\hat{g}$ is a MPF-sub LA-semigroup over $\hat{S}$, we have $\hat{g}_n(xy) \geq \hat{g}_n(x) \wedge \hat{g}_n(y) \geq t_n \wedge t_n = t_n$ for every $n \in \{1,2,3,...,m\}$. Thus $xy \in \hat{g}_t$. So $\hat{g}_t$ is a sub LA-semigroup over $\hat{S}$.

Conversely, assume that $\hat{g}_t \neq \varphi$ is a sub LA-semigroup over $\hat{S}$. On contrary, let $\hat{g}$ is not a MPF-sub LA-semigroup over $\hat{S}$. Consider $x, y \in \hat{S}$ with $\hat{g}_n(xy) < \hat{g}_n(x) \wedge \hat{g}_n(y)$ for $n \in \{1,2,3,..,m\}$. Take $t_n = \hat{g}_n(x) \wedge \hat{g}_n(y)$ for every $n \in \{1,2,3,...,m\}$. Then $x, y \in \hat{g}_t$ but $xy \notin \hat{g}_t$, this contradicts the hypothesis. Hence $\hat{g}(xy) \geq \hat{g}(x) \wedge \hat{g}(y)$. Thus $\hat{g}$ is a MPF-sub LA-semigroup over $\hat{S}$.

Similar methods can be applied to prove other cases.

Next, we define the multi-polar fuzzy generalized bi-ideal (MPFGB-ideal) over $\hat{S}$.

Definition 3.6 A MPF-subset $\hat{g} = (\hat{g}_1,\hat{g}_2,...,\hat{g}_m)$ over $\hat{S}$ is considered a MPFGB-ideal over $\hat{S}$ if for each x, y, z ∈ $\hat{S}$, $\hat{g}((xy)z) \geq \hat{g}(x) \wedge \hat{g}(z)$, that is $\hat{g}_n((xy)z) \geq \hat{g}_n(x) \wedge \hat{g}_n(z)$ for each n ∈ {1,2,...,m}.

Lemma 3.5 A subset $\hat{G}$ over $\hat{S}$ which is non-empty is a GB-ideal over $\hat{S}$ iff $\hat{C}_{\hat{G}}$ the multi-polar characteristic function of $\hat{G}$ is a MPFGB-ideal over $\hat{S}$.

Proof. It can be showed on the same lines of Lemma 3.2.

Lemma 3.6 A MPF-subset $\hat{g}$ over $\hat{S}$ is a MPFGB-ideal over $\hat{S}$ iff $(\hat{g} \circ \delta) \circ \hat{g} \leq \hat{g}$.

Proof. Suppose $\hat{g} = (\hat{g}_1,\hat{g}_2,...,\hat{g}_m)$ be a MPFGB-ideal over $\hat{S}$, i.e. $\hat{g}_n((xy)z) \geq \hat{g}_n(x) \wedge \hat{g}_n(z)$ for each n ∈ {1,2,3,...,m} and x, y, z ∈ $\hat{S}$. Consider a ∈ $\hat{S}$. If a ≠ bc for some b, c ∈ $\hat{S}$ thus $((\hat{g} \circ \delta) \circ \hat{g})(a) = 0$. Therefore, $(\hat{g} \circ \delta) \circ \hat{g} \leq \hat{g}$. But if a = xy for some x,y ∈ $\hat{S}$. Thus for every n ∈ {1,2,3,...,m}.

$$((\hat{g}_n \circ \delta_n) \circ \hat{g}_n))(a) = \vee_{a=xy}\{(\hat{g}_n \circ \delta_n)(x) \wedge \hat{g}_n(y)\}$$

$$= \vee_{a=xy}\{\vee_{x=uv}\{\hat{g}_n(u) \wedge \delta_n(v)\} \wedge \hat{g}_n(y)\}$$

$$= \vee_{a=xy}\{\vee_{x=uv}\{\hat{g}_n(u) \wedge \hat{g}_n(y)\}\}$$

$$\leq \vee_{a=xy}\{\vee_{x=uv}\hat{g}_n((uv)y)\}$$

$$= \vee_{a=xy}\{\hat{g}_n(xy)\}$$

$$= \hat{g}_n(a) \text{ for all } n \in \{1,2,3,...,m\}.$$

So $(\hat{g} \circ \delta) \circ \hat{g} \leq \hat{g}$.

Conversely, let $(\hat{g} \circ \delta) \circ \hat{g} \leq \hat{g}$ and x, y, z ∈ $\hat{S}$. Then

$$\hat{g}_n((xy)z) \geq ((\hat{g}_n \circ \delta_n) \circ \hat{g}_n)((xy)z)$$

$$= \vee_{(xy)z=uv}\{(\hat{g}_n \circ \delta_n)(u) \wedge \hat{g}_n(v)\}$$

$$\geq (\hat{g}_n \circ \delta_n)(xy) \wedge \hat{g}_n(z)$$

$$= \vee_{xy=ab}\{\hat{g}_n(a) \wedge \delta_n(b)\} \wedge \hat{g}_n(z)$$

$$\geq \{\hat{g}_n(x) \wedge \delta_n(y)\} \wedge \hat{g}_n(z)$$

$$= \hat{g}_n(x) \wedge \hat{g}_n(z) \text{ for every } n \in \{1,2,3,...,m\}.$$

Hence, $\hat{g}((xy)z) \geq \hat{g}(x) \wedge \hat{g}(z)$. Thus $\hat{g}$ is a MPFGB-ideal over $\hat{S}$.

Proposition 3.2 Consider $\hat{g} = (\hat{g}_1,\hat{g}_2,...,\hat{g}_m)$ is a multi-polar fuzzy subset over $\hat{S}$. Thus $\hat{g}$ is a MPFGB-ideal over $\hat{S}$ iff $\hat{g}_t = \{x \in \hat{S} \mid \hat{g}(x) \geq t\} \neq \varphi$ is a GB-ideal over $\hat{S}$ for every $t = (t_1,t_2,t_3,...,t_m) \in (0,1]^m$.

Proof. Suppose that $\hat{g}$ be a MPFGB-ideal over $\hat{S}$. Let x, z ∈ $\hat{g}_t$ and y ∈ $\hat{S}$. So $\hat{g}_n(x) \geq t_n$ and $\hat{g}_n(z) \geq t_n$ for every n ∈ {1,2,...,m}. Due to the fact that $\hat{g}$ is a MPFGB-ideal, we obtain $\hat{g}_n((xy)z) \geq \hat{g}_n(x) \wedge \hat{g}_n(z) \geq t_n \wedge t_n = t_n$ for every n ∈ {1,2,...,m}. Thus (xy)z ∈ $\hat{g}_t$, that is $\hat{g}_t$ is a GB-ideal over $\hat{S}$.

Conversely, let $\hat{g}_t \neq \varphi$ is a GB-ideal over $\hat{S}$. On contrary considered that $\hat{g}$ is not a MPFGB-ideal over $\hat{S}$. Suppose x, y, z ∈ $\hat{S}$ with $\hat{g}_n((xy)z) < \hat{g}_n(x) \wedge \hat{g}_n(z)$ for any n ∈ {1,2,...,m}. Suppose $t_n = \hat{g}_n(x) \wedge \hat{g}_n(z)$ for every n ∈ {1,2,...,m}. Then x, z ∈ $\hat{g}_t$ but (xy)z ∉ $\hat{g}_t$, this contradicts the hypothesis. Hence $\hat{g}((xy)z) \geq \hat{g}(x) \wedge \hat{g}(z)$, that is $\hat{g}$ is a MPFGB-ideal over $\hat{S}$. Now, we define the multi-polar fuzzy bi-ideal (MPFB-ideal) over $\hat{S}$.

Definition 3.7 A multi-polar fuzzy sub LA-semigroup $\hat{g} = (\hat{g}_1,\hat{g}_2,...,\hat{g}_m)$ over $\hat{S}$ is a MPFB-ideal over $\hat{S}$ if for each x, y, z ∈ $\hat{S}$, $\hat{g}((xy)z) \geq \hat{g}(x) \wedge \hat{g}(z)$ that is, $\hat{g}_n((xy)z) \geq \hat{g}_n(x) \wedge \hat{g}_n(z)$ for each n ∈ {1,2,3,...,m}.

Lemma 3.7 A subset $\hat{H}$ over $\hat{S}$ which is non-empty is a bi-ideal over $\hat{S}$ iff $\hat{C}_{\hat{H}}$ is a MPFB-ideal over $\hat{S}$.

Proof. It is followed by Lemmas 3.2 and 3.5.

Lemma 3.8 A multi-polar fuzzy sub LA-semigroup $\hat{g}$ of $\hat{S}$ is a MPFB-ideal over $\hat{S}$ iff $(\hat{g} \circ \delta) \circ \hat{g} \leq \hat{g}$.

Proof. Follows from Lemma 3.6.

Proposition 3.3 Let $\hat{g} = (\hat{g}_1,\hat{g}_2,...,\hat{g}_m)$ is a MPF-sub LA-semigroup over $\hat{S}$. So $\hat{g}$ is a MPFB-ideal over $\hat{S}$ iff $\hat{g}_t = \{x \in \hat{S} \mid g(x) \geq t\} \neq \varphi$ is a bi-ideal over $\hat{S}$ for every $t = (t_1,t_2,t_3,...,t_m) \in (0,1]^m$.

Proof. It is followed by Proposition 3.2.

Remark 3.1 Every MPFB-ideal of $\hat{S}$ is a MPFGB-ideal over $\hat{S}$.

The example below illustrate that the converse may not hold.

Example 3.3 Let $\hat{S}$ = {p, q, r, s} be an LA-semigroup under binary operation "·" described below in Table 4.

Table 4. LA-semigroup

•	p	q	r	s
p	s	s	q	q
Q	s	s	s	s
R	s	s	q	s
S	s	s	s	s

Consider $\hat{g} = (\hat{g}_1,\hat{g}_2,\hat{g}_3,\hat{g}_4)$ be a 4-polar fuzzy subset over $\hat{S}$ with $\hat{g}$(p) = (0.2,0.4,0.4,0.5), $\hat{g}$(q) = (0,0,0,0), $\hat{g}$(r) = (0,0,0,0), $\hat{g}$(s) = (0.6,0.7,0.8,0.9). Thus it is simple to reveal that $\hat{g}$ is a 4-polar fuzzy generalized bi-ideal over $\hat{S}$. Now, $\hat{g}$(q) = $\hat{g}$(p·s) = (0,0,0,0) $\ngeq$ (0.2,0.4,0.4,0.5) = $\hat{g}$(p) ∧ $\hat{g}$(s). So $\hat{g}$ is not a bi-ideal over $\hat{S}$.

Now we express the multi-polar fuzzy quasi-ideal (MPFQ-ideal) over $\hat{S}$.

Definition 3.8 A MPF-subset $\hat{g} = (\hat{g}_1,\hat{g}_2,...,\hat{g}_m)$ over $\hat{S}$ is a MPFQ-ideal over $\hat{S}$ if $(\hat{g} \circ \delta) \wedge (\delta \circ \hat{g}) \leq \hat{g}$, means that $(\hat{g}_n \circ \delta_n) \wedge (\delta_n \circ \hat{g}_n) \leq \hat{g}_n$ for every n ∈ {1,2,3,...,m}.

Lemma 3.9 A subset $\hat{J}$ over $\hat{S}$ which is non-empty is a quasi-ideal over $\hat{S}$ iff the multi-polar characteristic function $\hat{C}_{\hat{J}}$ of $\hat{J}$ is a MPFQ-ideal over $\hat{S}$.

Proof. Consider that $\hat{J}$ be a quasi-ideal over $\hat{S}$, i.e $\hat{J}\hat{S} \cap \hat{S}\hat{J} \subseteq \hat{J}$. We show that $(\hat{C}_{\hat{J}} \circ \delta) \wedge (\delta \circ \hat{C}_{\hat{J}}) \leq \hat{C}_{\hat{J}}$, means that

$((\hat{C}_{\hat{J}} \circ \delta) \wedge (\delta \circ \hat{C}_{\hat{J}}))(x) \leq \hat{C}_{\hat{J}}(x)$ for all x ∈ $\hat{S}$.

Let we have two cases,

Case1 : If x ∈ $\hat{J}$, then $\hat{C}_{\hat{J}}(x) = (1,1,...,1) \geq ((\hat{C}_{\hat{J}} \circ \delta) \wedge (\delta \circ \hat{C}_{\hat{J}}))(x)$.

Therefore $(\hat{C}_{\hat{J}} \circ \delta) \wedge (\delta \circ \hat{C}_{\hat{J}}) \leq \hat{C}_{\hat{J}}$.

Case 2 : If x ∉ $\hat{J}$, so x ∉ $\hat{J}\hat{S} \cap \hat{S}\hat{J}$. This implies that x ≠ ab or x ≠ cd for any a ∈ $\hat{J}$, b ∈ $\hat{S}$, c ∈ $\hat{S}$, d ∈ $\hat{J}$. Thus either $(\hat{C}_{\hat{J}} \circ \delta)(x) = (0,0,...,0)$ or $(\delta \circ \hat{C}_{\hat{J}})(x) = (0,0,...,0)$, means that $((\hat{C}_{\hat{J}} \circ \delta) \wedge (\delta \circ \hat{C}_{\hat{J}}))(x) = (0,0,...,0) \leq \hat{C}_{\hat{J}}(x)$. So that $(\hat{C}_{\hat{J}} \circ \delta) \wedge (\delta \circ \hat{C}_{\hat{J}}) \leq \hat{C}_{\hat{J}}$.

Conversely, let z ∈ $\hat{J}\hat{S} \cap \hat{S}\hat{J}$. Thus z = ax and z = yb, where x, y ∈ $\hat{S}$ and a, b ∈ $\hat{J}$. Since $\hat{C}_{\hat{J}}$ is a MPFQ-ideal over $\hat{S}$, we get

$\hat{C}_{\hat{J}}(z) \geq ((\hat{C}_{\hat{J}} \circ \delta) \wedge (\delta \circ \hat{C}_{\hat{J}}))(z)$

$= (\hat{C}_{\hat{J}} \circ \delta)(z) \wedge (\delta \circ \hat{C}_{\hat{J}})(z)$

$= \{\bigvee_{z=uv}\{\hat{C}_{\hat{J}}(u) \wedge \delta(v)\}\} \wedge \{\bigvee_{z=pq}\{\delta(p) \wedge \hat{C}_{\hat{J}}(q)\}\}$

$\geq \{\hat{C}_{\hat{J}}(a) \wedge \delta(x)\} \wedge \{\delta(y) \wedge \hat{C}_{\hat{J}}(b)\}$

= (1,1,...,1) since z = ax and z = yb.

Thus $\hat{C}_{\hat{J}}(z)$ = (1,1,...,1). Hence z ∈ $\hat{J}$.

Proposition 3.4 Consider $\hat{g} = (\hat{g}_1,\hat{g}_2,...,\hat{g}_m)$ be a MPF-subset over $\hat{S}$. Thus $\hat{g}$ is a MPFQ-ideal over $\hat{S}$ iff $\hat{g}_t = \{s \in \hat{S} \mid \hat{g}(s) \geq t\} \neq \varphi$ is a quasi-ideal over $\hat{S}$ for every $t = (t_1,t_2,t_3,...,t_m) \in (0,1]^m$.

Proof. Consider $\hat{g}$ be a MPFQ-ideal over $\hat{S}$. To show that $\hat{g}_t\hat{S} \cap \hat{S}\hat{g}_t \subseteq \hat{g}_t$. Let z ∈ $\hat{g}_t\hat{S} \cap \hat{S}\hat{g}_t$. Then z ∈ $\hat{g}_t\hat{S}$ and z ∈ $\hat{S}\hat{g}_t$. So z = ax and z = yb for some x,y ∈ $\hat{S}$ and a,b ∈ $\hat{g}_t$. Thus $\hat{g}_n(a) \geq t_n$ and $\hat{g}_n(b) \geq t_n$ for every n ∈ {1,2,3,...,m}. Now,

$(\hat{g}_n \circ \delta_n)(z) = \bigvee_{z=uv}\{\hat{g}_n(u) \wedge \delta_n(v)\}$

$\geq \hat{g}_n(a) \wedge \delta_n(x)$ because z = ax

$= \hat{g}_n(a) \wedge 1$

$= \hat{g}_n(a)$

$\geq t_n$

So, $(\hat{g}_n \circ \delta_n)(z) \geq t_n$ for each n ∈ {1,2,...,m}. Now,

$(\delta_n \circ \hat{g}_n)(z) = \bigvee_{z=uv}\{\delta_n(u) \wedge \hat{g}_n(v)\}$

$\geq \delta_n(y) \wedge \hat{g}_n(b)$ because z = yb

$= 1 \wedge \hat{g}_n(b)$

$= \hat{g}_n(b)$

$\geq t_n$

So, $(\delta_n \circ \hat{g}_n)(z) \geq t_n$ for every n ∈ {1,2,...,m}.

Thus, $((\hat{g}_n \circ \delta_n) \wedge (\delta_n \circ \hat{g}_n))(z)$

$= ((\hat{g}_n \circ \delta_n)(z) \wedge (\delta_n \circ \hat{g}_n)(z) \geq t_n \wedge t_n = t_n$

for every n ∈{1,2,3,...,m}. So, $((\hat{g} \circ \delta) \wedge (\delta \circ \hat{g}))(z) \geq t$. As $\hat{g}(z) \geq ((\hat{g} \circ \delta) \wedge (\delta \circ \hat{g}))(z) \geq t$, thus z ∈ $\hat{g}_t$. Therefore it is proved that $\hat{g}_t$ is a quasi-ideal over $\hat{S}$.

Conversely, on contrary, let $\hat{g}$ is not a MPFQ-ideal over $\hat{S}$. Let $z \in \hat{S}$ be such that $\hat{g}_n(z) < (\hat{g}_n \circ \delta_n)(z) \wedge (\delta_n \circ \hat{g}_n)(z)$ for any $n \in \{1,2,...,m\}$. Take $t_n \in (0,1]$ with $t_n = (\hat{g}_n \circ \delta_n)(z) \wedge (\delta_n \circ \hat{g}_n)(z)$ for every $n \in \{1,2,3,...,m\}$. It follows that $z \in (\hat{g}_n \circ \delta_n)t_n$ and $z \in (\delta_n \circ \hat{g}_n)t_n$ but $z \notin (\hat{g}_n)t_n$ for some n. Therefore, $z \in (\hat{g} \circ \hat{S})t$ and $z \in (\hat{S} \circ \hat{g})_t$ but $z \notin \hat{g}_t$. Which leads to contradiction.

This proves that $(\hat{g} \circ \delta) \wedge (\delta \circ \hat{g}) \leq \hat{g}$.

Lemma 3.10 Every multi-polar fuzzy one-sided ideal over $\hat{S}$ is a MPFQ-ideal over $\hat{S}$.

Proof. It is followed by Lemma 3.3.

The subsequent example demonstrates that the converse may not hold.

Example 3.4 Let $\hat{S} = \{r, s, t, u\}$ be an LA-semigroup under binary operation "·" described below in Table 5.

Table 5. LA-semigroup

•	r	s	t	U
R	r	s	t	U
S	u	t	t	T
T	t	t	t	T
U	s	t	t	T

Define a 5-polar fuzzy subset $\hat{g} = (\hat{g}_1,\hat{g}_2,\hat{g}_3,\hat{g}_4,\hat{g}_5)$ of $\hat{S}$ as follows:

$\hat{g}(s) = \hat{g}(t) = (0.4,0.4,0.5,0.5,0.6)$, $\hat{g}(r) = \hat{g}(u) = (0,0,0,0,0)$. Thus it is simple to reveal that $\hat{g}_t$ is a quasi-ideal over $\hat{S}$. Therefore by using Proposition 4, $\hat{g}$ is a 5-polar FQ-ideal over Ŝ. Now,

$$\hat{g}(u) = \hat{g}(s.r) = (0,0,0,0,0)$$

$$\ngeq (0.4,0.4,0.5,0.5,0.6) = \hat{g}(s).$$

So $\hat{g}$ is not a 5-polar FR-ideal over $\hat{S}$.

Lemma 3.11 Suppose that $\hat{g} = (\hat{g}_1,\hat{g}_2,...,\hat{g}_m)$ and $\hat{h} = (\hat{h}_1,\hat{h}_2,...,\hat{h}_m)$ be MPFR-ideal and MPFL-ideal over $\hat{S}$. Then $\hat{g} \wedge \hat{h}$ is a multi-polar FQ-ideal over $\hat{S}$.

Proof. Consider $\hat{g} = (\hat{g}_1,\hat{g}_2,...,\hat{g}_m)$ and $\hat{h} = (\hat{h}_1,\hat{h}_2,...,\hat{h}_m)$ be MPFR-ideal and MPFL-ideal over $\hat{S}$. Let $s \in \hat{S}$. If $s \neq ab$ for $a,b \in \hat{S}$. We have

$$((\hat{g} \wedge \hat{h})\circ\delta) \wedge (\delta \circ (\hat{g} \wedge \hat{h})) \leq (\hat{g} \wedge \hat{h}).$$

If $s = pq$ for $p,q \in \hat{S}$, then

$$(((\hat{g}_n \wedge \hat{h}_n) \circ \delta_n) \wedge (\delta_n \circ (\hat{g}_n \wedge \hat{h}_n)))(s)$$

$$= ((\hat{g}_n \wedge \hat{h}_n) \circ \delta_n)(s) \wedge (\delta_n \circ (\hat{g}_n \wedge \hat{h}_n))(s)$$

$$= \begin{Bmatrix} \bigvee_{s=pq}\{(\hat{g}_n \wedge \hat{h}_n)(p) \wedge \delta_n(q)\} \wedge \\ \bigvee_{s=pq}\{\delta_n(p) \wedge (\hat{g}_n \wedge \hat{h}_n)(q)\} \end{Bmatrix}$$

$$= \bigvee_{s=pq}\{(\hat{g}_n \wedge \hat{h}_n)(p)\} \wedge \bigvee_{s=pq}\{(\hat{g}_n \wedge \hat{h}_n)(q)\}$$

$$= \bigvee_{s=pq}\{(\hat{g}_n \wedge \hat{h}_n)(p) \wedge (\hat{g}_n \wedge \hat{h}_n)(q)\}$$

$$= \bigvee_{s=pq}\{(\hat{g}_n(p) \wedge \hat{h}_n(p)) \wedge (\hat{g}_n(q) \wedge \hat{h}_n(q))$$

$$\leq \bigvee_{s=pq}\{\hat{g}_n(p) \wedge \hat{h}_n(q)\}$$

$$\leq \bigvee_{s=pq}\{(\hat{g}_n(pq) \wedge \hat{h}_n(pq)\}$$

$$= \bigvee_{s=pq}\{(\hat{g}_n \wedge \hat{h}_n)(pq)\}$$

$$= (\hat{g}_n \wedge \hat{h}_n)(s) \text{ for every } n \in \{1,2,...,m\}.$$

Thus $((\hat{g}\wedge\hat{h})\circ\delta) \wedge (\delta\circ(\hat{g}\wedge\hat{h})) \leq (\hat{g}\wedge\hat{h})$, that is $\hat{g} \wedge \hat{h}$ be a MPFQ-ideal over $\hat{S}$.

Now, we define the multi-polar fuzzy interior-ideal (MPFI-ideal) over $\hat{S}$.

Definition 3.9 A multi-polar fuzzy sub LA-semigroup $\hat{g} = (\hat{g}_1,\hat{g}_2,...,\hat{g}_m)$ of $\hat{S}$ is a MPFI-ideal over $\hat{S}$ if for each $x, a, y \in \hat{S}$, $\hat{g}((xa)y) \geq \hat{g}(a)$, that is $\hat{g}_n((xa)y) \geq \hat{g}_n(a)$ for every $n \in \{1,2,3,...,m\}$.

Lemma 3.12 A subset $\hat{I}$ over $\hat{S}$ which is non-empty is an interior ideal over $\hat{S}$ iff the multi-polar characteristic function $\hat{C}_{\hat{I}}$ over $\hat{I}$ is a MPFI-ideal over $\hat{S}$.

Proof: Consider that $\hat{I}$ is an interior ideal over $\hat{S}$. From Lemma 2, $\hat{C}_{\hat{I}}$ is a multi-polar fuzzy sub LA-semigroup over $\hat{S}$. Now, we show that $\hat{C}_{\hat{I}}((pq)r) \geq \hat{C}_{\hat{I}}(q)$ for every $p,q,r \in \hat{S}$. Let we have the four cases,

Case 1 : Consider that $q \in \hat{I}$ and $p, r \in \hat{S}$. Then $\hat{C}_{\hat{I}}(q) = (1,1,...,1)$. Since $\hat{I}$ is an interior ideal over $\hat{S}$, so $(pq)r \in \hat{I}$. Then $\hat{C}_{\hat{I}}((pq)r) = (1,1,...,1)$. Hence $\hat{C}_{\hat{I}}((pq)r) \geq \hat{C}_{\hat{I}}(q)$.

Case 2 : Let $q \notin \hat{I}$ and $p,r \in \hat{S}$. Then $\hat{C}_{\hat{I}}(q) = (0,0,...,0)$. Clearly, $\hat{C}_{\hat{I}}((pq)r) \geq \hat{C}_{\hat{I}}(q)$. Hence the multi-polar characteristic function $\hat{C}_{\hat{I}}$ over $\hat{I}$ is an multi-polar FI-ideal over $\hat{S}$.

Conversely, consider that $\hat{C}_{\hat{I}}$ is a MPFI-ideal over $\hat{S}$. Then by Lemma 2, $\hat{I}$ is a sub LA-semigroup over $\hat{S}$. Let $p,r \in \hat{S}$ and $q \in \hat{I}$. Then, $\hat{C}_{\hat{I}}(q) = (1,1,...,1)$. By the hypothesis, $\hat{C}_{\hat{I}}((pq)r) \geq \hat{C}_{\hat{I}}(q) = (1,1,...,1)$. Hence $\hat{C}_{\hat{I}}((pq)r) = (1,1,...,1)$. This proves that $(pq)r \in \hat{I}$, that is $\hat{I}$ is an interior ideal over $\hat{S}$.

Lemma 3.13 Let $\hat{g}$ be a MPF-sub LA-semigroup over $\hat{S}$. Then $\hat{g}$ is a MPFI-ideal over $\hat{S}$ iff $(\delta \circ \hat{g}) \circ \delta \leq \hat{g}$.

Proof. Let $\hat{g} = (\hat{g}_1,\hat{g}_2,...,\hat{g}_m)$ be a multi-polar FI-ideal over $\hat{S}$. We demonstrate that $(\delta \circ \hat{g}) \circ \delta \leq \hat{g}$. Let $z \in \hat{S}$. Then for every $n \in \{1,2,...,m\}$.

$$((\delta_n \circ \hat{g}_n) \circ \delta_n)(z) = \bigvee_{z=uv}\{(\delta_n \circ \hat{g}_n)(u) \wedge \delta_n(v)\}$$

$$= \bigvee_{z=uv}\{(\delta_n \circ \hat{g}_n)(u)\}$$

$$= \bigvee_{z=uv}\{\bigvee_{u=ab}\{\delta_n(a) \wedge \hat{g}_n(b)\}$$

$$= \bigvee_{z=uv}\{\bigvee_{u=ab}\{\hat{g}_n(b)\}$$

$$= \bigvee_{z=(ab)v}\{\hat{g}_n(b)\}$$

$$\leq \bigvee_{z=(ab)v}\{\hat{g}_n((ab)v)\}$$

$$= \hat{g}_n(z) \text{ for every } n \in \{1,2,...,m\}.$$

Thus $(\delta \circ \hat{g}) \circ \delta \leq \hat{g}$.

In the reverse, assume that $(\delta \circ \hat{g}) \circ \delta \leq \hat{g}$. We only prove that $\hat{g}_n((xa)y) \geq \hat{g}_n(a)$ for each $x,a,y \in \hat{S}$ and for every $n \in \{1,2,...,m\}$. Let $z = (xa)y$. Now for every $n \in \{1,2,...,m\}$.

$$\hat{g}_n((xa)y) \geq ((\delta_n \circ \hat{g}_n) \circ \delta_n)((xa)y)$$

$$= \bigvee_{(xa)y=uv}\{(\delta_n \circ \hat{g}_n)(u) \wedge \delta_n(v)\}$$

$$\geq (\delta_n \circ \hat{g}_n)(xa) \wedge \delta_n(y)$$

$$= (\delta_n \circ \hat{g}_n)(xa)$$

$$= \bigvee_{xa=pq}\{(\delta_n(p) \wedge \hat{g}_n(q)\}$$

$$\geq \delta_n(x) \wedge \hat{g}_n(a)$$

$$= \hat{g}_n(a) \text{ for all } n \in \{1,2,...,m\}.$$

So, $\hat{g}_n((xa)y) \geq \hat{g}_n(a)$ for each $n \in \{1,2,...,m\}$. Thus $\hat{g}$ is a MPFI-ideal over $\hat{S}$.

Proposition 3.5 Consider $\hat{g} = (\hat{g}_1,\hat{g}_2,...,\hat{g}_m)$ be a MPF-subset over $\hat{S}$. Then $\hat{g}$ is a multi-polar FI-ideal over $\hat{S}$ iff $\hat{g}_t = \{x \in \hat{S} \mid \hat{g}(x) \geq t\} \neq \varphi$ is an interior ideal over $\hat{S}$ for each $t = (t_1,t_2,t_3,...,t_m) \in (0,1]^m$.

Proof. It can be proved on the same lines of Propositions 3.1 and 3.2.

4. REGULAR LA-SEMIGROUPS CHARACTERIZED BY MULTI-POLAR FUZZY IDEALS

Definition 4.1 If for every element s in the LA-semigroup $\hat{S}$, there exists $r \in \hat{S}$ such that s can be expressed as $s = (sr)s$ then $\hat{S}$ is a regular LA-semigroup.

Theorem 4.1 [15] Let $\hat{S}$ possesses e with $(ae)\hat{S} = a\hat{S}$ for each $a \in \hat{S}$. So the subsequent assertions are equivalent.

(1) $\hat{S}$ is regular

(2) For all R-ideal $\hat{R}$ and L-ideal $\hat{L}$ over $\hat{S}$ we have $\hat{R} \cap \hat{L} = \hat{R}\hat{L}$.

(3) $\hat{J} = (\hat{J}\hat{S})\hat{J}$ for all Q-ideal $\hat{J}$ over $\hat{S}$.

Theorem 4.2 If $\hat{S}$ possesses e with $(re)\hat{S} = r\hat{S}$ for each $r \in \hat{S}$. Then any MPFQ-ideal over $\hat{S}$ is a MPFB-ideal over $\hat{S}$.

Proof. Consider $\hat{g} = (\hat{g}_1,\hat{g}_2,...,\hat{g}_m)$ be any MPFQ-ideal over $\hat{S}$. Take $p,q \in \hat{S}$. Then,

$$\hat{g}_n(pq) \geq ((\hat{g}_n \circ \delta_n) \wedge (\delta_n \circ \hat{g}_n))(pq)$$

$$= (\hat{g}_n \circ \delta_n)(pq) \wedge (\delta_n \circ \hat{g}_n)(pq)$$

$$= \begin{Bmatrix} \bigvee_{pq=ab}\{\hat{g}_n(a) \wedge \delta_n(b)\} \wedge \\ \bigvee_{pq=uv}\{\delta_n(u) \wedge \hat{g}_n(v)\} \end{Bmatrix}$$

$$\geq \{\hat{g}_n(p) \wedge \delta_n(q)\} \wedge \{\delta_n(p) \wedge \hat{g}_n(q)\}$$

$$= \{\hat{g}_n(p) \wedge 1\} \wedge \{1 \wedge \hat{g}_n(q)\}$$

$$= \hat{g}_n(p) \wedge \hat{g}_n(q) \text{ for all } n \in \{1,2,...,m\}.$$

So, $\hat{g}(pq) \geq \hat{g}(p) \wedge \hat{g}(q)$.

Now, let $p,q,r \in \hat{S}$. Then,

$$(\delta_n \circ \hat{g}_n)((pq)r) = \bigvee_{(pq)r=uv}\{\delta_n(u) \wedge \hat{g}_n(v)\}$$

$$\geq \delta_n(pq) \wedge \hat{g}_n(r)$$

$$= 1 \wedge \hat{g}_n(r)$$

$$= \hat{g}_n(r)$$

So, $(\delta_n \circ \hat{g}_n)((pq)r) \geq \hat{g}_n(r)$ for all n ∈ {1,2,...,m}.

Since $(pq)r = (pq)(er) = (pe)(qr) \in (pe)\hat{S} = p\hat{S}$, so $(pq)r = ps$ for some $s \in \hat{S}$. Thus,

$(\hat{g}_n \circ \delta_n)((pq)r) = \bigvee_{(pq)r=ab}\{\hat{g}_n(a) \wedge \delta_n(b)\}$

$\geq \hat{g}_n(p) \wedge \delta_n(s)$ since $(pq)r = ps$

$= \hat{g}_n(p) \wedge 1$

$= \hat{g}_n(p)$

So, $(\hat{g}_n \circ \delta_n)((pq)r) \geq \hat{g}_n(p)$ for every n ∈ {1,2,...,m}.

Now, by our assumption

$\hat{g}_n((pq)r) \geq ((\hat{g}_n \circ \delta_n) \wedge (\delta_n \circ \hat{g}_n))((pq)r)$

$= (\hat{g}_n \circ \delta_n)((pq)r) \wedge (\delta_n \circ \hat{g}_n)((pq)r)$

$\geq \hat{g}_n(p) \wedge \hat{g}_n(r)$ for every n ∈ {1,2,...,m}.

Thus, $\hat{g}((pq)r) \geq \hat{g}(p) \wedge \hat{g}(r)$. This proves that $\hat{g}$ is an MPFB-ideal over $\hat{S}$.

Theorem 4.3 The subsequent statements are equivalent for an LA-semigroup $\hat{S}$.

(1) $\hat{S}$ is regular

(2) $\hat{g} \wedge \hat{h} = \hat{g} \circ \hat{h}$ for any MPFR-ideal $\hat{g}$ and MPFL-ideal $\hat{h}$ over $\hat{S}$.

Proof. (1) ⇒ (2): Consider $\hat{g} = (\hat{g}_1,\hat{g}_2,...,\hat{g}_m)$ and $\hat{h} = (\hat{h}_1,\hat{h}_2,...,\hat{h}_m)$ be any MPFR-ideal and MPFL-ideal of $\hat{S}$. Let $a \in \hat{S}$, we get

$(\hat{g}_n \circ \hat{h}_n)(a) = \bigvee_{a=yz}\{\hat{g}_n(y) \wedge \hat{h}_n(z)\}$

$\leq \bigvee_{a=yz}\{\hat{g}_n(yz) \wedge \hat{h}_n(yz)\}$

$= \hat{g}_n(a) \wedge \hat{h}_n(a)$

$= (\hat{g}_n \wedge \hat{h}_n)(a)$ for all n ∈ {1,2,...,m}.

So, $(\hat{g} \circ \hat{h}) \leq (\hat{g} \wedge \hat{h})$.

By assertion (1), for each $a \in \hat{S}$, we have $a = (ax)a$ for some $x \in \hat{S}$. So we get

$(\hat{g}_n \wedge \hat{h}_n)(a) = \hat{g}_n(a) \wedge \hat{h}_n(a)$

$\leq \hat{g}_n(ax) \wedge \hat{h}_n(a)$

$\leq \bigvee_{a=yz}\{\hat{g}_n(y) \wedge \hat{h}_n(z)\}$

$= (\hat{g}_n \circ \hat{h}_n)(a)$ for all n ∈ {1,2,...,m}.

Thus, $(\hat{g} \circ \hat{h}) \geq (\hat{g} \wedge \hat{h})$. Hence proved that $(\hat{g} \wedge \hat{h}) = (\hat{g} \circ \hat{h})$.

(2) ⇒ (1): Suppose that $a \in \hat{S}$. Thus $a\hat{S}$ is a L-ideal over $\hat{S}$ and $a\hat{S} \cup \hat{S}a$ is a R-ideal over $\hat{S}$ generated by a say $a\hat{S} = \hat{L}$ and $a\hat{S} \cup \hat{S}a = \hat{R}$. Now $\hat{C}_{\hat{L}}$ and $\hat{C}_{\hat{R}}$ the multi-polar characteristic functions of $\hat{L}$ and $\hat{R}$ are MPFL-ideal and MPFR-ideal over $\hat{S}$ by using Lemma 3.2. Hence, from Lemma 3.1 and assertion (2) we get

$\hat{C}_{\hat{R}\hat{L}} = (\hat{C}_{\hat{R}} \circ \hat{C}_{\hat{L}})$ from Lemma 3.1

$= (\hat{C}_{\hat{R}} \wedge \hat{C}_{\hat{L}})$ from 2

$= \hat{C}_{\hat{R} \cap \hat{L}}$ by Lemma 3.1.

This proves that $\hat{R} \cap \hat{L} = \hat{R}\hat{L}$. Thus $\hat{S}$ is regular from Theorem 4.1.

Theorem 4.4 Consider $e \in \hat{S}$ with $(ae)\hat{S} = a\hat{S}$ for each $a \in \hat{S}$. Thus the subsequent assertions are equivalent.

(1) $\hat{S}$ is regular

(2) $\hat{g} = (\hat{g} \circ \delta) \circ \hat{g}$ for any MPFGB-ideal $\hat{g}$ over $\hat{S}$.

(3) $\hat{g} = (\hat{g} \circ \delta) \circ \hat{g}$ for each MPFB-ideal $\hat{g}$ over $\hat{S}$.

Proof. (1) ⇒ (2): Consider $\hat{g} = (\hat{g}_1,\hat{g}_2,...,\hat{g}_m)$ be a MPFGB-ideal over $\hat{S}$. Let $a \in \hat{S}$, so by assertion (1), $a = (ax)a$ for some $x \in \hat{S}$. So, we get

$((\hat{g}_n \circ \delta_n) \circ \hat{g}_n)(a)$

$= \bigvee_{a=yz}\{(\hat{g}_n \circ \delta_n)(y) \wedge \hat{g}_n(z)\}$ for some $y, z \in \hat{S}$

$\geq (\hat{g}_n \circ \delta_n)(ax) \wedge \hat{g}_n(a)$ since $a = (ax)a$

$= \bigvee_{ax=pq}\{\hat{g}_n(p) \wedge \delta_n(q)\} \wedge \hat{g}_n(a)$

$\geq \{\hat{g}_n(a) \wedge \delta_n(x)\} \wedge \hat{g}_n(a)$

$= \hat{g}_n(a)$ for all n ∈ {1,2,...,m}.

Hence proved that $(c \circ \delta) \circ \hat{g} \geq \hat{g}$.

Because $\hat{g}$ is a MPFGB-ideal over $\hat{S}$. Thus, we get

$((\hat{g}_n \circ \delta_n) \circ \hat{g}_n)(a)$

$= \bigvee_{a=yz}\{(\hat{g}_n \circ \delta_n)(y) \wedge \hat{g}_n(z)\}$ for some $y,z \in \hat{S}$
$= \bigvee_{a=yz}\{\bigvee_{y=pq}\{\hat{g}_n(p) \wedge \delta_n(q)\} \wedge \hat{g}_n(z)\}$ for $p,q \in \hat{S}$

$= \vee_{a=yz}\{\vee_{y=pq}\{\hat{g}_n(p) \wedge \hat{g}_n(z)\}\}$

$\leq \vee_{a=yz}\{\vee_{y=pq}\{\hat{g}_n((pq)z)\}\}$

$= \vee_{a=yz}\{\hat{g}_n(yz)\}$

$= \hat{g}_n(a)$ for all n ∈ {1,2,...,m}.

So, $(\hat{g} \circ \delta) \circ \hat{g} \leq \hat{g}$. Thus $\hat{g} = (\hat{g} \circ \delta) \circ \hat{g}$.

(2) ⇒ (3): It is straightforward.

(3) ⇒ (1): Consider $\hat{J}$ be any quasi-ideal over $\hat{S}$. Since $(\hat{J}\hat{S})\hat{J} \subseteq (\hat{J}\hat{S})\hat{S} = (\hat{J}\hat{S})(e\hat{S}) = (\hat{J}e)(\hat{S}\hat{S}) = (\hat{J}e)\hat{S} = \hat{J}\hat{S}$ and $(\hat{J}\hat{S})\hat{J} \subseteq (\hat{S}\hat{S})\hat{J} = \hat{S}\hat{J}$. Therefore $(\hat{J}\hat{S})\hat{J} \subseteq \hat{J}\hat{S} \cap \hat{S}\hat{J} \subseteq \hat{J}$.

Now, let a ∈ $\hat{J}$ such that a = yz for some y, z ∈ $\hat{S}$. Since by Lemma 3.9, $\hat{C}_J$ is a MPFQ-ideal over $\hat{S}$. Therefore $\hat{C}_J$ is an MPFB-ideal over $\hat{S}$ by Theorem 4.2. Thus, we get

$((\hat{C}_J \circ \delta) \circ \hat{C}_J)(a) = \hat{C}_J(a)$ by using condition (3)

$= (1,1,...,1)$

Hence $((\hat{C}_J \circ \delta) \circ \hat{C}_J)(a) = (1,1,...,1)$. So, there are elements u, v ∈ $\hat{S}$ so that $(\hat{C}_J \circ \delta)(u) = (1,1,...,1)$ and $\hat{C}_J(v) = (1,1,...,1)$ with a = uv. Since $(\hat{C}_J \circ \delta)(u) = (1,1,...,1)$. So there are elements w, e ∈ $\hat{S}$ such that $\hat{C}_J(w) = (1,1,...,1)$ and δ(e) = (1,1,...,1) with u = we. Thus w, v ∈ $\hat{J}$ and e ∈ $\hat{S}$ and so a = uv = (we)v ∈ $(\hat{J}\hat{S})\hat{J}$. Hence $\hat{J} \subseteq (\hat{J}\hat{S})\hat{J}$. So, $\hat{J} = (\hat{J}\hat{S})\hat{J}$. Thus $\hat{S}$ is regular from Theorem 4.1.

Theorem 4.5 Consider e ∈ $\hat{S}$ with $(ae)\hat{S} = a\hat{S}$ for each a ∈ $\hat{S}$. Thus the subsequent statements are equivalent.

(1) $\hat{S}$ is regular

(2) Consider any MPFR-ideal $\hat{g}$, any MPFGB-ideal $\hat{h}$, and any MPFL-ideal $\hat{I}$ over $\hat{S}$, this

$(\hat{g} \circ \hat{h}) \circ \hat{I} \geq (\hat{g} \wedge \hat{h}) \wedge \hat{I}$ holds.

(3) Consider any MPFR-ideal $\hat{g}$, any MPFB-ideal $\hat{h}$, and any MPFL-ideal $\hat{I}$ over $\hat{S}$, this

$(\hat{g} \circ \hat{h}) \circ \hat{I} \geq (\hat{g} \wedge \hat{h}) \wedge \hat{I}$ holds.

(4) Consider any MPFR-ideal $\hat{g}$, any MPFQ-ideal $\hat{h}$, and any MPFL-ideal $\hat{I}$ of $\hat{S}$, this

$(\hat{g} \circ \hat{h}) \circ \hat{I} \geq (\hat{g} \wedge \hat{h}) \wedge \hat{I}$ holds.

Proof. (1) ⇒ (2): Consider $\hat{g} = (\hat{g}_1,\hat{g}_2,...,\hat{g}_m)$, $\hat{h} = (\hat{h}_1,\hat{h}_2,...,\hat{h}_m)$, and $\hat{I} = (\hat{I}_1,\hat{I}_2,...,\hat{I}_m)$ be any MPFR-ideal, MPFGB-ideal and MPFL-ideal $\hat{I}$ over $\hat{S}$, respectively. Suppose that a ∈ $\hat{S}$, so by assertion (1) a = (ar)a for some r ∈ $\hat{S}$. It follows that, a = (ar)a = (ar)(ea) = (ae)(ra) = a(ra) since $(ae)\hat{S} = a\hat{S}$ for each a ∈ $\hat{S}$. Hence we get

$((\hat{g} \circ \hat{h}) \circ \hat{I})(a) = \vee_{a=uv}\{(\hat{g} \circ \hat{h})(u) \wedge \hat{I}(v)\}$

$\geq (\hat{g} \circ h)(a) \wedge \hat{I}(ra)$ as a = a(ra)

$\geq \vee_{a=pq}\{\hat{g}(p) \wedge \hat{h}(q)\} \wedge \hat{I}(a)$

$\geq (\hat{g}(ar) \wedge \hat{h}(a)) \wedge \hat{I}(a)$ as a = (ar)a

$\geq (\hat{g}(a) \wedge \hat{h}(a)) \wedge \hat{I}(a)$

$= ((\hat{g} \wedge \hat{h})(a)) \wedge \hat{I}(a)$

$= ((\hat{g} \wedge \hat{h}) \wedge \hat{I})(a)$

Hence proved that $(\hat{g} \circ \hat{h}) \circ \hat{I} \geq (\hat{g} \wedge \hat{h}) \wedge \hat{I}$.

(2) ⇒ (3) ⇒ (4): These are straight forward.

(4) ⇒ (1): Consider $\hat{g} = (\hat{g}_1,\hat{g}_2,...,\hat{g}_m)$ and $\hat{I} = (\hat{I}_1,\hat{I}_2,...,\hat{I}_m)$ be any MPFR-ideal and MPFL-ideal over $\hat{S}$. As δ be a MPFQ-ideal over $\hat{S}$, by the supposition, we get

$(\hat{g} \wedge \hat{I})(a) = ((\hat{g} \wedge \delta) \wedge \hat{I})(a)$

$\leq ((\hat{g} \circ \delta) \circ \hat{I})(a)$

$= \vee_{a=pq}\{(\hat{g} \circ \delta)(p) \wedge \hat{I}(q)\}$

$= \vee_{a=pq}\{(\vee_{p=uv}\{\hat{g}(u) \wedge \delta(v)\}) \wedge \hat{I}(q)\}$

$= \vee_{a=pq}\{(\vee_{p=uv}\{\hat{g}(u) \wedge 1\}) \wedge \hat{I}(q)\}$

$= \vee_{a=pq}\{(\vee_{p=uv}\hat{g}(u)) \wedge \hat{I}(q)\}$

$\leq \vee_{a=pq}\{(\vee_{p=uv}\{\hat{g}(uv)\}) \wedge \hat{I}(q)\}$

$= \vee_{a=pq}\{\hat{g}(p) \wedge \hat{I}(q)\}$

$= (\hat{g} \circ \hat{I})(a)$

Thus $(\hat{g} \circ \hat{I}) \geq (\hat{g} \wedge \hat{I})$ for any MPFR-ideal $\hat{g}$ and any MPFL-ideal $\hat{I}$ over $\hat{S}$. But $(\hat{g} \circ \hat{I}) \leq (\hat{g} \wedge \hat{I})$. This gives $(\hat{g} \circ \hat{I}) = (\hat{g} \wedge \hat{I})$. Thus $\hat{S}$ is regular by Theorem 4.3.

5. CONCLUSION

In this research paper, we have put forward the idea of MPF-sets which is an expansion of BPF-sets. Infact, the BPF-sets are useful mathematical model to demonstrate the positivity and negativity of goods. In this study we have examined the multi-information about the given data by defining the multi-polar fuzzy sets in LA-semigroups. Mainly, we have confined our attention to investigate how we can generalize the results of BPF-sets in terms of multi-polar fuzzy sets. Also detailed exposition of multi-polar fuzzy ideals in $\hat{S}$ have been studied. Moreover, this study can be used as a design for aggregation or classification and to define multi-valued relations. One such structure is the Pythagorean MPF-set which is hybrid model of both PFS and MPF-sets is presented by Naeem *et al.* [17]. Another related model is the Pythagorean MPF-sets, which was proposed by Riaz *et al.* [18]. The interval [0,1] is the range of a membership function, which illustrates a fuzzy set (F-set). A membership degree serves as an illustration of how individuals of a set are related.

6. CONFLICT OF INTEREST

The authors declare no conflict of interest.

7. REFERENCES

1. J. Chen, S. Li, S. Ma, and X. Wang. m-Polar Fuzzy Sets: An Extension of Bipolar Fuzzy Sets. *The Scientific World Journal* 2014: 416530 (2014).
2. D.T. Ho, and J.M. Garibaldi. Context modelling in fuzzy systems. *Proceedings of the WCCI 2012 IEEE World Congress on Computational Intelligence, Brisbane, Australia* 1-7 (2012).
3. M.A. Nazim, and M. Naseerudin. On almost-semigroup. *The Aligarh Bulletin of Mathematics* 2: 1-7 (1972).
4. N. Kuroki. Fuzzy bi-ideals in semigroups. *Commentarii mathematici Universitatis Sancti Pauli* 27: 17-21 (1979).
5. K.M. Lee. Bipolar-valued fuzzy sets and their operations. *Proceedings of the International conference on Intelligent Technologies, Bangkok, Thailand* 307-312 (2000).
6. K.M. Lee. Comparison of interval-valued fuzzy sets, intuitionistic fuzzy sets and bipolar-valued fuzzy sets. *Journal of Fuzzy Logic and Intelligent Systems* 14: 125-129 (2004).
7. N. Malik, and M. Shabir. A consensus model based on rough bipolar fuzzy approximations. *Journal of Intelligent & Fuzzy Systems* 36: 3461–3470 (2019).
8. J.N. Mordeson, D. S. Malik, and N. Kuroki. Fuzzy semigroups. *Springer-Verlag, Berlin, Germany* (2003).
9. Q. Mushtaq, and S.M. Yusuf. On LA-semigroups. *The Aligarh Bulletin of Mathematics* 8: 65-70 (1978).
10. Q. Mushtaq, and S.M. Yusuf. On locally associative LA-semigroups. *Journal of natural sciences and mathematics* 19: 57-62 (1979).
11. P.V. Protic, and N. Stevanovic. The structural theorem for AG groupoids. *Series Mathematics and Informatics* 10: 25-33 (1995).
12. A. Rosenfeld. Fuzzy groups. *The Journal of Mathematical Analysis and Applications* 35: 512-517 (1971).
13. L.A. Zadeh. The concept of a linguistic variable and its applications to approximate reasoning. *Information Sciences* 8: 199-249 (1975).
14. L.A. Zadeh. Fuzzy Sets. *Information and Control* 8: 338-353 (1965).
15. R. Zenab. Some Studies in Fuzzy AG Groupoids. *M. Phil Dissertation, Quaid-i-Azam University, Islamabad* (2009).
16. M. Riaz, M. Saba, M. Abdullah, and M. Aslam. The novel concepts of m-polar spherical fuzzy sets and new correlation measures with application to pattern recognition and medical diagnosis. *AIMS Mathematics* 10: 11346-11379 (2021).
17. K. Naeem, M. Riaz, and D. Afzal. Pythagorean m-polar fuzzy sets and TOPSIS method for the selection of advertisement mode. *Journal of Intelligent & Fuzzy Systems* 37: 8441–8458 (2019).
18. M. Riaz, K. Naeem, and D. Afzal. Pythagorean m-polar fuzzy soft sets with TOPSIS method for MCGDM. *Punjab University Journal of Mathematics* 52: 21–46 (2020).

Proceedings of the Pakistan Academy of Sciences: A Physical and Computational Sciences 59(3): 69-80 (2022)

ISSN (Print): 2518-4245; ISSN (Online): 2518-4253
https://doi.org/10.53560/PPASA(59-3)775

Pakistan Academy of Sciences

Research Article

Design of Three Level Neutral Point Clamped Inverter with Fuzzy Logic based MPPT for PV Applications

Farhan Siddique[1], Saud Ahmad[1*], Hassan Ullah Khan[1], Muhammad Sohrab[1], and Tasneem Afeefa[2]

[1]Department of Electronic Engineering, University of Engineering and Technology, Peshawar
[2]Department of Chemistry, Quaid-i-Azam University, Islamabad

Abstract: In this paper a solar photovoltaic (PV) system with maximum power point tracking (MPPT) for domestic low power applications. The proposed system contains a PV array which provides electrical power, while a DC/DC converter is incorporated to regulate the power derived from PV panels. Fuzzy logic control (FLC) based MPPT has been proposed. To convert the DC voltages and currents obtained from Solar panels to AC voltages and currents, a Neutral point clamped multilevel inverter is included. Furthermore, harmonics are removed by using the LCL filter. The PV system working, design of the DC/DC Boost converter, Novel MPPT techniques, Multilevel inverter topologies and LCL filter design are explained. Results reveal that the FLC based MPPT has much lesser total harmonic distortion (THD) in the PV system. With this property, FLC possesses faster convergence than the perturb & observe (P&O) and other MPPT techniques.

Keywords: Photovoltaic (PV), Fuzzy logic control (FLC), Maximum power point tracking (MPPT), Multilevel Inverters, Neutral point clamped inverter, Perturb & Observe (P&O), Renewable energy (RE), PV Cell.

1. INTRODUCTION

Solar panels have become more efficient and inexpensive in recent years, making them an increasingly appealing alternative for people and companies looking to decrease their carbon footprint and minimize their energy expenses. Solar panels, as a renewable and sustainable energy source, have the potential to play a critical role in lowering greenhouse gas emissions and combatting climate change. PV panels have efficiency on the lower side however research and advances have led to technologies like MPPT (maximum power point tracking), which attains maximum available power at the output of a PV panel at any instant of time. Maximum power point tracking is available for PV panels, and wind power plants. There are several techniques to track maximum power points (MPP) [1, 2]. Such as perturbation and observation (P & O), incremental conductance, fractional open circuit, fractional short circuit, Fuzzy logic based MPPT etc. P & O is the simplest, inexpensive, easy to implement, and hence the most commonly used method in MPPT, however, it introduces fluctuations in the power, has a slower convergence rate and fails to track MPP under rapid changes in the environmental conditions. FLC based MPPT is fast, more efficient and performs better under various harsh conditions. Getting power from the panel effectively is not the solution, but it is also important to regulate this power and deliver it for useful work. To do this, an inverter (DC to AC converter) is used [3]. The output voltage of a multi-level inverter is greater than two levels. As a result, the inverter output voltage has reduced harmonic distortion and produces high-quality waveforms at the inverter output. These features make MLI available for applications that require higher power and high voltage levels [4]. Although there are various multilevel inverters, diode clamped or NPC inverters are widely used in industry because of their low electromagnetic interference and high efficiency. Over the years, the multi-level inverter is being used popularly in high-power applications because of its lesser interference than the typical two-level inverter and its ability to operate at lower switching frequencies. Transformers are the most efficient electrical machines and they are the most

Received: April 2022; Accepted: September 2022
*Corresponding author: Saud Ahmad <ahmadsaud436@gmail.com>

important member of any electrical system. In this research, a step-up transformer was used to obtain galvanic isolation and the desired output voltage. The implementation of MPPT was discussed by Chim *et al.* [5], and Du *et al.* [6] compared different methods of MPPT with different solar irradiance profiles. Edouard *et al.* [7], and Busquets-Monge *et al.* [8] presented Perturb & Observe and Fuzzy logic MPPT.

2. PROPOSED SYSTEM

Figure 1 represents the block diagram of the modelled solar photovoltaic system with MPPT for domestic low-power applications. The proposed system essentially consists of a PV panel, DC-DC converter, inverter, transformer and filter, and FLC-based MPPT. Details of the system design are explained in the following sections.

3. PV PANEL

Photovoltaic solar panels are used to convert the solar energy into electrical energy. This section discusses the output of solar panels & factors affecting the performance of Solar panels [1, 20].

3.1.1 Introduction

PV panels are the arrangement of semiconductor components which are used to convert the solar light into electric current. A PV module is a collection of PV cells that uses sunlight as energy and generates a direct current. The collection of PV modules is called a PV array. These arrays are used in PV systems and their job is to supply electrical energy to the electrical loads.

3.1.2 Working of Solar Panel

Solar panel includes many smaller units called PV cells. Light energy from the sun hits the PV cell, it transfers the light energy to the cell and causes the electrons to get loosen from the atom. To conclude, solar panels work by detaching electrons from atoms by photons or particles of light, generating electrical currents [7, 9, 10].

3.1.3 Factors Affecting Output of Solar Panel

The following are some crucial factors that influence the output of solar panels.

3.1.4 Temperature

With the increase in temperature, the output of the PV cell decreases, and the performance of PV is better in cold weather as compared to hot. A 25 ˚C rated PV panel can be very different from the actual external environment. For each degree increase in temperature above 25 ˚C then 0.25 % decays the output of the PV panels. The effect of temperature is explained in Figure 2, with an increase in temperature, the output power decreases.

3.1.5 Irradiance

The power per square meter area from sun is solar irradiance. As the power from sun changes, so do the I-V and P-V properties. As solar radiation rises, open voltage and short current rise as well, shifting the maximum power point. From Figure 3, it is clear that more the irradiance, greater amount of power is produced.

4. MAXIMUM POWER POINT TRACKING (MPPT)

MPPT stands for Maximum Power Point Tracking and refers to an electronic system used to optimize the efficiency of solar panels. Solar panels generate electricity when exposed to sunlight, but the

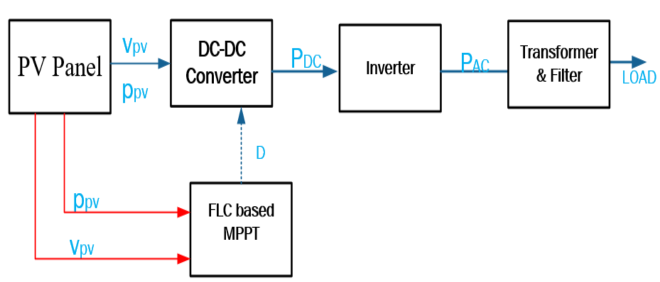

Fig. 1. Block diagram of proposed system

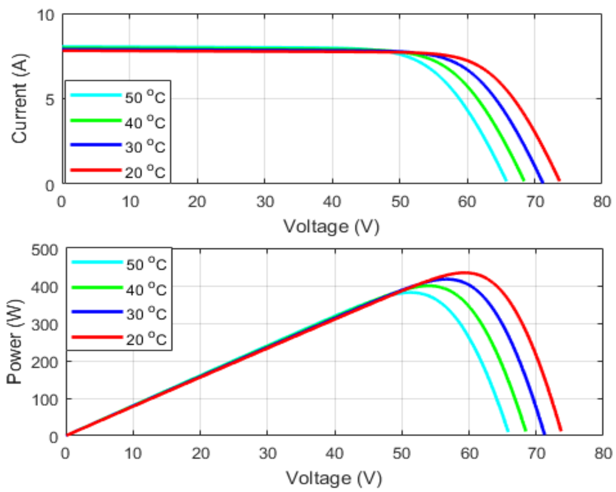

Fig. 2. Temperature effects on solar panels

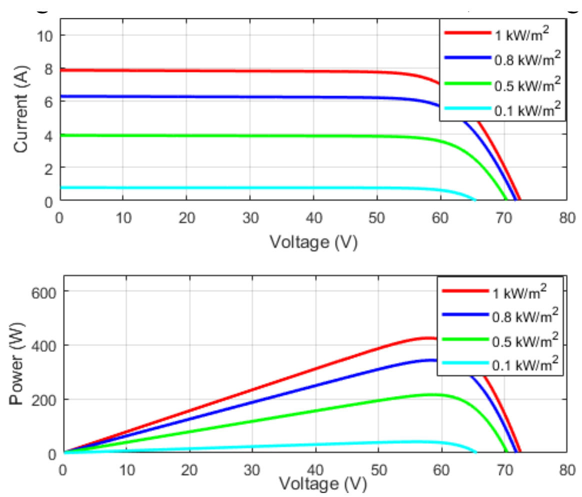

Fig. 3. Irradiance effects on solar panels

amount of electricity produced can vary depending on factors such as the angle and intensity of the sunlight and the temperature of the panels. MPPT systems work by constantly adjusting the voltage and current of the solar panel to ensure it is operating at its maximum power point i.e. Mpp the point where the module produces the most power under certain conditions. By optimizing the performance of the solar panel, MPPT systems can increase the efficiency of the entire solar power system and ensure that the maximum amount of energy is harvested from available sunlight. MPPT systems are widely used in on-grid solar power systems, off-grid solar power systems and in other applications where maximum efficiency is important [11].

4.1 Different MPPT Techniques

Many MPPT methods are implemented to reach the MPP. These MPP techniques vary from each other in many aspects such as the number of sensing devices, complexity, convergence speed, cost, range of effectiveness, accurate tracking etc. A few popular techniques are: [2, 12]

- Perturb and Observe
- Neural networks
- Fuzzy logic

In this research work FLC based maximum power point tracking technique is used, due to its fast and exploratory nature.

4.2 Fuzzy Logic based MPPT

FLC Maximum Power Point Tracking (FLC-MPPT), is a type of MPPT system that optimizes the efficiency of a solar panel using fuzzy logic. Fuzzy logic is a sort of mathematical logic that accepts imprecise or uncertain inputs, making it

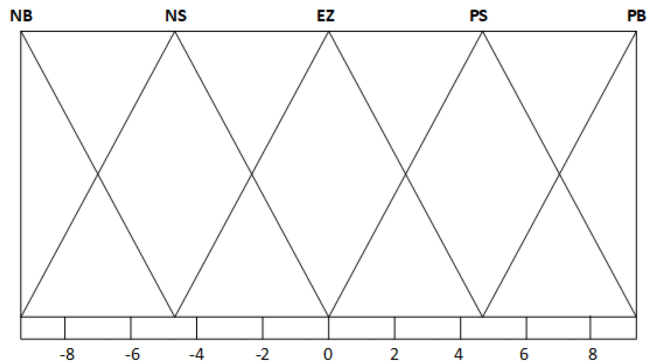

Fig. 4. Input membership function Vpv

especially effective in systems with complicated and changeable situations, such as solar power plants.

The input variables in an FL-MPPT system, such as sun irradiance and temperature, are translated into linguistic variables using fuzzy sets. The controller then applies rules based on expert knowledge or data to identify the solar panel's optimal operating position. The controller's output is a crisp value that is utilized to modify the duty cycle of DC/DC converters & regulate the solar panel's voltage and current to operate at its mpp. The FL-MPPT system offers several advantages over traditional MPPT systems. They can handle the non-linear and non-stationary behavior common in solar energy systems and can adapt to changing environmental conditions. Additionally, FL-MPPT systems are relatively simple and inexpensive to implement, making them a viable option for small-scale solar power systems. However, they may require more expertise to design and configure than traditional MPPT systems [13, 14].

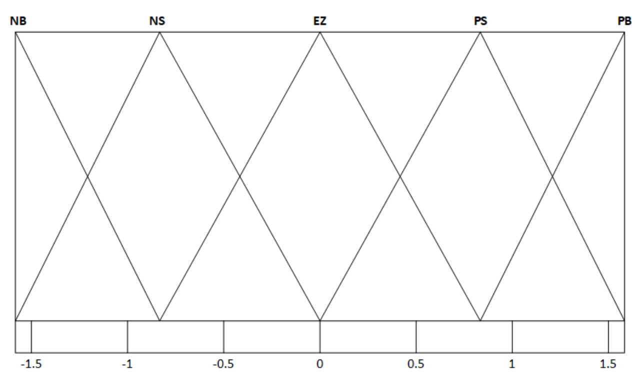

Fig. 5. Input membership function Ipv

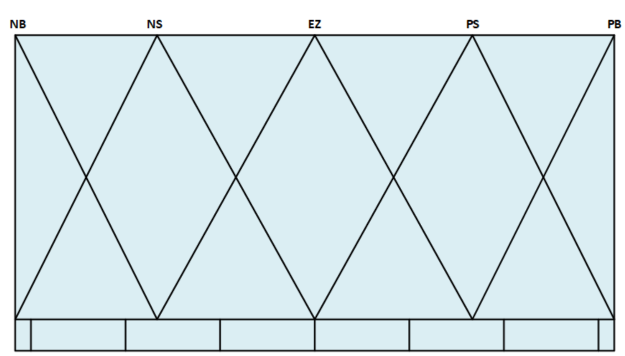

Fig. 6. Output membership function PWM

4.2.1 Design of FLC

FLC is designed by following steps:

- Variables are identified
- Fuzzy subsets are configured
- Fuzzy rule base is configured
- Fuzzification
- Combining the fuzzy outputs
- Defuzzification

The nature of FLC is robust as compared to conventional methods. FLC is based on three fundamental elements named 1st Fuzzification, 2nd Inference engine and 3rd defuzzification [3].

4.2.2 FLC based MPPT Design

During this research work, the following linguistic variables were used to define the membership functions [15].
NB: Neg Big
NS: Neg Small
EZ: Zero
PS: Pos Small
PB: Pos Big

The above-mentioned rules can be represented as the following Fuzzy rule base.

The fuzzy rules based on the if-then approach were:
1. (Vpv==NB) & (Ipv==BN) => (PWM=PB)(1)
2. (Vpv==NB) & (Ipv==NS) => (PWM=PS) (1)
3. (Vpv==NB) & (Ipv==ZE) => (PWM=NB) (1)
.
.
25. (Vpv==ZE) & (Ipv==PS) => (PWM=PB) (1)

The above-mentioned rules can be represented as the following Fuzzy rule base.

Figure 4 & Figure 5 are input membership functions, extracted for FLC. The variations in these functions lead to the generation of the output based on the membership functions provided in Figure 6. The pictorial representation of the PWM generated at the output of the FLC controller is shown in Figure 7.

5. DC/DC CONVERTER

A DC/DC converter is an electronic device used to convert direct current (DC) voltage levels from one level to another. It works by taking a DC type voltage at the input, changing its level to another DC output voltage, and using electronic circuitry to control current flow through the device. DC/DC converters can be used in a variety of applications including power supplies, battery charging systems, and solar power systems. This is especially useful in situations where the input voltage fluctuates, such as in solar power systems where the solar panel voltage can fluctuate with sunlight intensity. There are several different types of DC-to-DC converters, including:

- **Buck converters:** These converters step down the voltage at input to a lower output voltage.
- **Boost converters:** These converters step up the input voltage to a higher output voltage.

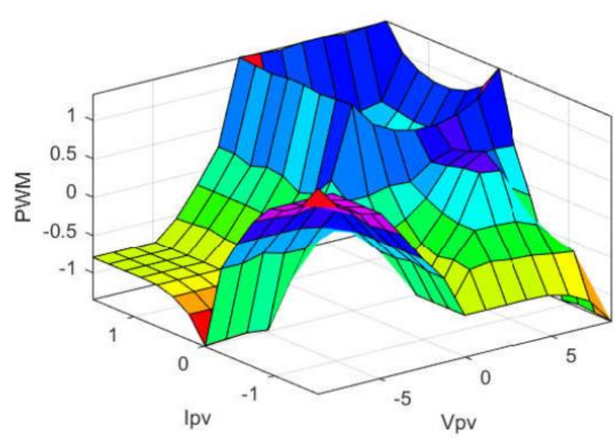

Fig. 7. Fuzzy rule surface

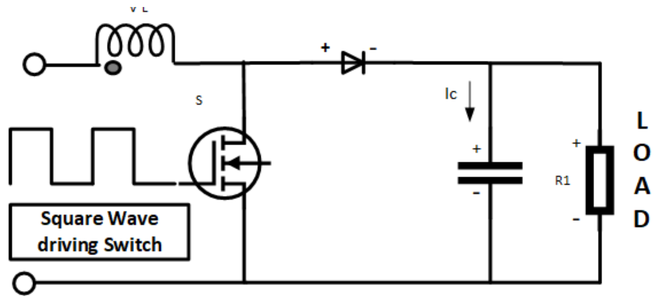

Fig. 8. Boost converter

- **Buck-boost converters:** These converters can both step up and step down the input voltage, depending on the needs of the system.
- **Flyback converters:** These converters store energy in a magnetic field and release it to the output in a series of pulses.

Depending on the requirements of the application, DC/DC converters can be implemented using different topologies and control methods. They are essential components of many electronic systems and play a key role in efficient power conversion and power management.

Among all DC/DC converter topologies, boost is an important topology used to step up the input voltage level given at the output. In this research work, a boost converter is used.

5.1 Boost Converter

A converter which shifts the level of input Dc voltage to the higher value at output is known as Boost converter. In the Figure 8, Switch S is controlled by the PWM scheme, generated by the MPPT algorithm.

5.1.1 Operation of Boost Converter

Firstly, when the switch is ON during time $0 \leq t \leq T_0$ which is the ON period for the switch, the output voltage is zero $V_0 = 0$ at that time, and the switch act as a short circuit. Current from the supply flows through the inductor and it starts charging. Therefore, the inductor current linearly rises; during ON time, the polarity of the Induce Emf is taken Positive, i.e, the left-hand side of the inductor is positive. When the switch is turned OFF during this cycle, this is the OFF period of switch $T_{off} = T\text{-}T_{on}$. In this period, the magnitude of the inductor current starts decreasing precisely in the same direction as in the ON period through an inductor, and the diode becomes forward-biased. The polarity of induced emf on the left-hand side is negative but added with supply voltage, making the current in the same direction. The current linearly decreases, keeping the voltage at a higher and constant level [16].

5.1.2 Design of Boost Regulator

The inductor and capacitor for the boost converter can be designed using the following equations: [17, 18]

$$Cmin = Vmpp \times Dmpp/2\Delta Vout \times RL \times fs \quad (1)$$

$$RL = Rmpp/(1 - Dmpp)^2 \quad (2)$$

$$Lmin = Vmpp \times Dmpp/2 \times \Delta Iout \times fs \quad (3)$$

6. INVERTERS

An inverter is an electronic device for converting direct current (DC) to alternating current (AC). Alternating current is the standard form of electricity used in most home and business appliances, while direct current is commonly used in batteries and other types of energy storage systems. A multilevel inverter is an electronic device used to convert direct current to alternating current by synthesizing a nearly sinusoidal step signal. It is designed to overcome the limitations of traditional 2-level inverters, which have limitations in output waveform quality, power loss and over-voltage of switching elements. The multilevel inverter uses a series of power solid state switches to produce a series of stepped voltage levels that approximate a sine wave. The number of voltage levels produced by the inverter determines the quality of the output waveform, with more levels providing a better approximation of a sine wave. Multi-level inverters offer many advantages over traditional two-level inverters, such as: B. Reduced harmonic distortion, reduced EMI and improved power efficiency. They are typically used in high power applications such as grid-connected solar power systems, motor drives and industrial applications [19].

6.1 Multilevel Inverter Classification

Multi-level Inverters can be classified into the following categories:

- Neutral point clamped Inverters
- Cascade Multilevel Inverters
- Capacitor clamped Inverters

This paper focuses on a neutral point clamped inverter.

6.2 Neutral Point Clamped Inverter

Diode clamped multilevel inverter (DCMLI), also known as neutral point clamp multi-level inverter. To produce L-levels of phase voltages, the DC bus of the inverter contains (L-1) capacitors. For three level inverter, DC bus consists of two capacitors, C1, C2. The DC voltage on each capacitor is Vdc/2 [4, 8].

No of capacitors L-1

No of switching devices 2(L-1)

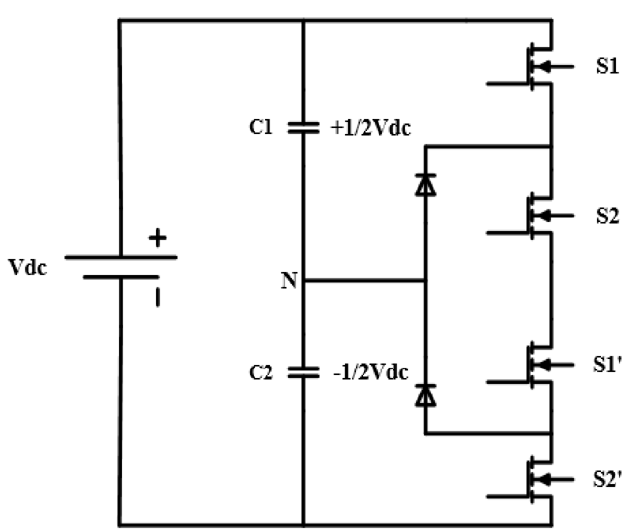

Fig. 9. One leg of typical NPC inverter

No of clamping devices (L-1)(L-2)

6.2.1 Principle of Operation

To achieve a waveform resembling a staircase output voltage, let us consider only one leg of the three-level inverter, as shown in Figure 9.

Table 1. Switching sequence for the one leg of NPC inverter

S1	S2	S1’	S2’	VRO
H	H	L	L	0.5Vdc
L	H	H	L	0
L	L	H	H	-0.5Vdc

To get the waveform shown in Figure 10, the switching sequence given in Table 1 is used. Figure 11 provides the circuit diagram for the full- bridge 3L NPC inverter.

Figure 12 shows the line voltage waveform of the NPC inverter. The Line voltage of the 3L NPC-MLI is obtained by taking, positive (+) voltage of one leg and negative (-) voltage other leg**.** For the above three-level inverter, the acquired line voltage is a 5-level step waveform. An L-level inverter gives k-levels of phase voltage and (2L-1) line voltage levels. The circuit diagrams shown in Figures 11 & 12 provides the base for simulation of the system.

7. TRANSFORMER & FILTER DESIGN

7.1 Transformer Design

A transformer where the output voltage is shifted to a higher level than its input voltage is called a step-

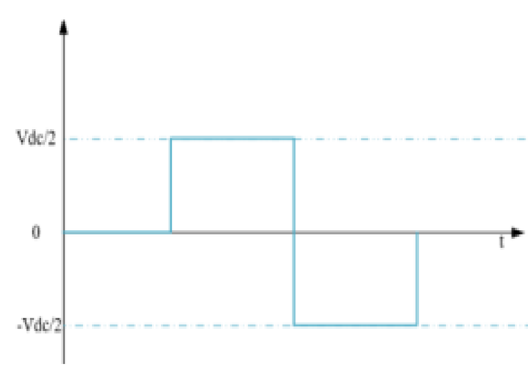

Fig. 10. Output of single phase of NPC inverter

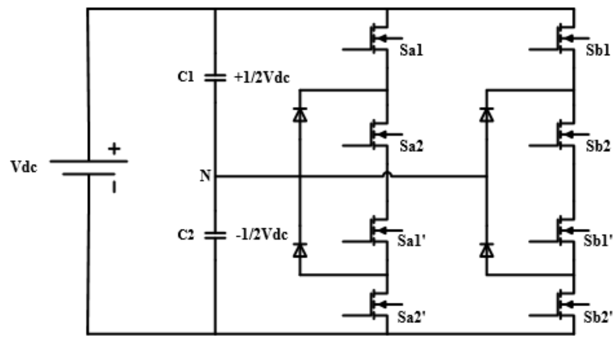

Fig. 11. Full bridge 3L NPC inverter

up transformer. In the step-up transformer amount of current reduces to maintain the input and output power of the same system.

The "step up" or "step down" transformer is decided by the voltage ratios of primary to secondary wire turns or called the turn ratio.

Voltage Transformation=Nsec/Npri
Current transformation =Npri/Nsec

Here N represents the No. of turn in the transformer winding.

The square root of a transformer's main to secondary inductance (L) ratio is called the transformer's transformation ratio. The working of the step-up transformer is given in Figure 13.
Voltage transformation=√((Lsec/Lpri))

7.2 Filter Design

During the course of this work, LC filter was used & was designed using following equations:

$$fc < \left(\frac{1}{10}\right) fswitchng \quad (4)$$

$$C = (\frac{1}{2} * S)/(2\pi V^2)f \quad (5)$$

$$L < \frac{0.2 \times Vac}{2\pi f I} \quad (6)$$

8. RESULTS & DISCUSSION

8.1 Simulation of Complete System

Figure 14 shows the simulation overview of the designed Photovoltaic system. As such, it reflects the simulation model of the designed system.

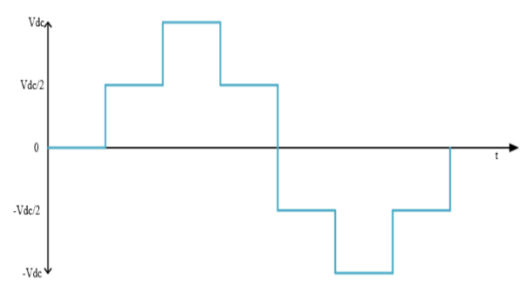

Fig. 12. Line voltage of 3L NPC inverter

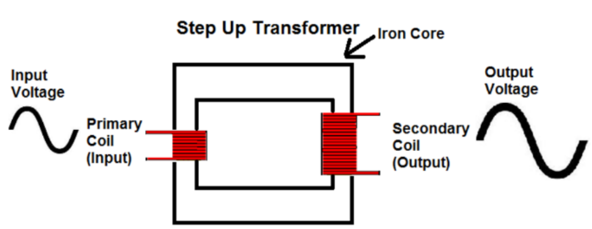

Fig. 13. Working of step-up transformer

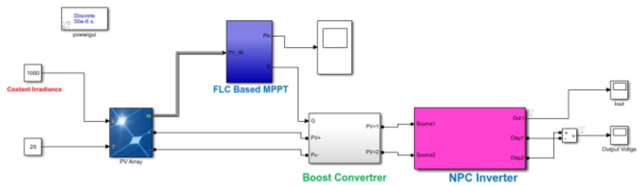

Fig. 14. MATLAB representation of complete system

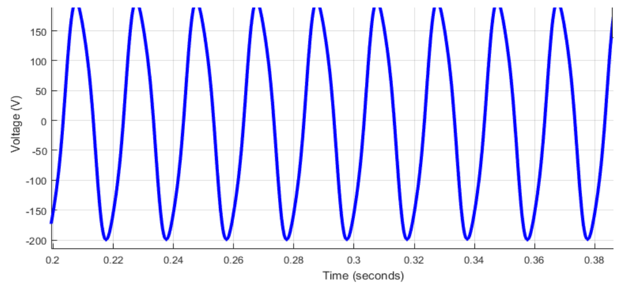

Fig. 15. Output voltage of the system

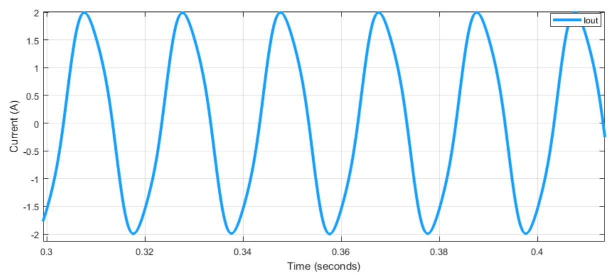

Fig. 16. Output current of the system

The output voltage and the output current of the system are shown in Figures 15 & 16 respectively, while Figure 17 shows the THD analysis of the designed system. The results shown in these three figures indicate that the system represented in this research work performs better than the conventional MPPT techniques mentioned by Nedumgatt *et al.* [12].

8.2 Simulated Results of Fuzzy Logic based MPPT and Full Bridge NPC Inverter

Figures 18 through 21 present the output of the simulated systems. Figure 18 shows the simulation of the designed Fuzzy logic controller, while Figure 19 shows the Simulink model of the inverter. Figure 20 & Figure 21 reflect the phase voltage & line voltage waveforms respectively. The aforementioned figures are simulated justifications for the Figure 11 & Figure 12.

9. CONCLUSION

A novel FLC based MPPT for Solar PV systems with NPC-MLI has been investigated. From the THD analysis of the system, it is concluded that the FLC based MPPT has much lesser THD in the system. With this property, FLC possesses faster convergence than the Perturb & Observe (P&O) and other MPPT techniques. Due to all of the above-explained reasons, the FLC based MPPT stands out as a very competitive alternative for P&O. Nevertheless, further research work is needed under various circumstances, which were not taken into consideration during this work.

10. CONFLICT OF INTEREST

The authors declare no conflict of interest.

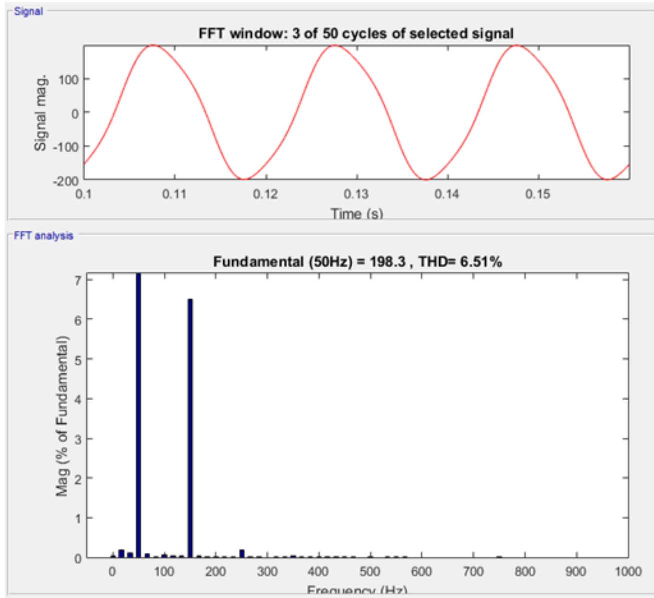

Fig. 17. THD analysis of the system

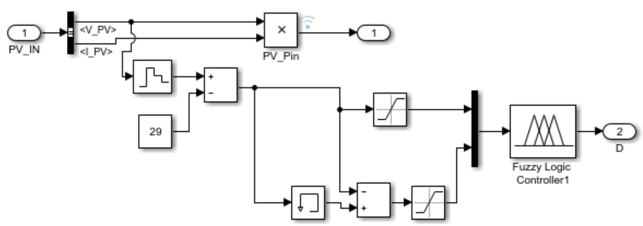

Fig. 18. FLC simulation in MATLAB Simulink

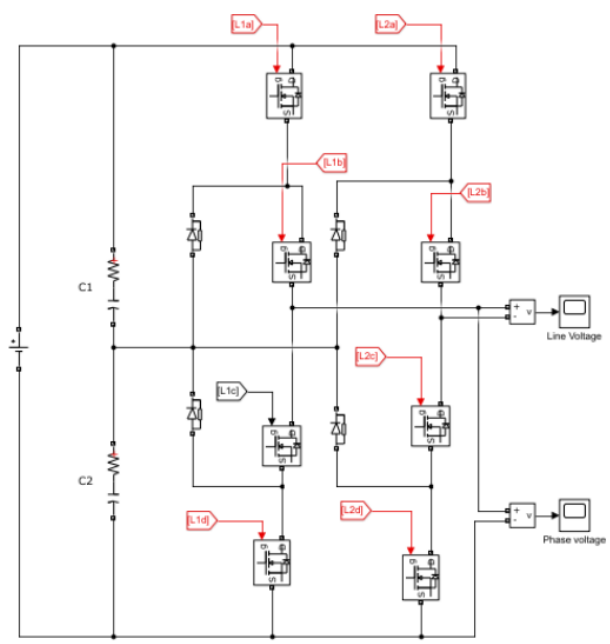

Fig. 19. Simulation of full bridge NPC inverter

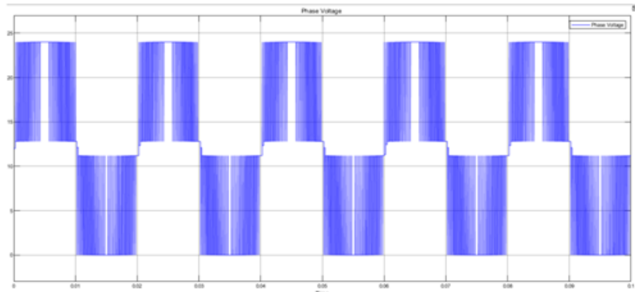

Fig. 20. Phase voltage of 3L NPC inverter

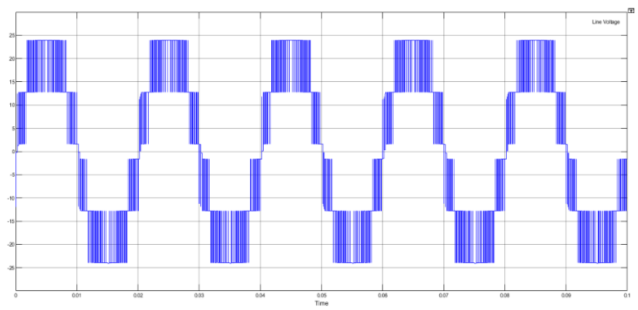

Fig. 21. Line voltage of 3L NPC inverter

11. REFERENCES

1. K. Bakirci. General models for optimum tilt angles of solar panels: Turkey case study. *Renewable and Sustainable Energy Reviews* 16: 6149–6159 (2012).
2. A.A. Abdulrazzaq, and A.H. Ali. Efficiency Performances of Two MPPT Algorithms for PV System With Different Solar Panels Irradiances. *International Journal of Power Electronics and Drive System (IJPEDS)* 9: 1755–1764 (2018).
3. F. Boico, and L. Brad. Single sensor MPPT algorithm for multiple solar panels configurations. *IEEE Power Electronics Specialists Conference* (2007).
4. M.T. Fard, and J. He. Fault Tolerant Five-Level Active NPC Inverter for High-Reliability Photovoltaic Applications. *IEEE 13th International Symposium on Diagnostics for Electrical Machines, Power Electronics and Drives (SDEMPED)* (2021).
5. C.S. Chim, P. Neelakantan, H.P. Yoong, and K.T.K. Teo. Fuzzy logic based MPPT for photovoltaic modules influenced by solar irradiation and cell temperature. *UkSim 13th International Conference on Computer Modelling and Simulation* (2011).
6. Y. Du, and D.D.-C. Lu. Battery-integrated boost converter utilizing distributed MPPT configuration for photovoltaic systems. *Solar Energy* 85: 1992–2002 (2011).
7. M. Edouard, and D. Njomo. Mathematical modeling and digital simulation of PV solar panel using Matlab software. *International Journal of Emerging Technology and Advanced Engineering* 3: 24–32 (2013).
8. S. Busquets-Monge, J. Bordonau, D. Boroyevich, and S. Somavilla. The nearest three virtual space vector PWM-a modulation for the comprehensive neutral-point balancing in the three-level NPC inverter. *IEEE Power Electronics Letters* 2: 11–15 (2004).
9. A.M. Serenelli. New results on standard solar models. *Astrophysics and Space Science* 328: 13–21 (2010).
10. M. Taherbaneh, G. Farahani, and K. Rahmani. Evaluation the accuracy of one-diode and two-diode models for a solar panel based open-air climate measurements. *Solar Cells-Silicon Wafer-Based Technologies* 4: 201–228 (2011).
11. M. Rosu-Hamzescu, and S. Oprea. Practical guide to implementing solar panel MPPT algorithms. *Microchip Technology Inc. Application Note, AN1521* (2013).
12. J.J. Nedumgatt, K.B. Jayakrishnan, S. Umashankar, D. Vijayakumar, and D. P. Kothari. Perturb and observe MPPT algorithm for solar PV systems-modeling and simulation. *Annual IEEE India Conference* (2011).
13. C. Robles Algarín, J. Taborda Giraldo, and O. Rodriguez Alvarez. Fuzzy logic based MPPT controller for a PV system. *Energies* 10: 2036 (2017).
14. C.K. Sundarabalan, K. Selvi, and K.S. Kubra. Performance investigation of fuzzy logic controlled MPPT for energy efficient solar PV systems. *Power Electronics and Renewable Energy Systems, Springer* 326: 761–770 (2015).

15. M. Veerachary, T. Senjyu, and K. Uezato. Neural-network-based maximum-power-point tracking of coupled-inductor interleaved-boost-converter-supplied PV system using fuzzy controller. *IEEE Transactions on Industrial Electronics* 50: 749–758 (2003).
16. B.M. Hasaneen, and A.A.E. Mohammed. Design and simulation of DC/DC boost converter. *12th International Middle-East Power System Conference* (2008).
17. H.A. Mohamed, H.A. Khattab, A. Mobarka, and G.A. Morsy. Design, control and performance analysis of DC-DC boost converter for stand-alone PV system. *Eighteenth International Middle East Power Systems Conference (MEPCON)* (2016).
18. S.-H. Park, G.-R. Cha, Y.-C. Jung, and C.-Y. Won. Design and application for PV generation system using a soft-switching boost converter with SARC. *IEEE Transactions on Industrial Electronics* 57: 515–522 (2009).
19. J. Siahbalaee, and N. Sanaie. Comparison of conventional and new cascaded multilevel inverter topologies based on novel indices. *ISA Transactions* 119: 41–51 (2022).
20. K.C. Kong, M.B. Mamat, M.Z. Ibrahim, and A. Muzathik. New approach on mathematical modeling of photovoltaic solar panel. *Applied Mathematical Sciences* 6: 381–401 (2012).

Instructions for Authors

Manuscript Format

The manuscript may contain Abstract, Keywords, INTRODUCTION, MATERIALS AND METHODS, RESULTS, DISCUSSION (or RESULTS AND DISCUSSION), CONCLUSIONS, ACKNOWLEDGEMENTS, CONFLICT OF INTEREST and REFERENCES, *and any other information that the author(s) may consider necessary*.

Abstract (font size 10; max 250 words)**:** Must be self-explanatory**,** stating the rationale, objective(s), methodology, main results, and conclusions of the study. Abbreviations, if used, must be defined on the first mention in the Abstract as well as in the main text. Abstract of review articles may have a variable format.

Keywords (font size 10)**:** Three to eight keywords**,** depicting the article.

INTRODUCTION: Provide a clear and concise statement of the problem, citing relevant recent literature, and objectives of the investigation.

MATERIALS AND METHODS: Provide an adequate account of the procedures or experimental details, including statistical tests (if any), concisely but sufficient enough to replicate the study.

RESULTS: Be clear and concise with the help of appropriate Tables, Figures, and other illustrations. Data should not be repeated in Tables and Figures, but must be supported with statistics.

DISCUSSION: Provide interpretation of the RESULTS in the light of previous relevant studies, citing published references.

ACKNOWLEDGEMENTS: (font size 10)**:** In a brief statement, acknowledge the financial support and other assistance.

CONFLICT OF INTEREST: State if there is any conflict of interest.

REFERENCES (font size 10)**:** Cite references in the text **by number only** in **square brackets**, e.g. "Brown et al [2] reported ..." or "... as previously described [3, 6–8]", and list them in the REFERENCES section, in the order of citation in the text, Tables and Figures (not alphabetically). Only published (and accepted for publication) journal articles, books, and book chapters qualify for REFERENCES.

Declaration: Provide a declaration that: (i) the results are original; (ii) the same material is neither published nor under consideration elsewhere; (iii) approval of all authors have been obtained; and (iv) in case the article is accepted for publication, its copyright will be assigned to *Pakistan Academy of Sciences*. Authors must obtain permission to reproduce, where needed, copyrighted material from other sources and ensure that no copyrights are infringed upon.

Manuscript Formatting

Manuscripts must be submitted in Microsoft Word (2007 Version .doc or .docx format); **pdf** files not acceptable. Figures can be submitted in Word format, TIFF, GIF, JPEG, EPS, PPT. Manuscripts, in *Times New Roman*, 1.15spaced (but use single-space for Tables, long headings, and long captions of tables & figures). The text must be typed in a double-column across the paper width. The Manuscript sections must be numbered, i.e., **1. INTRODUCTION, 2. MATERIALS AND METHODS,** and so on… (a) **Title** of the article **(**Capitalize initial letter of each main word; font-size 16; **bold**), max 160 characters (no abbreviations or acronyms), depicting article's contents; (b) Author' first name, middle initial, and last name (font size 12, **bold**), and professional affiliation (i.e., each author's Department, Institution, Mailing address and Email; but no position titles) (font size 12); (c) Indicate the corresponding author with *; (d) **Short running title**, max 50 characters (font size 10).

Headings and Subheadings (font size 11): All flush left

LEVEL-1: **ALL CAPITAL LETTERS; Bold**

Level-2: **Capitalize Each Main Word (**Except prepositions**); Bold**

Level-3: Capitalize each main word (Except prepositions)***; Bold, Italic***

Level-4: *Run-in head*; *Italics*, *in the normal paragraph position. Capitalize the initial word only and end in a colon (i.e.,* ***:****)*

List of REFERENCES must be prepared as under:

a. Journal Articles *(Name of journals must be stated in full)*

1. I. Golding, J. Paulsson, S.M. Zawilski, and E.C. Cox. Real time kinetics of gene activity in individual bacteria. *Cell* 123: 1025–1036 (2005).
2. W. Bialek, and S. Setayeshgar. Cooperative sensitivity and noise in biochemical signaling. *Physical Review Letters* 100: 258–263 (2008).
3. R.K. Robert, and C.R.L.Thompson. Forming patterns in development without morphogen gradients: differentiation and sorting. *Cold Spring Harbor Perspectives in Biology* 1(6) (2009).
4. D. Fravel. Commercialization and implementation of biocontrol. *Annual Reviews of Phytopathology* 43: 337359 (2005).

b. Books

5. W.R. Luellen. Fine-Tuning Your Writing. *Wise Owl Publishing Company, Madison, WI, USA* (2001).
6. U. Alon, and D.N. Wegner (Ed.). An Introduction to Systems Biology: Design Principles of Biological Circuits. *Chapman & Hall/CRC, Boca Raton, FL, USA* (2006).

c. Book Chapters

7. M.S. Sarnthein, and J.D. Stanford. Basal sauropodomorpha: historical and recent phylogenetic developments. In: The Northern North Atlantic: A Changing Environment. P.R. Schafer, & W. Schluter (Ed.), *Springer, Berlin, Germany*, pp. 365–410 (2000).
8. J.E. Smolen, and L.A. Boxer. Functions of Europhiles. In: Hematology, 4th ed. W.J. Williams., E. Butler and M.A. Litchman (Ed.), *McGraw Hill, New York, USA*, pp. 103–101 (1991).

d. Reports

9. M.D. Sobsey, and F.K. Pfaender. Evaluation of the H2S method for Detection of Fecal Contamination of Drinking Water, Report WHO/SDE/WSH/02.08, *Water Sanitation and Health Programme, WHO, Geneva, Switzerland* (2002).

e. Online references

These should specify the full URL for reference and give the date on which it was consulted. Please check again to confirm that the work you are citing is still accessible:

10. L. Branston. SENSPOL: Sensors for Monitoring Water Pollution from Contaminated Land, Landfills and Sediment (2000). http://www.cranfield.ac.uk/biotech/senspol/ (accessed 22 July 2005)

Tables and Figures

Insert all tables as editable text, not as images. Number tables consecutively following their appearance in the text, Figures should appear in numerical order, be described in the body of the text, and be positioned close to where they are first cited. Each figure should have a caption that describes the illustration, and that can be understood independently of the main text (Caption Table 1. and Fig 1. font size 10; Bold; Captions should be in sentence case; left-aligned). All Figures should have sufficiently high resolution (minimum 1000 pixels width/height, or a resolution of 300 dpi or higher) to enhance the readability. Figures may be printed in two sizes: column width of 8.0 cm or page width of 16.5 cm; number them as **Fig. 1**, **Fig. 2**, … in the order of citation in the text. Parts in a figure can be identified by A, B, C, D, ... and cited as Figure 2A, Figure 2B, Figure 2C. Captions to Figures must be concise but self-explanatory. Laser printed line drawings are acceptable. Do not use lettering smaller than 9 points or unnecessarily large. Photographs must be of high quality. A scale bar should be provided on all photomicrographs.

Tables: with concise but self-explanatory headings must be numbered according to the order of citation (like **Table 1.**, **Table 2.**). *Do not* abbreviate the word "Table" to "Tab.". Round off data to the nearest three significant digits. Provide essential explanatory footnotes, with superscript letters or symbols keyed to the data. Do not use vertical or horizontal lines, except for separating column heads from the data and at end of the Table.

Figures: Figures may be printed in two sizes: column width of 8.0 cm or page width of 16.5 cm; number them as **Fig. 1**, **Fig. 2**, … in the order of citation in the text. Captions to Figures must be concise but self-explanatory. Laser printed line drawings are acceptable. Do not use lettering smaller than 9 points or unnecessarily large. Photographs must be of high quality. A scale bar should be provided on all photomicrographs.

Note: The template of the manuscript is available at http://www.paspk.org/proceedings/; http://ppaspk.org/

Reviewers: Authors may suggest four relevant reviewers, two National and two International (with their **institutional E-mail** addresses).

SUBMISSION CHECKLIST

The following list will be useful during the final checking of an article before sending it to the journal for review.

Ensure that the following items are present:

One author has been designated as the corresponding author with contact details:

- E-mail address (Correct and valid)
- Full address of Institute/organization
- Keywords
- All figure captions
- All tables (including title, description, footnotes)

Further considerations

- Manuscript has been 'spell-checked' and 'grammar checked'
- References are in the correct format for this journal
- All references mentioned in the Reference list are cited in the text, and vice versa
- Permission has been obtained for the use of copyrighted material from other sources (including the Internet)

In case of any difficulty while submitting your manuscript, please get in touch with:

Editor
Pakistan Academy of Sciences
3-Constitution Avenue, Sector G-5/2
Islamabad, Pakistan
Email: editor@paspk.org
Tel: +92-51-920 7140
Websites: http://www.paspk.org/proceedings/; http://ppaspk.org/

PROCEEDINGS OF THE
PAKISTAN ACADEMY OF SCIENCES: PART A
Physical and Computational Sciences

C O N T E N T S

Volume 59, No. 3, September 2022 **Page**

PAKISTAN ACADEMY OF SCIENCES, ISLAMABAD, PAKISTAN

HEC Recognized, Category Y; Scopus Indexed

Websites: http://www.paspk.org/proceedings/; http://ppaspk.org